To the Graduate Council:

I am submitting herewith a dissertation written by Bassam Jamal entitled "PLASTIC AND ELASTIC BEHAVIOR OF INFILLED FRAMES SUBJECTED TO IN-PLANE LOADING." I have examined the final copy of this dissertation for form and content and recommend that it be accepted in partial fulfillment of the requirements for the degree of Doctor of Philosophy, with a major in Civil Engineering.

Richard M. Bennett

Richard M. Bennett, Major Professor

We have read this dissertation
and recommend its acceptance:

Edwin G. Burdette

D.W. Goodpasture

Joseph W. Fortey

Accepted for the Council:

CW Minkel

Associate Vice Chancellor
and Dean of the Graduate School

PLASTIC AND ELASTIC BEHAVIOR

OF

INFILLED FRAMES SUBJECTED TO IN-PLANE LOADING

A Dissertation

Presented for the

Doctor of Philosophy

Degree

The University of Tennessee, Knoxville

Bassam Jamal

May 1993

ACKNOWLEDGEMENTS

The author wishes to express his great appreciation to Dr. Richard M. Bennett, Dr. Edwin G. Burdette, Dr. Joseph W. Fortey, and Dr. David Goodpasture for serving on the committee and providing invaluable assistance, ideas, and comments. The author is grateful to Dr. Richard M. Bennett for the guidance, encouragement, and technical expertise throughout the study. The author also wishes to show his sincere thanks to Dr. Edwin G. Burdette for his guidance and assistance during the graduate studies.

This study is part of a research project sponsored by Martin Marietta Energy Systems, Inc. Thanks are due to Mr. Roger D. Flanagan, senior engineer in MM-ES, for his contributions.

The author is grateful to the University of Tennessee Computing Center for providing financial support throughout the graduate studies. Acknowledgements are due to my supervisors at UTCC, Ms. Nancy Gnilka, Ms. Robin McNeil, and Mr. Jeff Day for their support and understanding.

ABSTRACT

Elastic and plastic finite element studies were conducted to evaluate the in-plane behavior of concrete masonry infilled steel frames. ABAQUS was used to develop the finite element model and perform a parametric analysis. The model was verified by comparing the results with the experimental program series carried out at the University of New Brunswick, Canada. The initial stiffness could be matched using an elastic model with an frame-infill interface element. The ultimate load and secant stiffness, at approximately 50% of the ultimate, could be matched using a plastic model. The ABAQUS plastic model used a concrete model for the infill and an elastic-plastic material for the steel frame. A softened interface was used to account for the localized mortar crushing that tends to occur at the corners of infilled frames. The parametric study results indicated that an appropriate equivalent strut could closely match the infilled frame behavior. The model had the same frame beam and columns. The masonry infill was replaced by an equivalent diagonal strut. The strut had the same infill net thickness and Young's modulus. The model connections were hinged regardless of the frame's actual connections. When the frame columns differed, the average properties were used to estimate the relative stiffness used in calculating the diagonal strut effective width. However, the exact frame columns were still used in the strut model. Therefore, the infill behavior depended on the load direction. An average value could be used in estimating the structural stiffness, and thereafter, the natural frequency. The study included one and multiple bay infilled frames. For the latter case, the properties, area and moment of inertia

of each middle column were equally divided between the two adjacent one bay infilled frames. Infilled frames under gravity loads were also examined.

Stafford-Smith and Carter's (1969) formula to estimate the diagonal strut effective width for rigidly connected frames matched the initial stiffness. The effective diagonal strut width was divided by a constant, $\sqrt{2}$, for hinged connection frames. The secant stiffness model used the same equation and constant. However, the strut used a secant modulus, 0.662 of the infill Young's elastic modulus. The equivalent strut model successfully reflected the positive influence that vertical loads had on the infilled frame stiffness. The ultimate load model used the same equation and a penalty factor, 0.387, to reduce the infill ultimate strength due to the infill imperfect plasticity. The model ultimate load was the smaller lateral load which caused the failure of the windward column or the diagonal strut. Vertical loads did not effect the ultimate load when the infill was weak or under moderate vertical loads when the infill was relatively strong. Heavy gravity loads decreased the infilled frame ultimate strength for strong infills. The study found that the ultimate load of a multiple bay infilled frame was the sum of the ultimate strength of each individual one bay infilled frame.

TABLE OF CONTENTS

LIST OF FIGURES

LIST OF TABLES

CHAPTER 1

INTRODUCTION

1.1 Introduction

Infilled partitions or walls are generally considered nonstructural elements. Yet, these elements may drastically alter the building behavior. The infills add considerable strength and stiffness to structures. A partition when enclosed by a frame creates a new type of structure, an infilled frame. Frames can be steel or reinforced concrete. The infill can be a block, brickwork, or a reinforced or plain concrete wall, Figure 1.1.

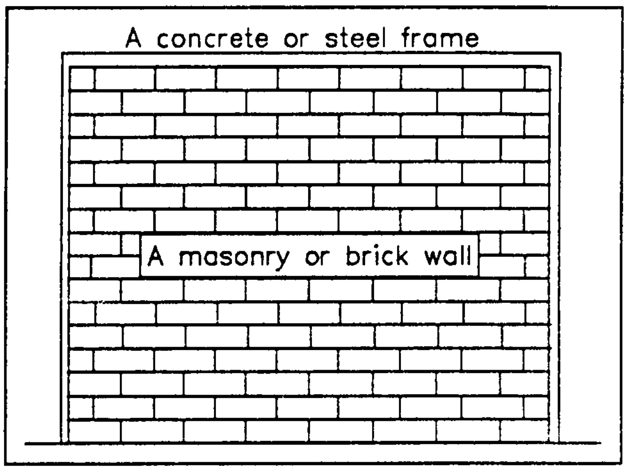

Figure 1.1. An infilled frame.

Bounding frames by themselves can be quite flexible under lateral loads. Walls are stiff, yet they are susceptible to cracking and failure under tensile stresses due to lateral loads, Figure 1.2. Both elements when combined contribute to the new structure. The infill provides the frame with the needed bracing. The frame

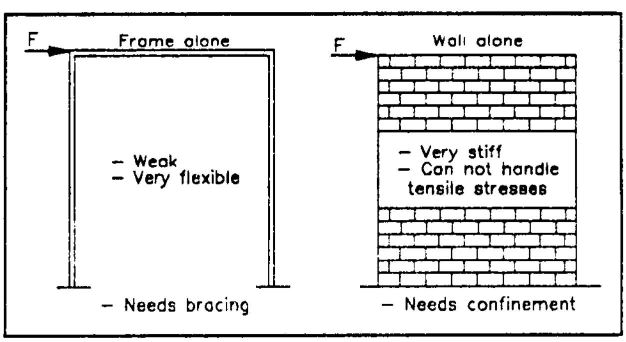

Figure 1.2. The behavior of infilled frame elements.

confines the infill and holds it together. The resultant structure can be considered as a well braced frame or a large moment of inertia section. The section consists of the windward column section in tension and the rest of the infill section and the leeward column in compression. This large section is significantly stiffer and stronger than the frame beam or column sections acting alone to support lateral loads. Infill significantly influences the structural behavior of the frames, even if the designers did not consider them during the original design.

The infilled frame behavior can be described by the initial and secant stiffness, and failure load, Figure 1.3. Stiffnesses are crucial in ascertaining the structural behavior against earthquake loads. They determine the structure's natural frequency. The initial stiffness is the stiffness at low lateral loads, without cracks, and thus, elastic. The secant stiffness is the stiffness after the infill has cracked under lateral loads and gone into the inelastic region. The ultimate load is the maximum lateral load the infilled frame can withstand. The ultimate load determines the structure's capacity to support lateral loads.

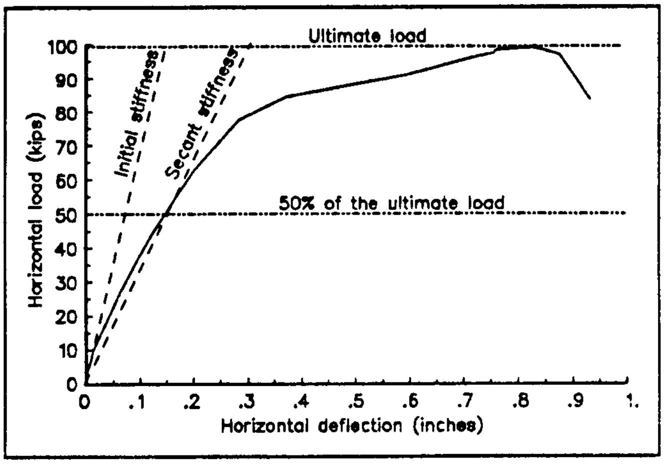

Figure 1.3. Infilled frame initial and secant stiffness and ultimate load.

Many researchers have studied the behavior of various types of infilled frames. They used analytical methods, finite element programs, and small and large scale test models. These studies enabled them to shed some light on the subject, but more is needed to fully understand the vital role infills play in the behavior of infilled frames. Infilled frames are highly indeterminate and complex to model and analyze. This fact explains the reluctance to consider them in design. A modest model and simple formulas are needed to describe the actual infilled frame behavior. Such formulas would enable designers to take advantage of infilled frames and achieve more realistic analyses.

1.2 Objectives

The purpose of this study is to contribute to the understanding of infilled frame behavior. The study analyzes the in-plane behavior of concrete masonry infilled steel frames. A literature review is conducted to determine the state of the art of infilled frame knowledge. A finite element model is developed and verified by comparison to experimental results. This is followed by a parametric study and a comparison of existing analytical method formulas. The study is performed on one and multiple bay infilled frames. Various types of infilled frame conditions are considered. These include rigid or hinged steel frame connections, frame-infill initial gaps, infill door or window openings, frame-infill shear connectors, infill reinforcements, and load reversal.

1.3 Scope of Work

The study develops a finite element model to perform the analytical analysis. The model consists of the appropriate finite elements and constitutive behavior to model the steel frame and the masonry infill. Special elements are used at the steel infill interface to account for the debonding and gapping. An elastic model is used to conduct the initial stiffness study. A plastic model is used to perform the secant stiffness and the ultimate load analyses. Modifications are made to define the steel and infill properties beyond the elastic range. The model is adjusted to account for local mortar crashing that tends to occur at the infill corners. The model is checked and refined with experimental data and other available analytical methods. These methods include equivalent strut and plastic collapse theories. The refined and accepted model is used in lieu of testing actual infilled frames to analyze several aspects of the in-plane behavior and perform a parametric study. These aspects include initial and secant stiffnesses and ultimate loads. The study is done on various types and infilled frame conditions. These include hinged or rigid frame connections, frame-infill initial gaps, infill door or window openings, frame-infill shear connectors, infill reinforcements, and load reversal. The parametric study determines that an equivalent strut model is capable of fully describing the infilled frame behavior. The behavior includes initial and secant stiffnesses, and failure loads. The study presents simple formulas to calculate the diagonal strut parameters. These formulas include existing, modified, and new ones.

CHAPTER 2

LITERATURE REVIEW

2.1 Introduction

The 1985 Mexico City earthquake was, unfortunately, a real test for the performance of many structures under seismic loadings. The investigation of an engineering team (Klingner et al., 1985) revealed the vital role infills played in resisting the earthquake. Many low-rise unreinforced masonry buildings, very common in Mexico City, survived due to their infills. The infill in most cases was not reinforced nor well tied to the surrounding frames. Therefore, it suffered severe damage, yet it prevented the building collapse. The infill played a beneficial role by stiffening the structures and reducing the natural period. Consequently, they reduced the inertial forces acting on the buildings. However, this is not always the case; stiffening structures in some seismic regions , e.g., California, could increase the inertial forces.

Despite the great influence infills may have on the structure behavior, they are not usually considered as structural elements. Their role should be understood and taken into consideration to obtain an accurate analysis and produce more realistic designs (Moghaddam and Dowling, 1988).

Analyzing the behavior of infilled frames under in-plane lateral loading is perplexing. Such a complex problem requires using various engineering tools. Seeking simplicity and resemblance to familiar structures, many researchers suggested that infilled frames behave as regular frames stiffened with diagonal struts. Others studied infilled frame behavior near failure and estimated the ultimate load using plastic collapse theories. Finite element methods also were used to idealize the complete infilled frame behavior up to failure. A series of full-scale infilled frames were tested experimentally to study their behavior and check the validity of analytical methods.

2.2 Equivalent Diagonal Strut Theory

2.2.1 Diagonal Strut Analogy

The infill provides bracing and adds considerable strength and stiffness to the bounding frame. Many researchers therefore suggested replacing the infill by an equivalent diagonal strut that provides the same bracing effect.

Early tests by Stafford-Smith (1962, 1966) on small-scale micro-concrete infilled frames showed that the frame and infill separate upon loading, leaving only portions near the loaded corners in contact. The tests also revealed that the windward column had high stresses, while the leeward column was almost stress free. Therefore, Stafford-Smith concluded that the infill acts as a diagonal strut, Figure 2.1.

2.2.2 Equivalent Strut Width

The effective width of the strut depends strongly on the infill aspect ratio (Stafford-Smith, 1962 and 1966). It also relies on the frame strength relative to the infill; the contact length is longer for a stronger frame. The strut width varies from about one-fourth of the infill diagonal length, d, for a square infilled frame to about d/11 for a rectangular infill with width to height ratio of 5, Figure 2.2. As a conservative value, Riddington and Stafford-Smith (1977) used a strut width of one tenth of the strut length.

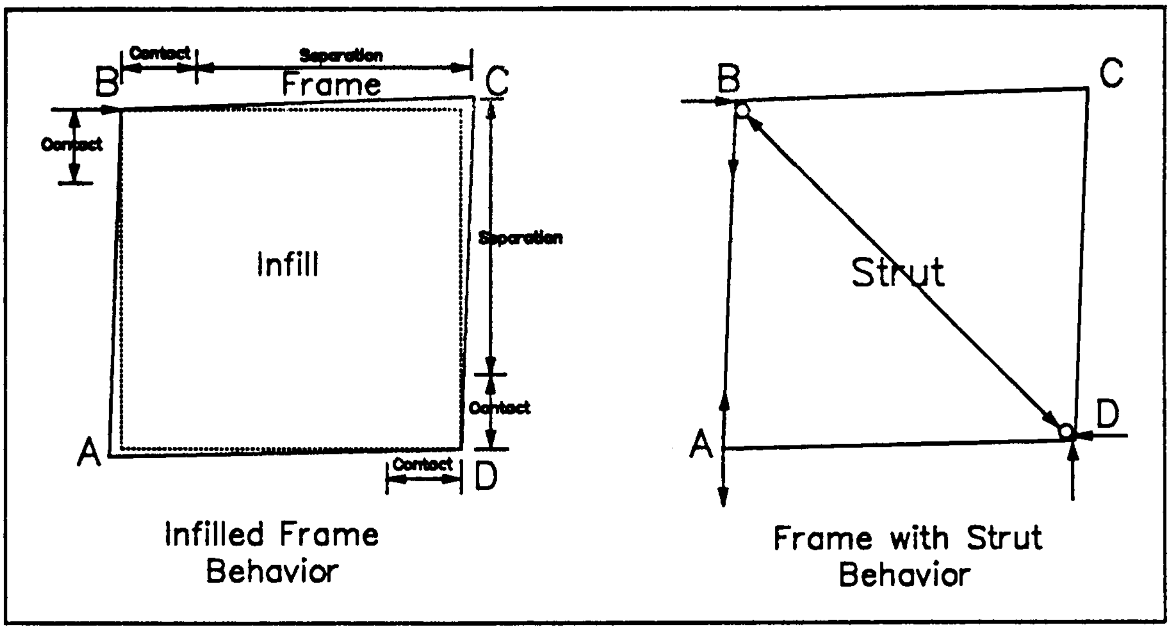

Figure 2.1. Strut and infill behavior similarities (after Stafford-Smith, 1962).

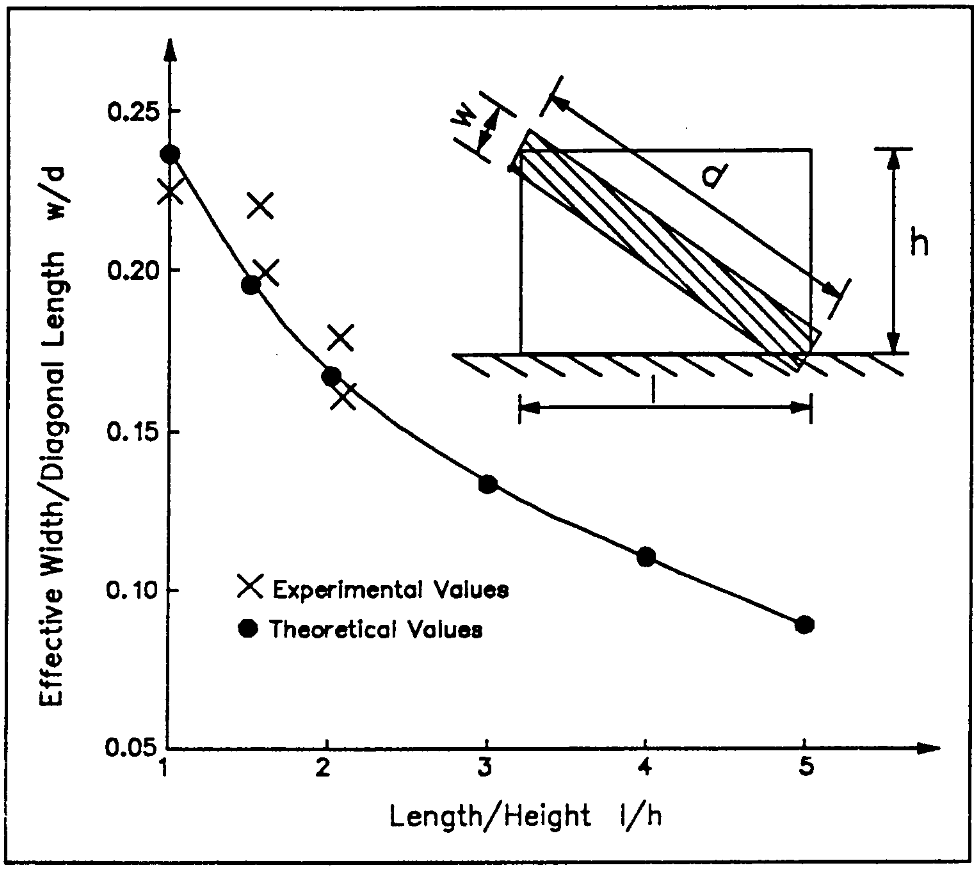

Figure 2.2. Effective strut width verses length to height ratio (after Stafford-Smith, 1962).

Holmes (1961) estimated the effective strut width to be one-third of the steel frame diagonal length. Stafford-Smith and Carter (1969) determined the strut effective width, a, using Equation 2.1. The parameter λ, a measure of the frame-infill relative stiffness, is given by Equation 2.2; Figure 2.3 shows the other parameters.

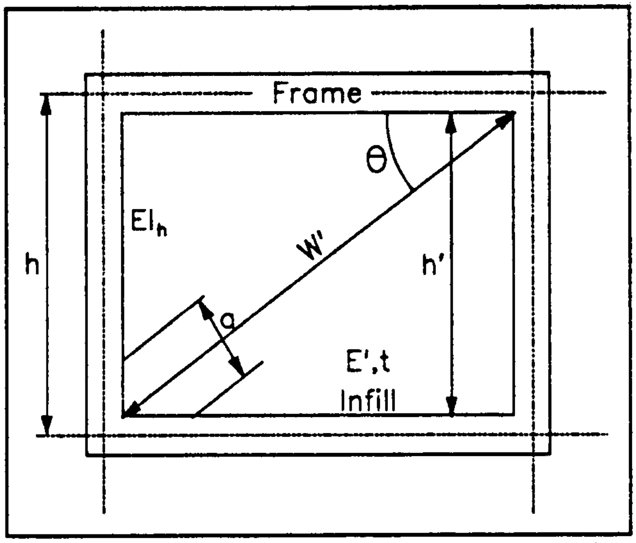

Figure 2.3. Frame and strut parameters (after Stafford-Smith and Carter, 1969).

$$a = \frac{\pi}{2\lambda} \tag{2.1}$$

$$\lambda = \sqrt[4]{\frac{E' \, t \, \sin 2\theta}{4 \, E \, I_h \, h'}} \tag{2.2}$$

Barua and Mallick (1977) tested several mortar infilled steel frames. They also conducted an analytical study. Their results agreed with Stafford-Smith's (1962 and 1966) observation concerning the infilled-frame strut similarity. They found that the steel-infill bond had little effect on the system behavior; the frame-infill separated in the early stages of loading. Simple expressions were proposed for length of contact, stiffness, strength, and share of load between the frame and infill. Equation 2.3 is the suggested formula for stiffness, S, given in terms of l, the frame length, λ, the frame-infill relative stiffness, and t and E', the infill thickness and Young's modulus respectively. This expression yields a lower stiffness than Stafford-Smith and Carter (1969) formulas, which overestimated the

$$\frac{S}{E' \, t} = \frac{0.2234}{\sqrt{\lambda \, l}} \tag{2.3}$$

system stiffness. The reason given for this discrepancy was due to Stafford-Smith and Carter (1969) neglecting steel-infill slippage.

Klingner (1980) suggested using Equation 2.4 to calculate the strut width.

$$\frac{a}{W'} = 0.175 \; (\lambda \; h)^{-0.4} \tag{2.4}$$

Chrysostomou et al. (1988), unlike the others, used different equations for different infill material and (λ h) values. When $4 \leq (\lambda \text{ h}) \leq 5$, Equation 2.4 is suitable for brick infills, while Equation 2.5 is for concrete infills. For (λ h) > 5, Equations 2.6 and 2.7 are for brick and concrete infills respectively. Equation 2.2 is still valid to calculate λ.

$$\frac{a}{W'} = 0.115 \; (\lambda \; h)^{-0.4} \quad (Concrete) \tag{2.5}$$

$$\frac{a}{W'} = 0.16 \; (\lambda \; h)^{-0.3} \quad (Brick) \tag{2.6}$$

$$\frac{a}{W'} = 0.11 \; (\lambda \; h)^{-0.3} \quad (Concrete) \tag{2.7}$$

Liauw and Kwan (1984) conducted a finite element parametric study. Neglecting friction, they suggested using Equation 2.8 to estimate the effective strut width, W. The parameters θ and h are the diagonal-horizontal angle and the frame height respectively.

$$\frac{W}{h \; \cos\theta} = \frac{0.86}{\sqrt{\lambda h}} \leq 0.45 \tag{2.8}$$

They also found that Equation 2.9 closely represents Barua and Mallick's (1977) experimental results.

$$\frac{W}{h\cos\theta} = \frac{0.95}{\sqrt{\lambda h}} \tag{2.9}$$

2.2.3 Infilled Frames With Openings

The previous section provides the equivalent strut width for solid infills. In practice, many infills have openings for several reasons, e.g., doors, windows, and vents. Liauw and Lee (1977) used a strain energy method and, assuming homogeneous and isotropic materials, developed formulas for the equivalent strut width for infilled frames with openings. Their analytical and experimental results were in good agreement. They concluded that infill openings did not change the basic structure behavior. Openings reduced the infilled-frame stiffness and strength moderately. They recommended using frame-infill connectors to increase the structure stiffness and strength.

Mallick and Grag (1971) studied the effects of openings and their position on the infilled frame behavior. They concluded that openings can reduce the stiffness and strength by as much as 75% and 90% respectively. They suggested locations of openings to minimize their undesirable effects. Doors should be located in the lower half near the center of the panel. Window openings are best located near the mid-height of either panel left or right half near the panel vertical edge.

Achyutha et al. (1988) put more emphasis on stiffening openings by frames to minimize the strength and stiffness reduction. Chrysostomou et el. (1988) suggested reducing the equivalent strut area to account for openings. The reduction percentage is equal to the opening-infill area ratio. Wolde-Tinsae et al. (1987) examined large openings at the top of the infill, such as occur when the infill is not full story height. They suggested that the equivalent strut frame into the column at the top of the infill in this case.

2.2.4 Nonlinear Behavior

After cracking, infilled frames behave inelastically. Klingner (1980) studied the elastic and inelastic response of infilled frames using the diagonal strut method. He used Equations 2.2 and 2.4 to estimate the strut width. An inelastic, degrading constitutive model was developed for the strut. The analytical and experimental results were in good agreement. Klingner (1980) concluded that the equivalent strut method is efficient to model the elastic and inelastic response of complex infilled frame structures.

Chrysostomou et el. (1988) developed a strut model to idealize the infilled frame's elastic and inelastic behavior. They proposed a decaying exponential expression to model the inelastic response. Figure 2.4 shows the elastic and inelastic parts of the model load-displacement curve separated by the infill cracking, where E, A, L, and f_c are the infill Young's modulus, area, length, and strength respectively. They used the suggested model to study the infill effects on the nonlinear dynamic characteristics of infilled frames. They concluded that the equivalent strut model can reasonably predict the infill inelastic behavior.

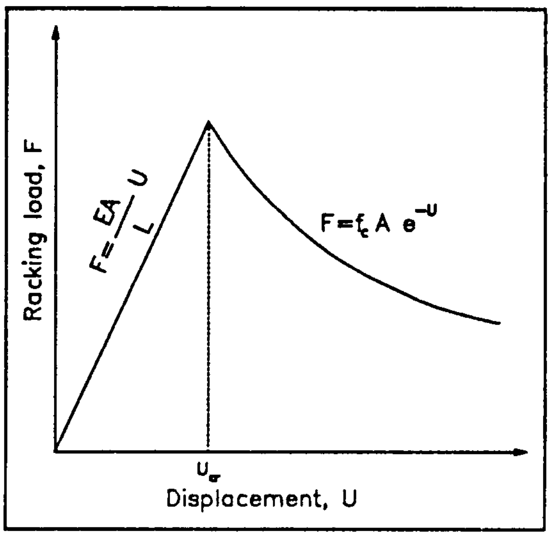

Figure 2.4. Model used to idealize the Load-Displacement behavior of infill walls (after Chrysostomou et al., 1988).

2.3 Plastic Theory of Infilled Frames

2.3.1 Introduction

Experimental tests (McBride, 1984) showed that the equivalent strut method (Stafford-Smith and Carter, 1969) did not correctly predict infilled frame failure loads. The plastic collapse theory (Liauw and Kwan, 1983), with a penalty factor (Wood, 1978), accurately predicted the ultimate loads. Consequently, plastic collapse theories have special significance in determining an important aspect of infilled frame behavior, the ultimate load.

2.3.2 Yield Zone Methods

Several researchers, e.g., Wood (1978) and May and Ma (1985), used yield line theories or strip methods to find work done along the yield lines. Thereafter, upper and lower bounds to the collapse loads could be obtained. The difference between the upper and lower bounds was negligible, confirming the validity of the theories.

A very complex equation calculates the work, W, done in yield zones or lines. However, for special cases of interest, simple formulas give W. These cases are positive, negative, or no rotation. May and Ma (1985) introduced Equations 2.10, 2.11, and 2.12 correspond to these cases respectively. They used a yield zone criterion, Figure 2.5, and assumed rigid-plastic no-tension infill material.

$$W = \frac{1}{2}\, \sigma_c\, t_w\, L\, \delta\, (1 - \sin\alpha) \tag{2.10}$$

$$W = 0 \tag{2.11}$$

$$W = \frac{1}{2}\ \sigma_c\ t_w\ L^2\ |\theta| \qquad (2.12)$$

Where:

W : work done in a yield line/zone

σ_c : infill crushing stress

t_w : infill thickness

L : yield zone length

δ : displacement

θ : rotation

α : displacement angle to y axis

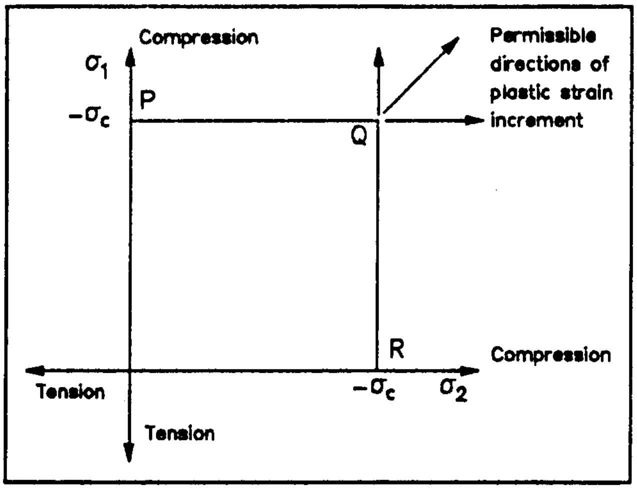

Figure 2.5. Infill square yield criterion (after May and Ma ,1985).

2.3.3 Wood's Work

Wood (1978) examined solid panel infilled frames. He applied a square yield criterion to develop work done along the yield lines. He calculated upper and lower bounds to the collapse load for each failure mode. The upper and lower bounds were quite close or identical. A penalty factor was applied to ultimate loads to account for the masonry's imperfect plasticity.

The infilled-frame ultimate load strongly depends on the collapse mode. Wood (1978) identified four different failure modes for infilled frames. These included shear, shear rotation, diagonal compression, and corner crushing, Figure 2.6.

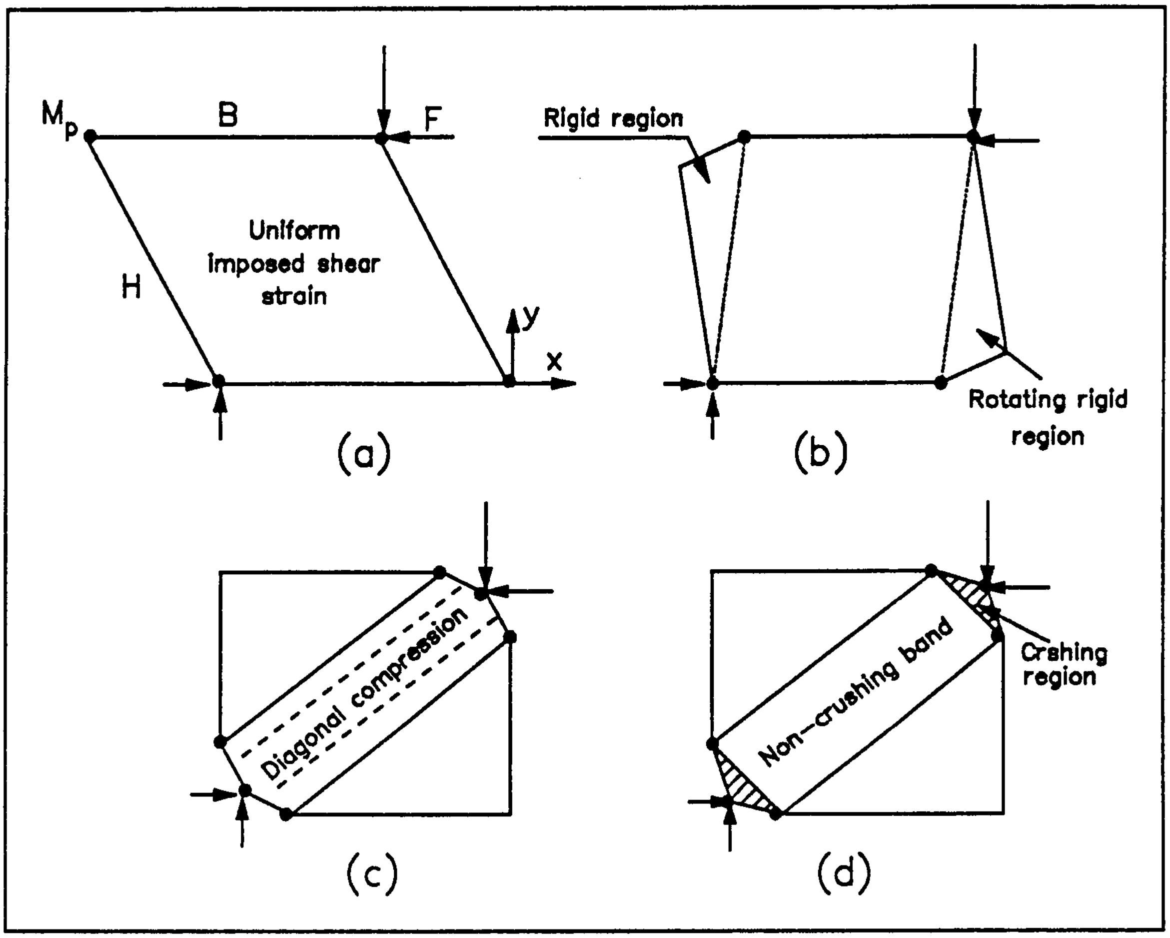

Figure 2.6. Idealized plastic failure modes for infill panel: (a) shear mode S, (b) shear rotation mode SR, (c) diagonal compression mode DC, (d) corner crushing mode CC (after Wood, 1978).

2.3.3.1 Shear Mode

In this mode, which happens when the infill is weak, four plastic hinges are formed in the frame corners, and the infill is under a pure shear, no rotation. Therefore, Equation 2.12 gives the internal work of the infill. Equation 2.13 is the work equation for this failure mode, with the left hand being the external work done by the collapse force, F. This leads to Equation 2.14 where H and B are the frame height and breadth respectively; Φ is the shear strain angle; M_p is the smaller plastic moment of the frame beam and column. For this failure mode, upper and lower bounds are identical.

$$FH\Phi = 4M_p\Phi + \frac{1}{2}\sigma_c\Phi BHt_W \qquad (2.13)$$

$$F = \frac{4M_p}{H} + \frac{1}{2}\sigma_c\, B\, t_W \qquad (2.14)$$

It is useful to introduce a non-dimensional factor, f, Equation 2.15. The term f is equal to unity for the shear failure mode which is considered the natural and strongest mode. Equation 2.16 defines m a non-dimensional measure of the frame-wall relative strength.

$$f = \frac{F}{\frac{4\,M_p}{H} + \frac{1}{2}\,\sigma_c\,t_w\,B} \qquad (2.15)$$

$$m = \frac{8\,M_p}{\sigma_c\,t_w\,B^2} \qquad (2.16)$$

2.3.3.2 Shear Rotation Mode

This mode occurs with a medium strength infill. The infill in this mode consists of a pure shear part and two rotating regions, Figure 2.6. Four hinges are formed in the frame, two in the loaded corners and two in the beams near the non-loaded corners. The non-dimensional factor f for this mode is given in Equations 2.17 and 2.18 for the upper and lower bounds respectively. The parameters X and C are numerically chosen to minimize and maximize f respectively. Equation 2.19 represents the lower bound for square panels.

$$f = \frac{1}{(1-X)\,(1+\frac{H}{mB})} + \frac{\frac{H}{mB}}{1+\frac{H}{mB}} \left\{ \sqrt{[1+(\frac{XB}{H})^2]} - \frac{XB}{H} \right\} \tag{2.17}$$

$$f = \frac{2}{1+\frac{mB}{H}} \left\{ \sqrt{(C-C^2)} + (1-C)\frac{B}{H} \left[\sqrt{(\frac{2m}{(1-C)})} - 1 \right] \right\} \tag{2.18}$$

$$f = \frac{2}{\sqrt{m+\frac{1}{\sqrt{m}}}} \tag{2.19}$$

2.3.3.3 Diagonal Compression and Corner Crushing Modes

The diagonal compression failure mode occurs with infilled frames composed of a strong wall and weak frame. The corner crushing mode happens with very weak frames. Equations 2.19 and 2.20 are the lower bound solutions for square and rectangular panels respectively. Equation 2.21 is the upper bound solution. The parameter D is the diagonal panel length.

$$f = \frac{\frac{2}{(1-X)}}{1+\frac{H}{mB}} \tag{2.20}$$

$$f = \frac{1 - \frac{2BH}{D^2} + 2(\frac{B}{D})\sqrt{2m}}{1 + \frac{mB}{H}} \tag{2.21}$$

2.3.4 Penalty Factor

Wood (1978) suggests using a penalty factor to reduce σ_c to account for imperfect plasticity of the infill. Applying a penalty factor gave consistent results with experiments (Dawe and McBride, 1985). Equation 2.22 calculates the penalty factor, ν_p. The term ($\nu_p\sigma_c$) is then used in lieu of σ_c in the collapse shear calculations.

$$\nu_p = 2.663\ m^2 - 1.371\ m + 0.406 \leq 0.45 \tag{2.22}$$

2.3.5 Infilled Frames With Openings

The previous analysis determines the ultimate load for replete infilled frames. Yet, infilled frames often have door, window, or ventilation openings. May and Ma (1985) extended the plastic collapse methods developed by Wood (1978) to include panels with openings. They used a yield zone criterion to get the upper and lower bound on the collapse load. The study shows that the difference between the upper and lower bound results is negligible, which confirms the analysis validity.

May and Ma (1985) consider panels with openings in the loaded or non-loaded corner, or center. The development for openings in the loaded corner will be reviewed. There are two basic failure modes, the shear and shear-rotation modes, Figure 2.7. The shear mode occurs when the frame is strong relative to the infill, and the shear-rotation mode when the frame is weak with respect to the infill.

The upper bound analysis of the shear mode is shown in Figures 2.8 and 2.9 for small and large openings. Using Equations 2.10 and 2.12, the work done in yield zones for a small opening is given by Equation 2.23. Equation 2.24 gives the non-dimensional factor, f, which determines the collapse shear, F, for this case. The study uses the same scheme to derive Equation 2.25 for the non-dimensional factor f for the large opening case.

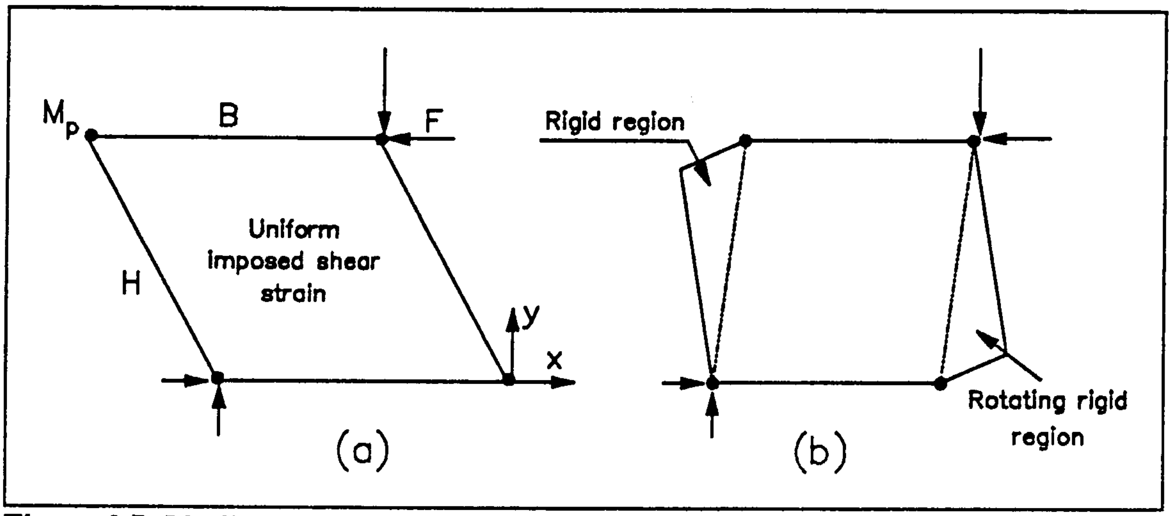

Figure 2.7. Idealized Plastic failure modes for wall-frame panels:
(a) shear mode-mode S; (b) shear rotation mode-mode SR (after May and Ma, 1985).

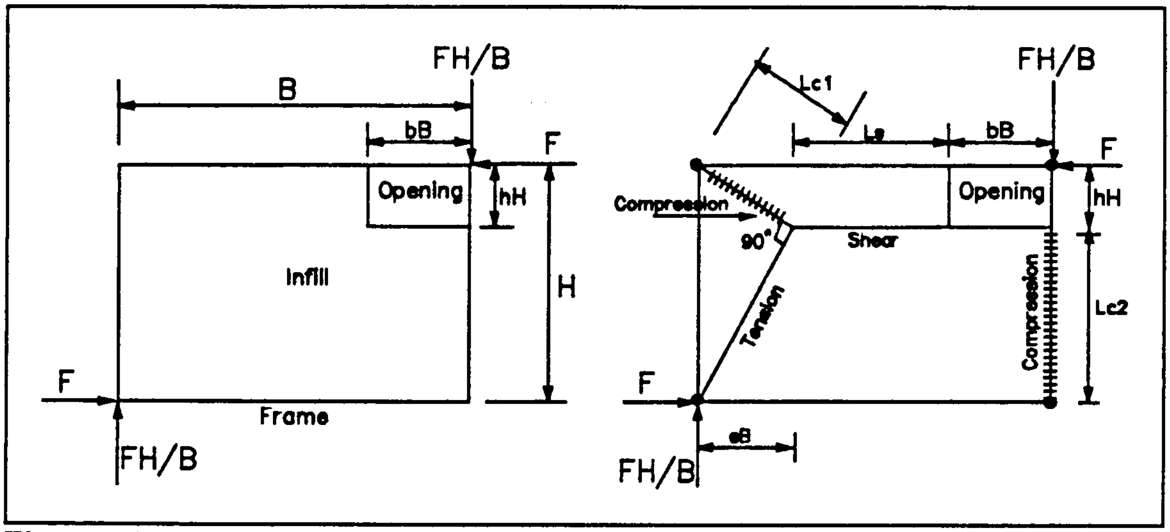

Figure 2.8. Details of a small opening panel and disposition of yield zones (after May and Ma, 1985).

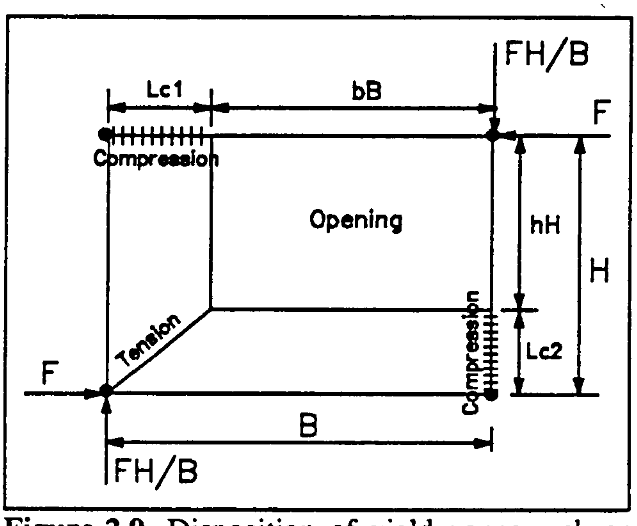

Figure 2.9. Disposition of yield zones - shear mode (after May and Ma, 1985).

$$4\,M_p\,\Phi + \frac{1}{2}\,\sigma_c\,t_w\,L^2_{c1}\,\Phi + \frac{1}{2}\,\sigma_c\,t_w\,L^2_{c2}\,\Phi + \frac{1}{2}\,\sigma_c\,t_w\,L_s\,H\,\Phi \quad (2.23)$$

Where: Φ = *The rigid region rotation*

$L_{c1} = H\sqrt{h}$

$L_{c2} = H\,(1-h)$

$L_s = B - e\,B - b\,B$

$$f = \frac{m\,\dfrac{B}{H} + \dfrac{H}{B}\,[h + (1-h)^2] + (1-b-e)}{1 + m\,\dfrac{B}{H}} \quad (2.24)$$

$$f = \frac{m\,\dfrac{B}{H} + \dfrac{B}{H}\,(1-b^2) + \dfrac{H}{B}\,(1-h)}{1 + m\,\dfrac{B}{H}} \quad (2.25)$$

The lower bound analysis for the small and large opening infills is illustrated in Figure 2.10. Equation 2.26 gives the non-dimensional factor f for both cases. The angles α and β are numerically varied to maximize f.

$$f = \frac{\dfrac{mB}{H} + \dfrac{2\,(1-b)\,B\,\sin\alpha\,\cos\alpha + (1-h)^2\,H\,\cos^2\beta - 2(z-\frac{z^2}{2})\,H\,\cos^2\alpha}{B}}{\dfrac{mB}{H} + 1} \quad (2.26)$$

The study (May and Ma, 1985) provides an appropriate analysis for infilled frames with openings. The given formulas are complex. They suggest that the penalty factor developed by Wood (1978) be used to reduce the infill strength.

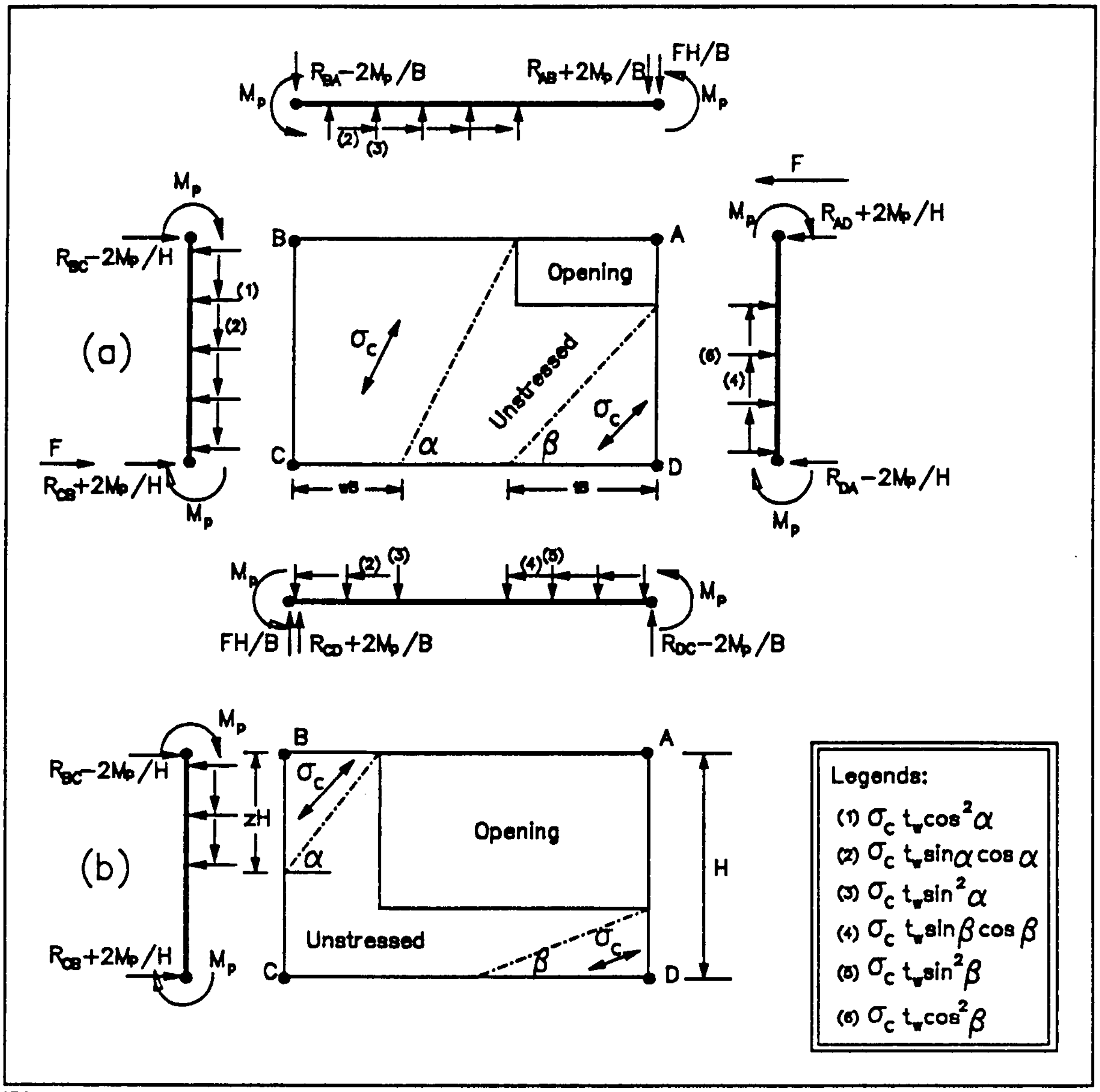

Figure 2.10. Rectangular panel with opening - shear mode: (a) a small opening; (b) a large opening (after May and Ma, 1985).

2.3.6 Liauw and Kwan's Work

Liauw and Kwan (1983) used a plastic collapse theory to calculate the ultimate loads for infilled frames. They considered three different failure modes. These included corner crushing with failure in columns, corner crushing with failure in beams, and diagonal failure, Figure 2.11.

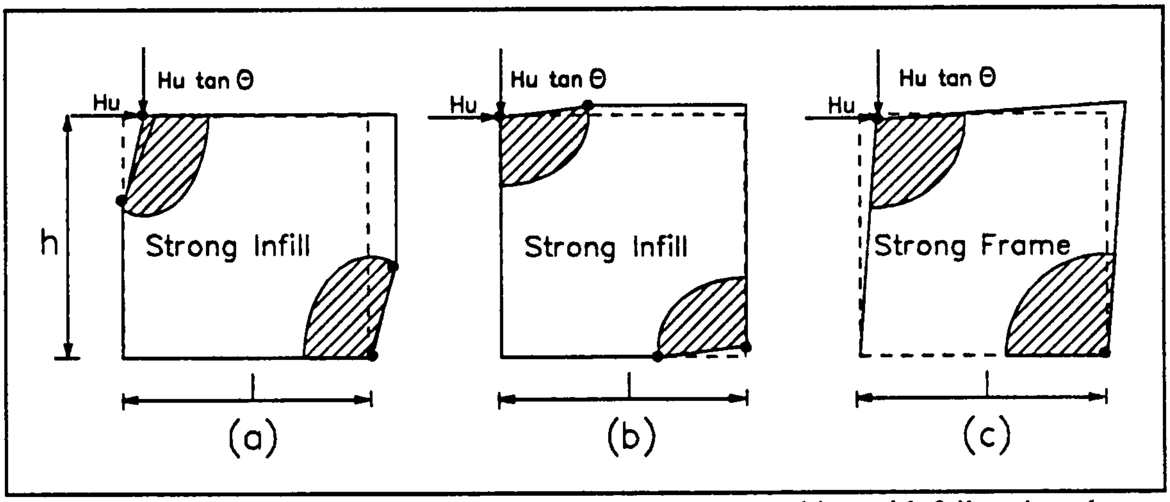

Figure 2.11. Failure modes of infilled frames: (a) corner crushing with failure in columns (weak columns); (b) corner crushing with failure in beams (weak beams); (c) diagonal crushing (after Liauw and Kwan, 1983).

2.3.6.1 Corner Crushing With Failure in Columns

This collapse mode, Figure 2.12, occurs when the frame is weak relative to the infill and the beams are strong compared to columns. In this mode, the loaded corners crush and plastic hinges form in the loaded joints and columns. The term σ_c is the crushing stress of the infill assuming perfect plasticity. The parameter F_b is the contribution of the infill-beam friction and the leeward side column shear. Horizontal and moment equilibrium about A for the segment AE gives Equations 2.27 and 2.28. The

$$H_u = \sigma_c \, t \, \alpha_c \, h + F_b \tag{2.27}$$

$$\frac{1}{2} \, \sigma_c \, t \, (\alpha_c \, h)^2 = M_{pj} + M_{pc} \tag{2.28}$$

parameters M_{pj} and M_{pc} are the joint and column plastic moments respectively. The contribution of column shear and the beam/infill friction, F_b, is small (Liauw and Kwan 1983); therefore, it can be neglected. This leads to Equations 2.29 and 2.30.

$$\alpha_c = \sqrt{\frac{2 \, (M_{pj} + M_{pc})}{\sigma_c \, t \, h^2}} \tag{2.29}$$

$$\frac{H_u}{\sigma_c \, t \, h} = \sqrt{\frac{2 \, (M_{pj} + M_{pc})}{\sigma_c \, t \, h^2}} \tag{2.30}$$

2.3.6.2 Corner Crushing With Failure in Beams

This collapse mode, Figure 2.13, happens when the frame is weak relative to the infill and the columns are strong compared to beams. In this mode the infill compressive corners crush with failure in the beams. Vertical and moment equilibrium about A for the segment AG gives Equations 2.31 and 2.32 in which θ is the beam-diagonal angle. For the same reasons as for mode a, F_c is neglected, which leads to Equations 2.33 and 2.34.

$$H_u \tan\theta = \sigma_c \, t \, \alpha_b \, l + F_c \tag{2.31}$$

$$\frac{1}{2} \, \sigma_c \, t \, (\alpha_b \, l)^2 = M_{pj} + M_{pb} \tag{2.32}$$

$$\alpha_b = \tan\theta \sqrt{\frac{2\,(M_{pj} + M_{pb})}{\sigma_c\, t\, h^2}} \tag{2.33}$$

$$\frac{H_u}{\sigma_c\, t\, h} = \frac{1}{\tan\theta} \sqrt{\frac{2\,(M_{pj} + M_{pb})}{\sigma_c\, t\, h^2}} \tag{2.34}$$

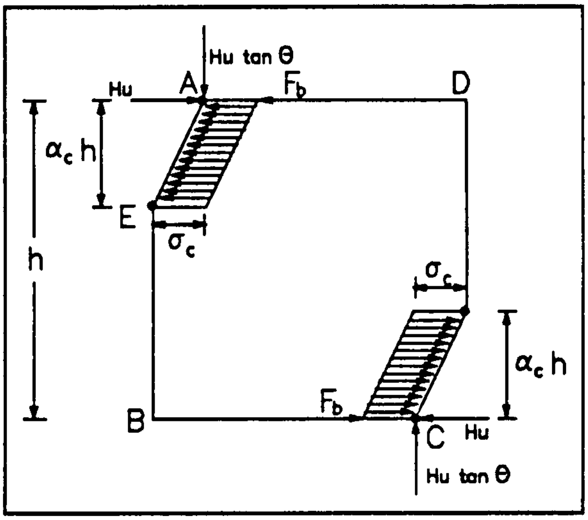

Figure 2.12. Mode (a) corner crushing with failure in columns (after Liauw and Kwan, 1983).

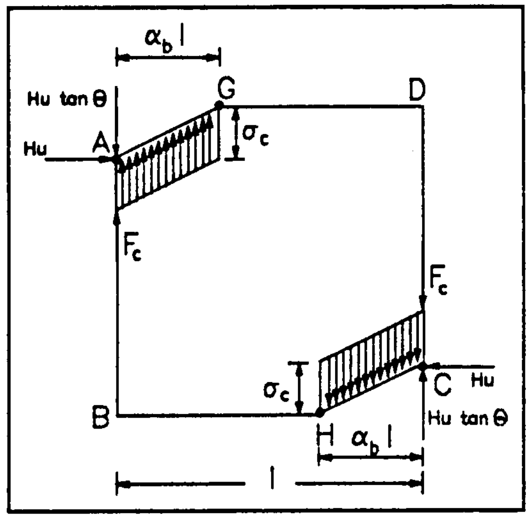

Figure 2.13. Mode (b) corner crushing with failure in beams (after Liauw and Kwan, 1983).

2.3.6.3 Diagonal Failure

This mode, Figure 2.14, occurs when the frame is strong relative to the infill; therefore, neither the beams nor the columns fail. Instead, plastic hinges form in all corners and the infill-crushed regions are deeper towards the infill interior. The contact stress σ_c is assumed to be parabolic along the infill-frame contact. Considering the case when the span is greater than height, resolving horizontal forces, and taking moments

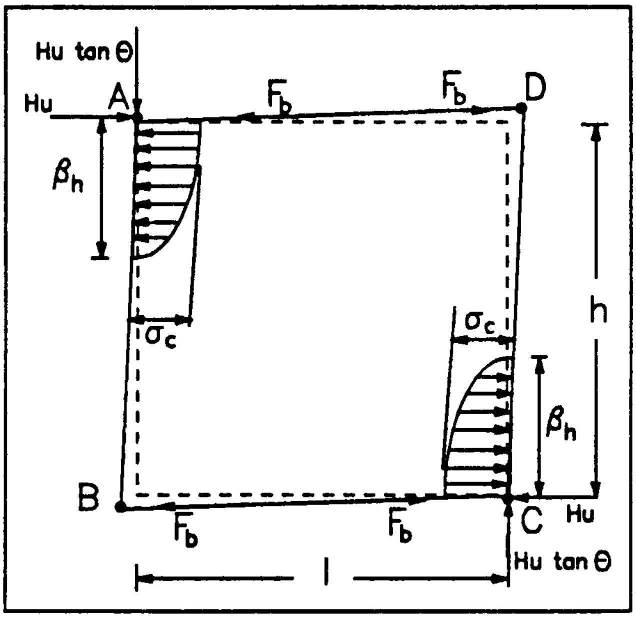

Figure 2.14. Mode (c) diagonal crushing (l>h) (after Liauw and kwan, 1983).

about A for column AB gives Equations 2.35 and 2.36. Taking ß as 1/3 which is accurate enough based on experimental results and eliminating F_b leads to Equation 2.37. In the same manner, Equation 2.38 is for the case when the height is greater than span.

$$H_u = \frac{2}{3}\ \sigma_c\ t\ \beta\ h + 2\ F_b \tag{2.35}$$

$$F_b\ h + (\frac{2}{3}\ \sigma_c\ t\ \beta\ h)\ (\frac{3}{8}\ \beta\ h) = 2\ M_{pj} \tag{2.36}$$

$$\frac{H_u}{\sigma_c\ t\ h} = \frac{4\ M_{pj}}{\sigma_c\ t\ h^2} + \frac{1}{6} \tag{2.37}$$

$$\frac{H_u}{\sigma_c\ t\ h} = \frac{4\ M_{pj}}{\sigma_c\ t\ h^2} + \frac{1}{6\ \tan^2\theta} \tag{2.38}$$

2.3.7 Collapse Shear

The collapse load is the minimum value derived from the collapse mode Equations 2.30, 2.34, and 2.37 or 2.38 depending on the span being greater or smaller than the height, respectively. Liauw and Kwan (1983) do not agree that Wood's penalty factor is mainly to account for the infill lack of plasticity. They believe Wood's theory overestimated the collapse shear because of the excessive friction assumption and neglecting the infill frame separation. Liauw and Kwan (1985) showed the accuracy of their plastic theory against experimental tests on micro-concrete infilled frames and nonlinear finite element analyses. However, applying Wood's (1978) penalty factor on Liauw and Kwan's (1983) plastic theory gave accurate results against tests on concrete masonry infilled frames (Dawe and McBride, 1985).

2.4 Finite Element Modeling

2.4.1 Introduction

Two approaches, macroscopic and local, are used to analyze the infilled frame behavior. Macroscopic techniques, e.g., an equivalent strut method, are more practical to analyze complex structures. Local approaches, e.g., finite element modeling, can more accurately analyze the behavior of infilled frames under a wide variety of conditions. Both approaches are complementary, and local methods are needed to develop more accurate macroscopic methods (Klingner, 1980).

2.4.2 Linear Modeling

Mallick and Severn (1967) were the pioneers in analyzing the behavior of infilled frames using finite element methods. They realized the importance of the frame-infill interface. Their elastic finite element model reflected the fact that there is infill-frame separation and slippage upon loading. They modeled one and multi-story infilled frames using linear plane stress infill elements. The finite element results were in good agreement with experimental tests. The study (Mallick and Severn, 1967) encouraged further effort to use more extensive finite element methods to analyze the infilled frame response.

Other researchers have used linear material properties in conjunction with some sort of interface elements. Liauw (1970) conducted elastic finite element analyses on infilled frames assuming the infill is bonded to the frame. Mallick and Garg (1971) proposed a linear elastic finite element model to examine opening location effects on the infilled frame behavior. Yong (1984) modeled the infilled frame precracking behavior and initial stiffness using linear elastic finite elements with gap elements. Achyutha et al. (1988) conducted a linear finite element analysis. They studied the effects of opening position on the behavior of infilled frames.

2.4.3 Rivero and Walker's Nonlinear Modeling

Rivero and Walker (1982) developed a nonlinear dynamic model to study the elastic and inelastic behavior of infilled frames. The model nonlinearities include the frame-wall discontinuities and interaction, the wall cracking, the wall bracing effect on the frame, and the frame inelastic behavior. The types of finite elements are shown in Figure 2.15.

Gap elements model the interface between the wall and frame and ascertain whether the frame and wall are in contact. Joint elements model the frame wall boundary where they are initially in contact. They allow continuity up to a certain stress level, then

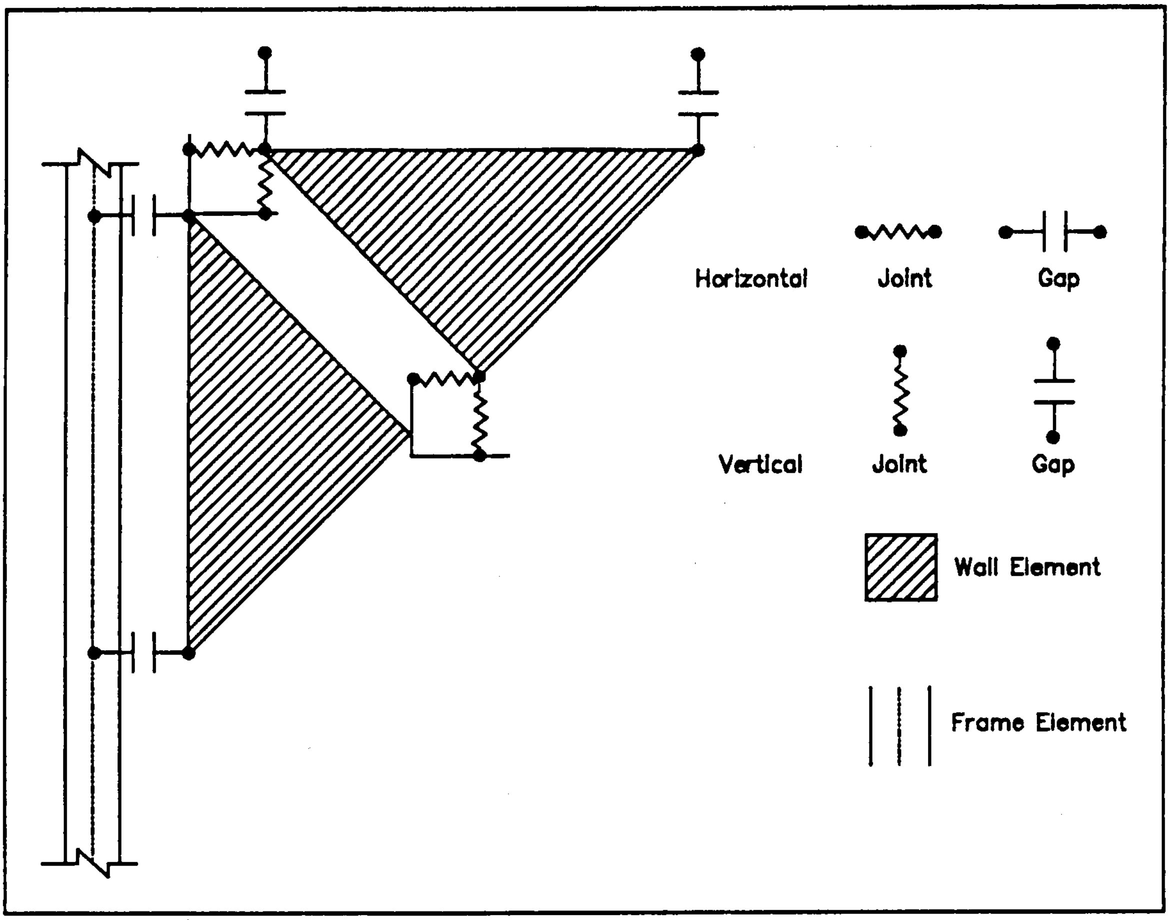

Figure 2.15. Schematic representation of the wall model (after Rivero and Walker, 1982).

they act like the gap elements. Joint elements have the failure surface shown in Figure 2.16. After failure, shear can be transferred through friction under a compression normal stress.

Homogeneous isotropic triangular elements are used to model the uncracked wall. These plane stress elements model several bricks and joints, and have linear elastic behavior up to failure. Joint elements, placed at the edges, model the masonry cracks; it is assumed cracks can only occur at the location of the joint elements. Figure 2.17 shows the assumed failure surface in the principal stresses coordinate system. Since the masonry is not isotropic and homogeneous, the failure surface depends also on the mortar joint

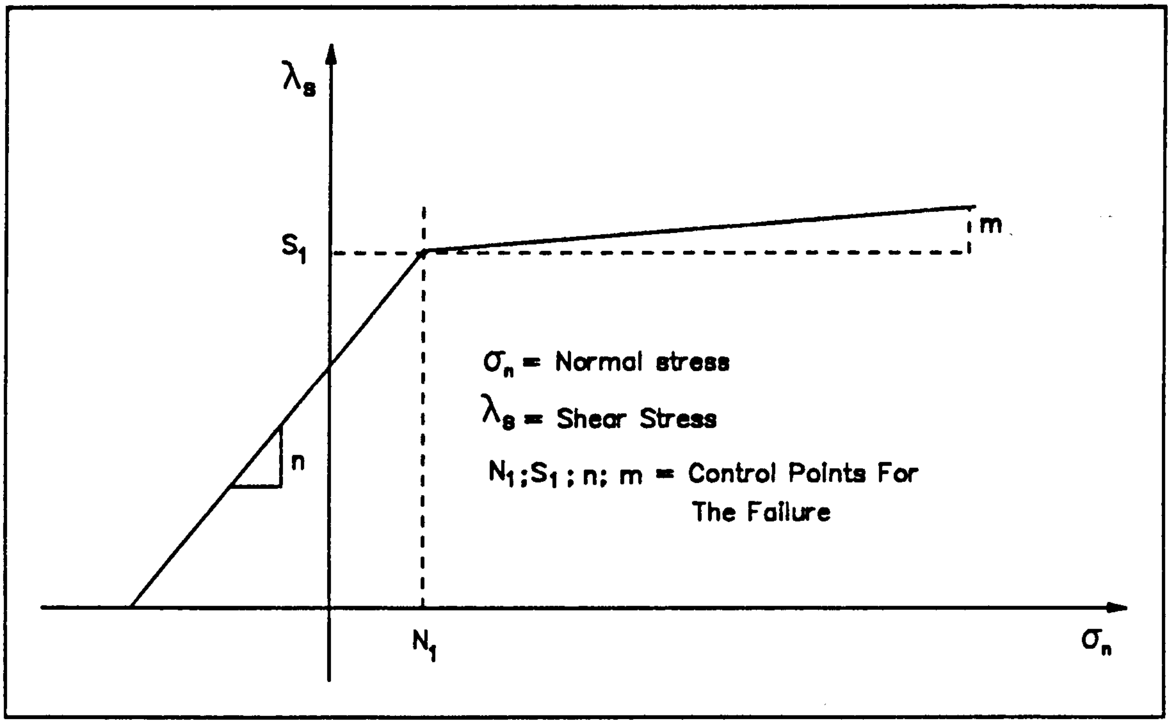

Figure 2.16. Joint element failure surface (after Rivero and Walker, 1982).

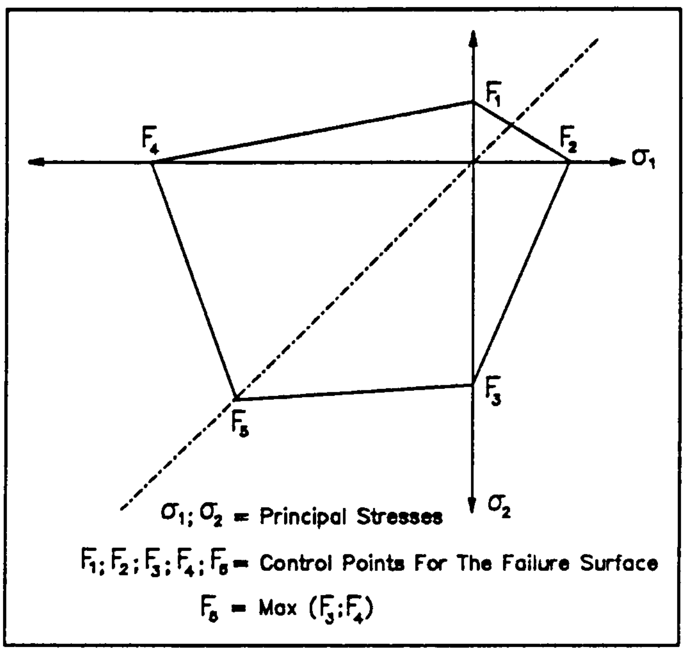

Figure 2.17. Masonry wall failure surface in principal stresses (after Rivero and Walker, 1982).

angle.

The functional shape of the failure surface is assumed invariant and the control points F1, F2, F3, F4, and F5 are functions of the angle to characterize this dependency. Based on experimental results, Figure 2.18 shows the control points F1 and F2 as functions of the angle. Figure 2.19 shows F3 and F4 as functions of the angle. F5 is the maximum of F3 or F4 multiplied by a less than unity constant.

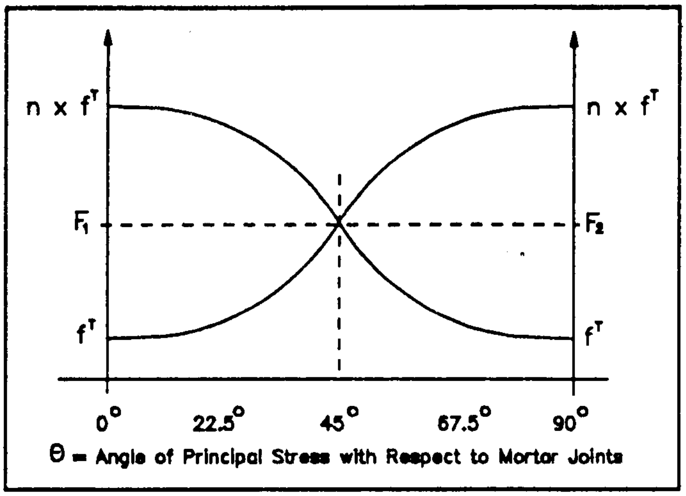

Figure 2.18. Uniaxial tensile strength of masonry verses angle of principal stress with respect to the mortar joints (after Rivero and Walker, 1982).

Line elements represent columns and beams. Plastic hinges can form at the end of these elements to model the inelastic behavior. Any degree of freedom can have a mass. Accelerations applied at the boundary produce dynamic loads. The analysis assumes small displacement, tangent stiffness method, and the nonlinear properties being constant during each time step.

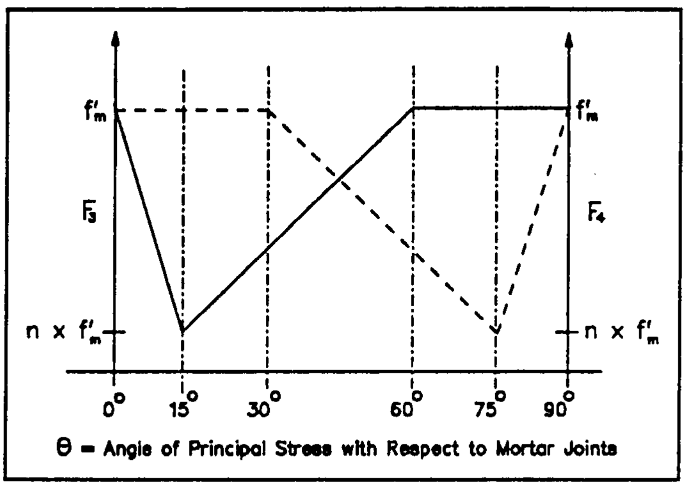

Figure 2.19. Uniaxial compression strength of masonry verses angle of principal stress with respect to the mortar joints (after Rivero and Walker, 1982).

Rivero and Walker (1982) used the finite element model to study the behavior of several one and three story, one-bay infilled frames under a ground motion. They concluded that modeling the discontinuity of the masonry wall and the gap is essential in modeling the infilled frames. The gap size, the infilled frame strength, and the time of the frame maximum response have the most effect on the system behavior. The wall braces the frame once they come in contact at the opposite diagonal corners. The natural period of the bare frame is far greater than that of the infilled frame.

2.4.4 Liauw and Kwan's Nonlinear Modeling

Liauw and Kwan (1982, 1984) presented a nonlinear finite element model. The model took into account the material and frame-infill interface nonlinearities. Anisotropy of the panel was assumed solely due to cracking. In tension, the material was assumed to elastic-brittle. In compression, a nonlinear uniaxial stress-strain curve was used. This model was used to examine the behavior of multistory infilled frames. This included cracking, crushing, and nonlinear infill and frame behavior. Depending on interface conditions, the model examined two cases. When shear connectors were provided, the no frame-infill slippage situation occurred. The friction case was when

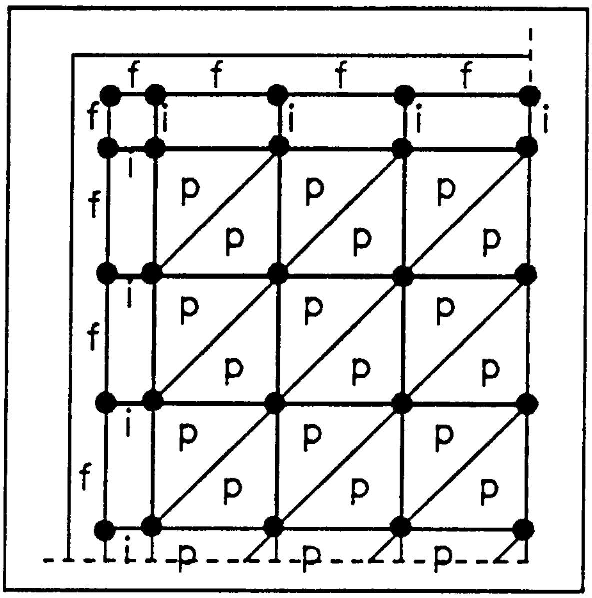

Figure 2.20. The finite elements i, interface, p, panel, and f, frame (after Liaum and Kwan, 1982).

slippage was allowed due to no infill-frame connectors. Figure 2.20 shows the basic model elements. The analytical results agreed with experimental observations.

Liauw and Kwan (1982) concluded that shear connectors improved the infilled frame behavior. The connectors reduced the joint moments and stress concentrations in the loaded corners.

2.4.5 Dhanasekar and Page's Nonlinear Modeling

Based on 180 biaxial tests of half-scale brickwork, Dhanasekar and Page (1986) developed a nonlinear constitutive model and failure surface. The constitutive model consisted of isotropic linear properties (Dhanasekar and Page, 1986) and plastic strains related to orientation of strain with respect to the bed joint (Dhanasekar and Page, 1986). The failure surface consisted of three intersecting elliptical cones in the σ_n, σ_p, τ space, where σ_n is the normal stress normal to the bed joint, σ_p is the normal stress parallel to the bed joint, and τ is the shear stress (Dhanasekar and Page, 1986). This model was used to examine infilled frame behavior (Dhanasekar and Page, 1986).

The finite element model had frame-infill and block-joint one-dimensional interface elements. These elements were to take care of frame-infill separation and shear failure respectively. Square and rectangular frames were used in the study. As the finite element model predicted, the square and rectangular frames had diagonal and corner crushing failure modes respectively. The analytical and experimental ultimate loads were in good agreement. Nonlinear behavior was primarily due to cracking, and not material nonlinearity (Dhanasekar and Page, 1986).

A parametric study (Dhanasekar and Page, 1886) revealed that the infill modulus of elasticity considerably affected the infilled frame characteristics, while Poisson's ratio did not. The infill compressive strength had great effects on the infilled frame ultimate strength if the failure mode was corner crushing. Consequently, increasing the infill compressive strength would change the failure mode to a diagonal failure, Figure 2.21. The infill tensile and shear bond strengths greatly affected the system strength and could change the failure mode. Therefore, proper modeling of the infill characteristics should receive great attention.

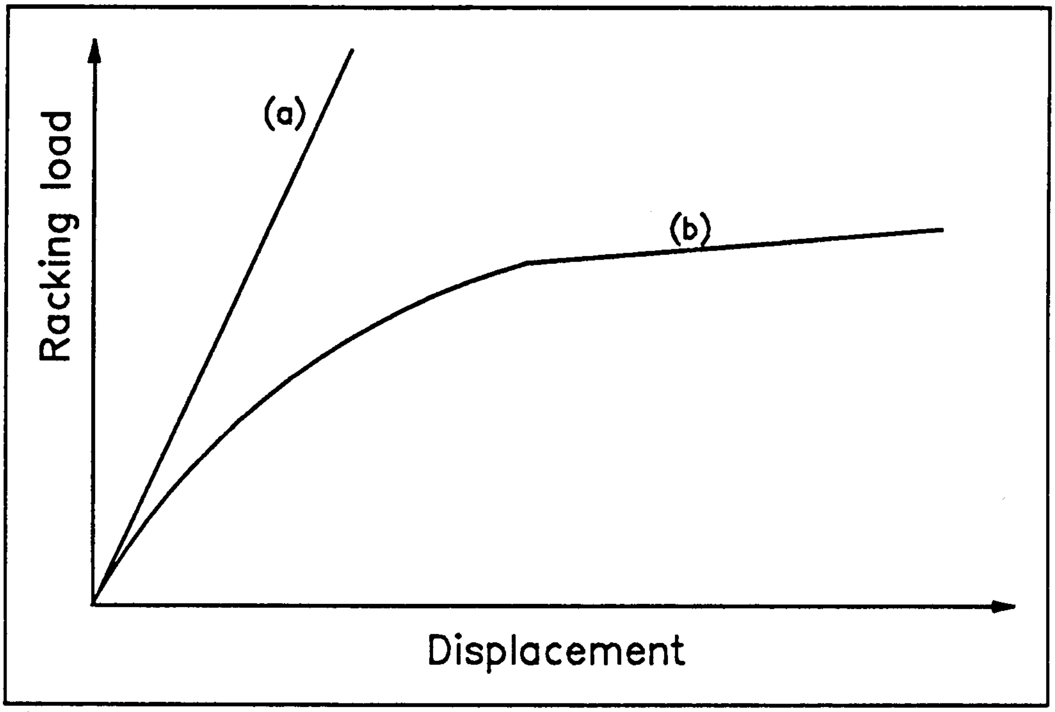

Figure 2.21. Load-displacement curves for infilled frames (a) crushing corner and (b) diagonal failure (after Dhanasekar and Page, 1986).

2.4.6 Initial Gap Effects

Riddington (1984) used a finite element model to investigate the effect of initial gaps on the behavior of infilled frames. The initial gaps are there for some reason, or they may result from shrinkage or poor construction. Riddington (1984) found that even relatively small initial gaps reduce the infilled-frame racking stiffness significantly. However, they do not have a significant effect on the cracking pattern or ultimate strength.

The behavior of infilled frames with initial gaps is divided into five stages, Figure 2.22 (Riddington, 1984). During stage 1, the system acts as a bare frame. Stage 2 starts when the frame contacts the infill. During stage 3, the infill slips and lifts to wedge into the loaded corner. The infill wedges into the opposite corner at the start of stage 4. The infill and the frame then start acting together up to the ultimate load. An infilled frame with no initial gaps goes only through stages 4 and 5.

The study (Riddington, 1984) shows that the finite element model reasonably models the actual infilled frame behavior. Still, the experimental infilled frame stiffness is less than that of the finite element model. The reason for this discrepancy is the crushing of the mortar in the loaded corners. Therefore, Riddington (1984) recommended using high strength mortar in the corners to improve the infilled frame stiffness. He concluded that serious efforts should be made to avoid having initial gaps since they have undesirable effects on the infilled frames stiffness.

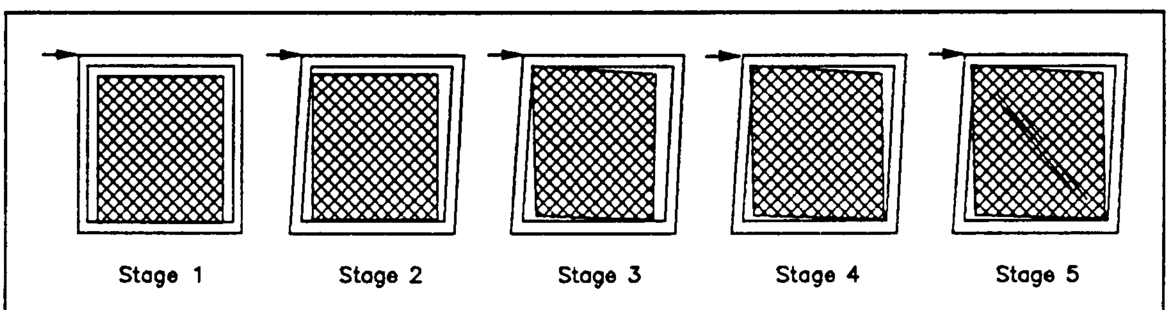

Figure 2.22. Behavior of infilled frames with top and side gaps (after Riddington, 1984).

2.5 Experimental Work

2.5.1 Introduction

An experimental test program investigating the in-plane behavior of infilled frames was carried out by several researchers at University of New Brunswick, Canada. The program consisted of four series, A through D, and was conducted by McBride (1984), Yong (1984), Amos (1985), and Richardson (1986) respectively. The researchers examined the effect of frames and infill characteristic on the infilled frame behavior. These included frame-infill interface conditions, column to infill ties, initial gaps, frame connection types, infill openings, reinforced bond beams, and loading conditions. The researchers examined the effect of these characteristics on the stiffness and strength of infilled frames.

The experimental tests consisted of 34 large-scale infilled frames. Each specimen

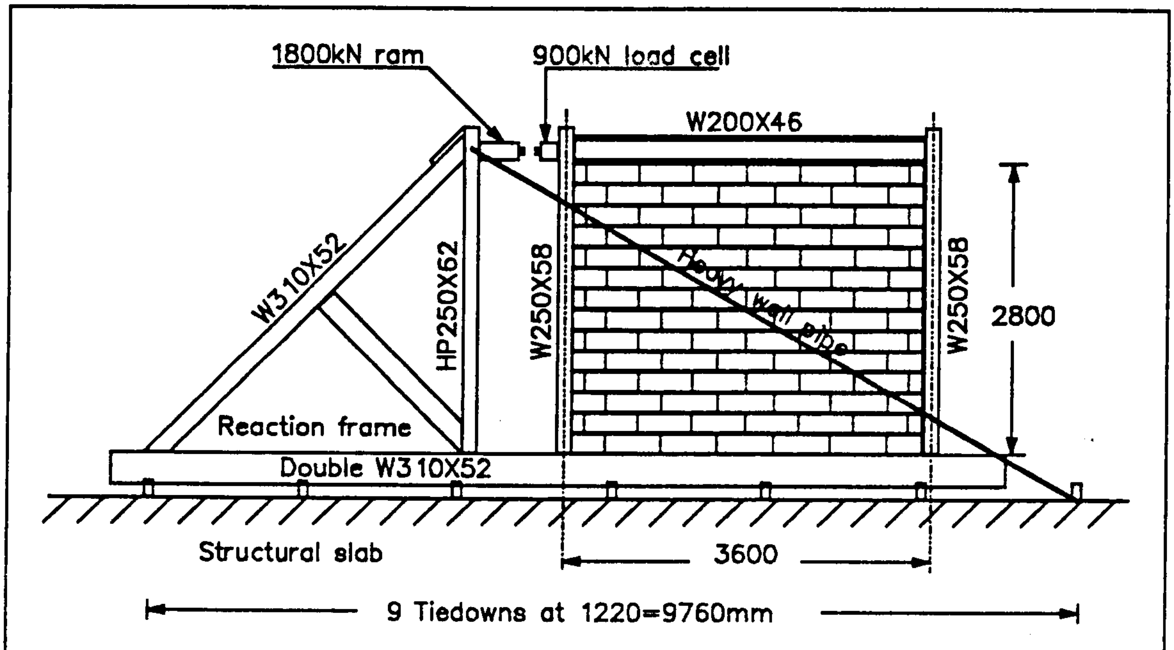

Figure 2.23. Test apparatus, side view (after McBride, 1984).

was a single-bay one-story full-scale concrete masonry infilled steel frame. All panels were 3600 mm long and 2800 mm high and constructed using 200 X 200 X 400 mm blocks. Steel frames were W250 X 58 columns and W200 X 46 top beams with rigid or pinned connections, Figure 2.23. Racking loads were applied in-plane at the roof-beam center. Columns were oriented in their weak direction, resisting the in-plane loads, while beams were oriented in their strong directions.

2.5.2 McBride's Tests

Mcbride (1984) initiated the test program with the first six tests. These test specimens, WA1 through WA6, were to evaluate the effect of bond beams, column panel ties, and joint reinforcement on the infilled frame behavior.

All panels were mortared snugly between column flanges. Except for WA4, all had horizontal joint reinforcement. In addition, WA5 had a column-panel tie system. The top and bottom of each tie were welded to the column. The tie bottom and top free portions were bent into the second cell which was fully grouted. WA6 had two bond beams, at one- and two-thirds of the panel height.

The test results (McBride, 1984) revealed that bond beams did not increase the ultimate load substantially, however, they increased the first major crack load to that of the ultimate; they also stiffened the system considerably. Joint reinforcement stiffened the system and decreased the number and severity of joint cracks, but did not notably affect the ultimate load. The tie system increased the stiffness and the first crack load considerably, yet did not significantly affect the ultimate load.

2.5.3 Yong's Tests

Yong (1984) tested six specimens with five different panel types. His objective was to study the effect of boundary conditions and initial gaps on infilled frame behavior. All panels had horizontal joint reinforcement and type S mortar between the column-web and panel. The steel frames had semi-rigid connections at the top and full-moment connections at the bottom.

All specimens had mortar packed between column-web and blocks. However, WB1 had additional mortar packed between column flanges and blocks. WB2 and WB3 specimens were standard. A 20 mm initial gap between the top beam and panel was the only difference between WB4 and standard specimens. WB5 and WB6 were identical to standard specimens but with column-panel flat-bar ties and a column-tie system respectively.

Yong (1984) concluded that initial gaps and boundary conditions affected the infilled frame behavior significantly. The infilled frame maximum strength was achieved when infills were untied and mortared only to the column webs. The reason for this was the infill ability, in this case, to rotate and to assume a better diagonal strut position. Tests also showed that frame-panel ties did not increase infilled frame stiffness nor strength. The roof beam panel initial gap reduced the strength considerably, about 60%. Ties did not improve the strength or stiffness for this case. The effect of mortar packed between column flanges and infill had the same effect as shear connectors.

2.5.4 Amos's Tests

Amos (1985) examined ten full scale infilled frames, WC1 through WC10. He investigated the effect of mortar quality, joint reinforcement, openings, frame-block bond, and frame-panel friction on the infilled frame behavior.

All panels had horizontal joint reinforcement except WC7. All walls were constructed using good quality type S mortar except WC2 which was built with poor sandy mortar. Mortar was packed between all panel webs and blocks, but not in between column flanges and blocks. WC1 and WC2 had 6 mil polyethylene between frames and blocks to eliminate steel-panel friction. WC3 and WC4 had a 0.8 m wide by 2.2 m high center opening. WC5 and WC6 had door openings offset 0.6 m from center toward and away from the loaded column respectively. Different loading conditions were applied on WC8 through WC10 which were standard; they had joint reinforcement, no openings, and no polyethylene.

The experimental tests (Amos, 1985) revealed that poor mortar or lubricant material, polyethylene, may reduce first crack and ultimate loads notably. Openings reduced first crack loads substantially and ultimate loads considerably. Offset openings toward the loaded corner reduced the strength more than that of central openings. Offset openings away from loaded column did not reduce the strength as much as central openings did. The tests also showed that cyclic loading decreased infilled frame strength and stiffness considerably. The strength and stiffness reduction was more intense with higher cycle loading magnitude. Amos's (1985) results agreed with McBride's (1984) in that joint reinforcement decreased the number and severity of joint cracks, but did not affect the ultimate load significantly.

2.5.5 Richardson's Tests

Richardson (1986) tested twelve specimens, WD1 through WD12. He studied the effect of several factors on the in-plane infilled-frame behavior. These include frame connection types, infill bond types, panel openings, reinforcements, initial gaps, and loading conditions.

To examine the effect of different types of beam-columns connections, WD1 through WD7 were rigid while the rest were pinned. WD1 and WD2 were standard panels having running bond infill. WD3 and WD4 had stack bond infill. WD5 had a 0.8 m wide by 2.2 m high center door opening with reinforcements in the sides and top. WD6 had reinforcements in the compression diagonal while WD7 and WD8 were standard panels. To study the effect of the lack of fit, the pin hole slack was removed during curing from WD9 through WD12; then uplift was applied to the top beam. WD11 had a 20mm gap between the infill and the top beam while WD12 had an opening as WD5 but without reinforcements in the sides.

Loading procedures were also varied; WD1 through WD4 were loaded with 250 pre-crack cycles before being loaded to failure in 22.2kN load increments. Using the same load increments, WD5 and WD6 were loaded up to the maximum in two directions while WD7 was loaded in one direction only. WD9 through WD12 were loaded monotonically up to the maximum loading in both directions.

The tests (Richardson, 1986) revealed the following conclusions. Under many low or few high magnitude load cycles, infilled frames gradually lose their strength and stiffness to those of the bare frame. Stack bonding does not reduce the ultimate strength, but it increases the first crack load so that it becomes very close to the ultimate load. Reinforcing the sides of an opening increases the strength slightly. Diagonal compression reinforcements do not increase the stiffness as much as horizontal reinforcements do. Yet both reduce the amount of cracking considerably. The infill generally fails by having severe diagonal tension cracks which in turn cause the confining frame to fail at the intersection points with the cracks. Infilled frames are much more ductile than the infill by itself. Beam-column connections have a great effect on the stiffness and the strength of the infilled frame. Therefore, to avoid severe strength reduction when pinned connections are used, serious effort should be made to avoid other bad circumstances. These include lack of fit in the connections, initial gaps, and large openings.

2.5.6 Further Investigations

Pook and Dawe (1986) examined the results of sixteen specimens from the experimental test program. Their analysis revealed that gaps and lack of frame-panel bond reduced the infilled frame stiffness and strength. They also showed that column panel tie system did not improve the system strength considerably. Increasing the surrounding frame connection rigidity increased the infilled frame strength.

More investigation of the program results were done by Dawe and Seah (1989). Their examination of twenty-eight specimens confirmed the important effect of gaps and interface conditions on the system performance. They confirmed that the tie system marginally affects the system strength. Bond beams had only a limited effect on the infilled frame ultimate strength.

CHAPTER 3

A FINITE ELEMENT MODEL

3.1 Introduction

The numerical analysis for in-plane behavior of infilled frames has two phases. The first is to build a finite element model capable of evaluating the behavior of infilled frames. The second is to use this finite element model, in lieu of actual specimens, to conduct an extensive parametric study.

ABAQUS, a general purpose finite element program, is used to develop the model. The model is checked, whenever applicable, against STRUDL, the deflection formula for a rectangular cantilever beam, plastic collapse theories (Liauw and Kwan, 1983), and experimental results (Richardson, 1986). These examinations test the model and add more refinements to it making it more closely follow the infilled frame behavior.

3.2 Finite Element Model Components

The proposed model has the appropriate finite elements to model the steel frame, the infilled tile wall, and the interface. The interface elements are to account for the debonding and gapping at the tile-steel interface.

Several infilled frames are modeled to test the finite element model. These include an infilled frame from the Y-12 plant in Oak Ridge, TN and the WD experimental series at The University of New Brunswick (Richardson, 1986).

The Oak Ridge infilled frame is constructed from a steel frame that confines a 12" hollow clay tile wall, Figures 3.1 and 3.2. The Young's modulus is taken to be 30,000 ksi and 1,500 ksi for the steel and clay tile respectively. Poisson's ratio for the clay tile is assumed to be 0.10 and 0.30 for the steel frame. Two extreme cases of frame connections, rigid and pinned, are studied.

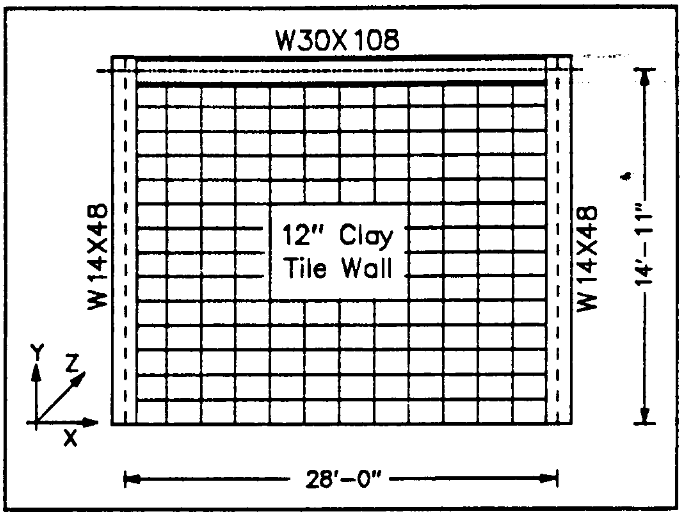

Figure 3.1. A panel from Y-12 plant in Oak Ridge.

All the WD panels (Richardson, 1986) have the same general dimensions, Figure 3.3. They were constructed using identical confining steel frames and 15.75 X 7.87 X 7.87 in (400 X 200 X 200 mm) standard blocks, Figure 3.4. The steel has a Young's modulus of 30,170 ksi (208,000 MPa). Young's modulus and Poisson's ratios for WD masonry infills vary as shown in Table 3.1.

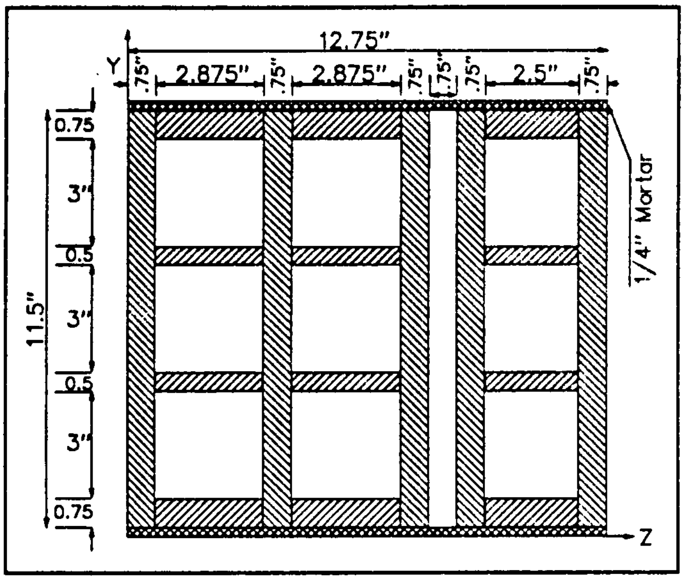

Figure 3.2. A section through YZ plane.

Table 3.1. Young's Modulus and Poisson's Ratio for WD specimens.

Specimen	Young's Modulus (ksi)	Poisson's Ratio
WD1	1459	0.06
WD2	1885	0.15
WD3	1885	0.09
WD4	1160	0.06
WD5	2756	0.13
WD6	2509	0.08
WD7	2611	0.06
WD8	2567	0.11
WD9	2872	0.12
WD10	2466	0.04
WD11	1798	0.04
WD12	2248	0.06

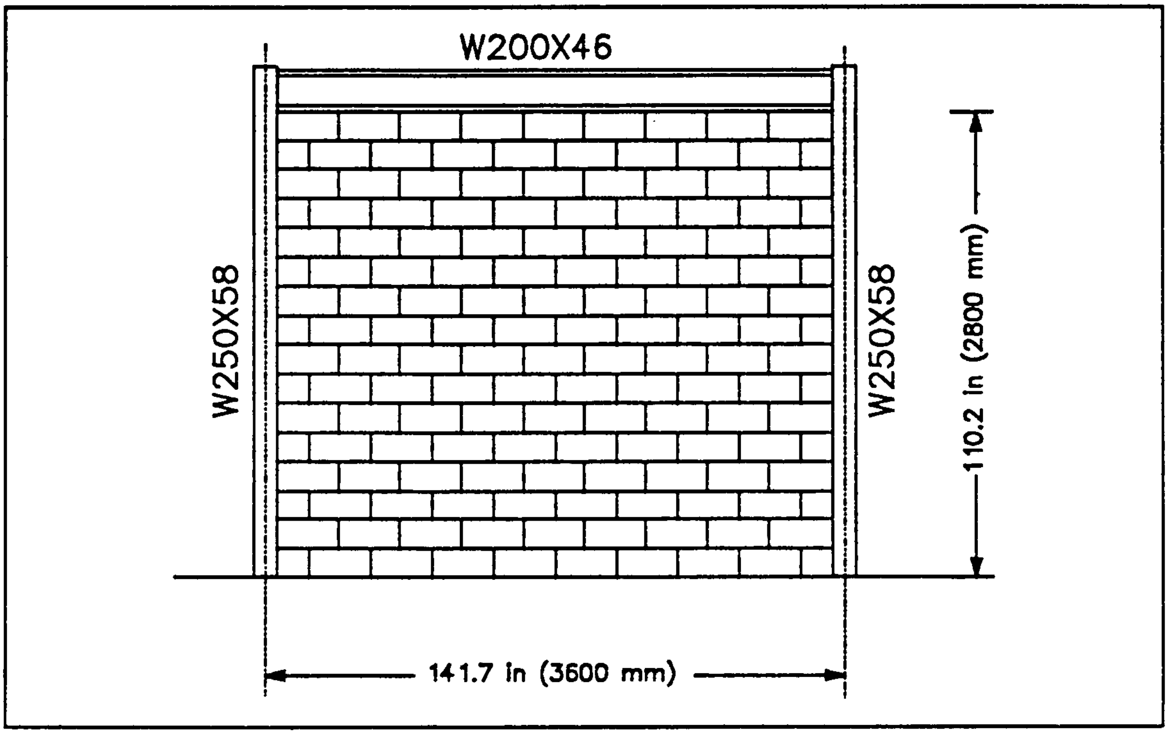

Figure 3.3. WD specimens (after Richardson, 1986).

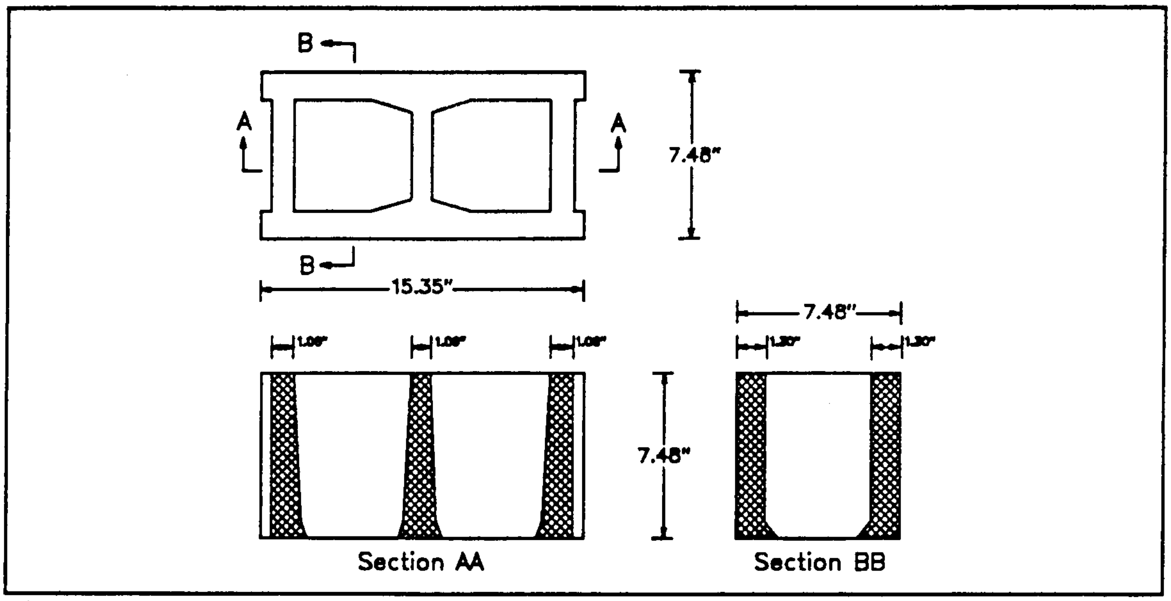

Figure 3.4. WD standard blocks (after Richardson, 1986).

3.2.1 Steel Frame

Several elements can model the in-plane behavior of steel frames. These include beam and solid elements. To investigate which element type is more suitable and practical to model steel frames, two models are built to model the same steel frame (Oak Ridge) using beam and solid elements respectively. ABAQUS in-plane beam-type elements, B21, are 2 noded, linear interpolation elements with three degrees of freedom at each node. ABAQUS plane stress solid elements, CPS4, are 4 noded bilinear interpolation elements with two degrees of freedom at each node. Beam elements can have the same area and moment of inertia of the frame components they represent. Solid elements have the same moments of inertia as the beam sections they represent by keeping the same section width and choosing an appropriate thickness. Beam elements can have hinged and rigid connections. Hinged connections can be simulated with solid elements by assuming very low values for Young's modulus for the elements where hinges exist. Another way to simulate a hinge when a single row of solid elements is used is to connect the elements to each other only at one node and leave the other unconnected.

Using ABAQUS, a finite element model was built for the Oak Ridge steel frame using beam elements. Assuming the two top corners are hinged connections, the model was run twice with a different number of elements each time. STRUDL is used to check the results, and Table 3.2 shows good agreement between the results. Table 3.3 shows the results for the rigid connection case.

Richardson (1986) gives experimental data on frame WD1 to check against the finite element model. The WD1 ABAQUS model consisting of 64 B21 beam elements requires a 13.82 kips (61.5 kN) horizontal force at the top to produce a 0.787 in (20 mm)

Table 3.2. ABAQUS versus STRUDL for the Oak Ridge steel frame (hinged connections).

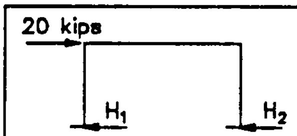		H_1 (kips)	H_2(kips)	Top Disp. (Inches)
ABAQUS	27 Elements	10.0130	9.9870	12.4000
	70 Elements	10.0130	9.9870	12.4000
STRUDL	27 Elements	10.0132	9.9868	12.3998

Table 3.3. ABAQUS versus STRUDL for the Oak Ridge steel frame (rigid connections).

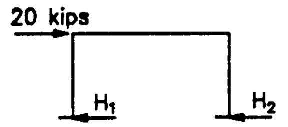		H_1 (kips)	H_2(kips)	Top Disp. (Inches)
ABAQUS	70 Elements	10.006	9.9940	3.141
STRUDL	27 Elements	10.005	9.9945	3.136

horizontal displacement at the top. STRUDL gives a comparable 0.783 in (19.90 mm) displacement under the same horizontal load. The experimental load which causes a 0.787 in (20 mm) displacement at the top is 20.68 kips (92 kN).

Solid elements, CPS4, are also used to model the WD1 steel frame. This ABAQUS model requires a 23 kip (102.3 kN) horizontal force get a 0.787 in (20 mm) horizontal displacement at the top if the corner elements have the same thickness as the top beam elements, or 20.9 kips (93.0 kN) if the corner elements are the same as the column elements. The latter choice gives good agreement with the experimental results. This result implies that solid elements are more suitable to model the WD1 steel frame. However, further study defies that conclusion; the solid element solution approaches the beam element solution as the solid elements increase in number, Figure 3.5 and Table 3.4.

A possible reason for the discrepancy between the experimental and analytical solution is the rigidity of the actual beam-column connections. The heavy connections

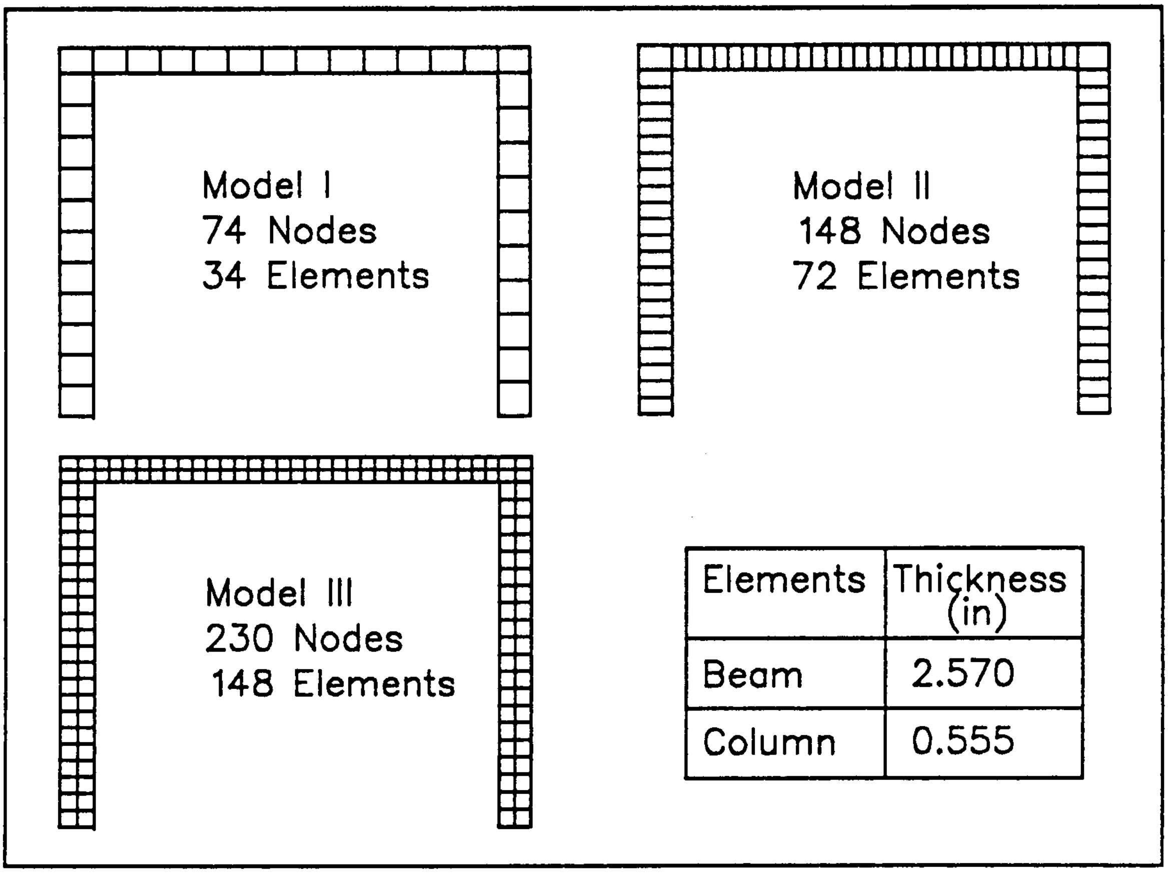

Figure 3.5. Solid element models with different element sizes.

Table 3.4. The effects of using different solid element sizes on the model behavior.

F 0.787in	Corner-elements thickness (in)	F required to produce a 0.787 in dis. (kips)		
		Model I	Model II	Model III
*Notes: STRUDL F is 13.89 kips Experimental F is 20.66 kips	0.555	20.90	16.16	15.06
	2.570	23.00	17.49	16.42
	5.910	23.46	17.78	16.74
	59.10	23.85	18.00	17.02

may make the portion near the corners stiffer than the members themselves. Increasing the moment of inertia by 300% over 10% of the member length at each end results in a 0.795 in (20.19 mm) deflection under a 20.66 kips (91.9 kN) load, Figure 3.6.

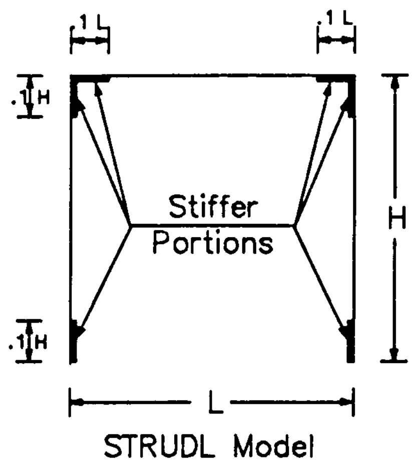

$I_{Stiffer\ Portions}$ / I_{Member}	Displacements Under 20.66 kips (in)
100 %	1.171
110 %	1.120
125 %	1.058
150 %	0.983
300 %	0.795
Experimental Displacement is 0.787 in	

Figure 3.6. The effect of stiffer portions due to the heavy connections on the displacements.

3.2.2 Infilled Wall

The solid elements, CPS4, are used to model the infilled wall. The Oak Ridge infilled wall is modeled using 600 (11.2" X 8.95") solid elements, Figure 3.7. A distributed force is applied along the top totaling 93 kips. The average horizontal top displacement was 0.0339 in. The deflection formula for a rectangular cantilever beam including shear deformations gives a displacement of 0.0332 in. The problem was also run using a Poisson's ratio of 0.25 instead of 0.1. The resultant displacement was 0.0366 in, as compared to 0.0364 in, given by the deflection formula.

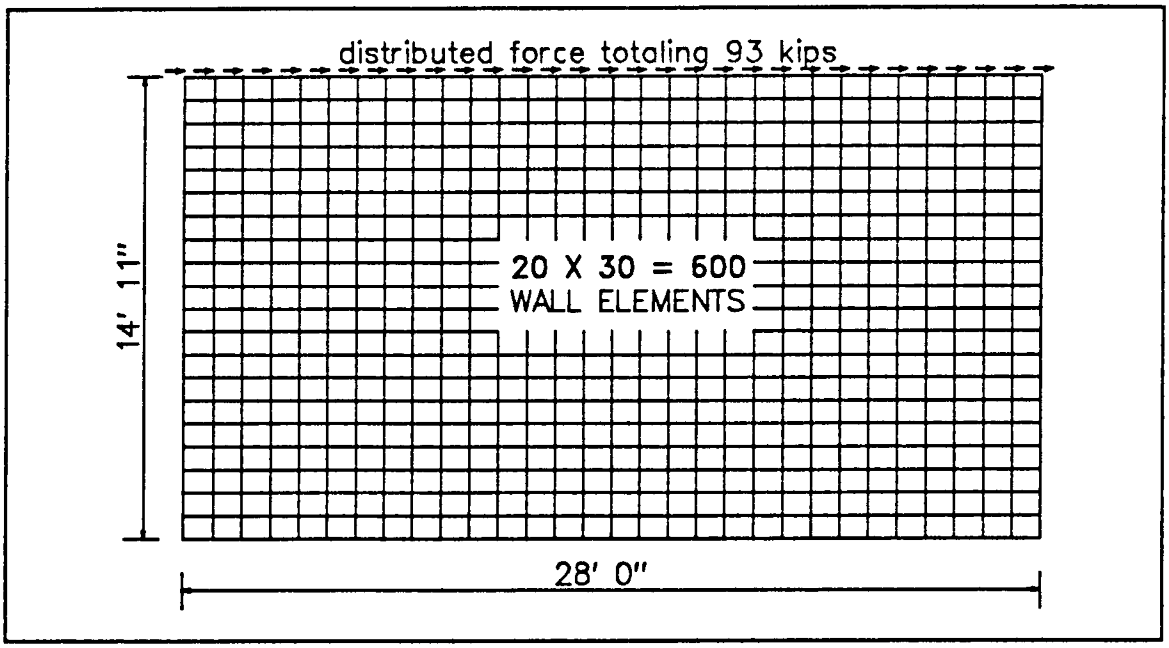

Figure 3.7. Wall elements for the Y-12 panel.

3.2.3 Steel-Infill Interface

Since the interface between the frame and the wall may have little or no strength, and there can be an initial gap or different friction factors between the frame and the wall, special contact elements are needed. These elements should be capable of transferring the compression and the shear forces from the frame to the wall or vice versa. Using interface elements or having different frame-wall connections will make a major difference in the behavior.

ABAQUS has "Gap" elements which are appropriate for the problem. The gap elements can be in one of two states, opened or closed, and only in the latter state can they transfer shear force through friction.

Another type of element available is "Interface" elements. These elements have the friction option, as gap elements do; in addition, they can handle modified pressure-clearance behavior which is useful to describe the localized corner mortar crushing effects. Both types of elements are examined in the model to find the advantages and disadvantages of each type.

3.3 Finite Element Model Behavior

Assuming linear properties for the frame and infill results in linear behavior. This model provides the infilled-frame elastic characteristics such as initial stiffness. The nonlinear behavior is achieved using nonlinear material properties for the model. These include secant stiffness and ultimate strength. The nonlinear model describes the infilled frame degrading behavior due to the infill cracking and deformation.

3.3.1 Elastic Behavior

A linear finite element model is built for the Oak Ridge infilled panel, Figure 3.1. The model has 600 solid elements to model the infill, 21 and 30 beam-type elements to model each column and the top-beam respectively, and 68 Gap elements to model the infill-steel interface, Figure 3.8.

Figure 3.9 shows the behavior of the steel frame, wall, and infilled frame model for the hinged frame connection case. Figure 3.10 is for the rigid frame connection case. The steel frame rigidity increases from 1.61 k/in to 6.37 k/in, about 400%, when rigid connections are used instead of pinned. The infilled frame rigidity increases from 827 k/in to 1021 k/in in going from pinned to rigid frame connections, only about 125%.

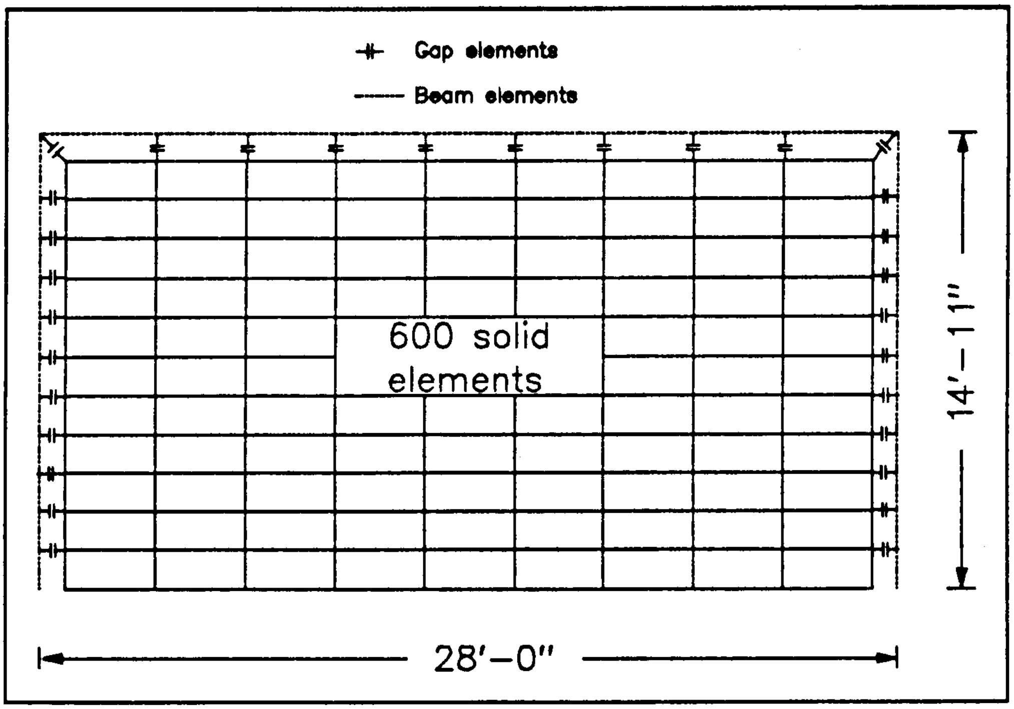

Figure 3.8. Finite element model for the Oak Ridge frame.

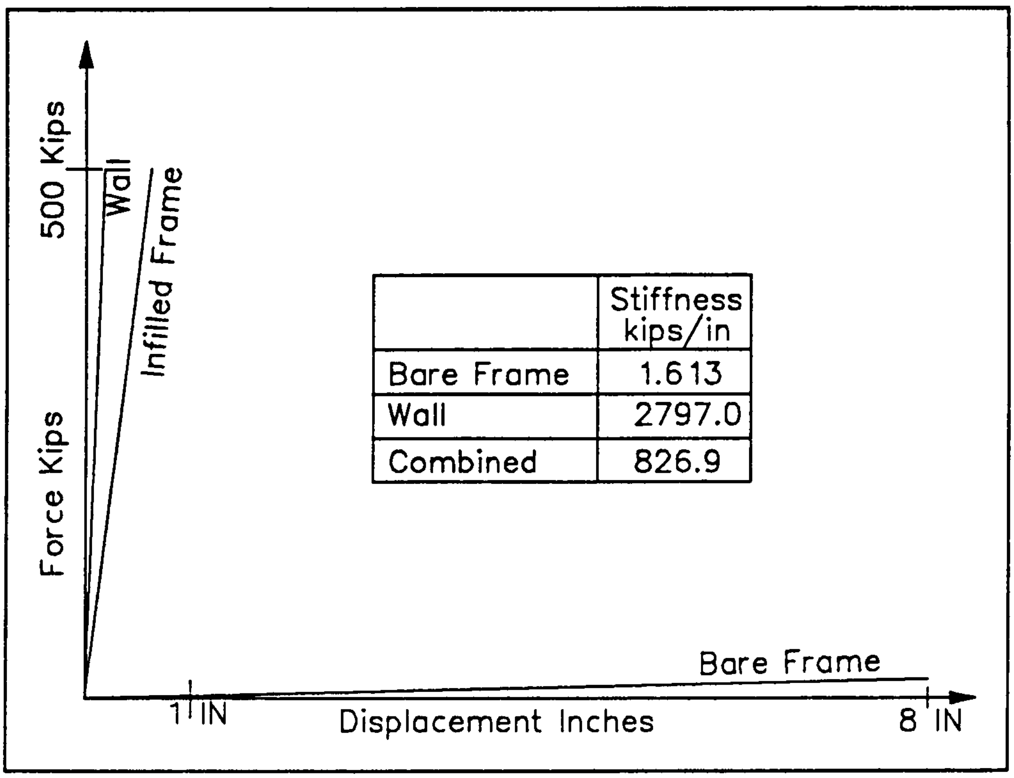

Figure 3.9. Horizontal load versus horizontal displacement for the hinge connected frame.

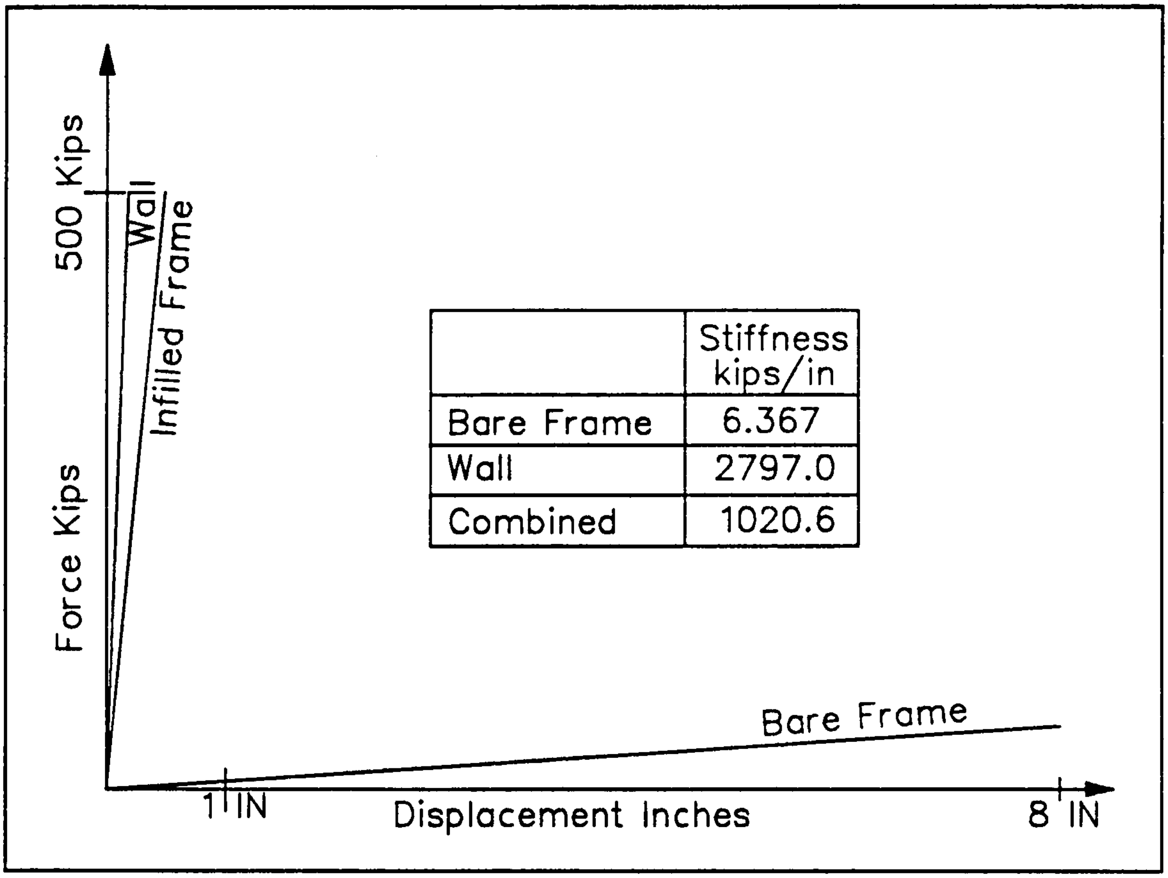

Figure 3.10. Horizontal load versus horizontal displacement for the rigid connected frame.

Linear models are also built for the WD specimens. Table 3.5 shows the initial stiffness from the ABAQUS models, experimental tests, and analytical methods. The first four methods are based on equivalent strut formulations. Method 1 uses Equation 2.1 (Stafford-Smith and Carter, 1969); method 2 uses Equation 2.4 (Klingner, 1980); method 3 uses Equations 2.5 and 2.7 (Chrysostomou et al., 1988); method 4 uses Equation 2.8 (Liauw and Kwan, 1984). Method 5 calculates the stiffness directly and uses Equation 2.3 (Barua and Mallick, 1977). These analytical methods do not apply to WD5 which has a central door opening.

Table 3.5 shows that ABAQUS results are comparable to the experimental data and to other analytical methods. Methods 2 and 3 result in lower stiffnesses. This suggests that these methods are for the stiffness at a higher level of loading, where stiffness is degrading.

When a finite element model is built for WD7 without using interface elements, that is the steel and infill are fully integrated, the initial stiffness is 1453 k/in (254 kN/mm). That is about twice the experimental result and shows the vital role of interface elements.

Table 3.5. Initial stiffness at 5 kips load for WD panels.

	Initial stiffness at a 5 k horizontal load (k/in)						
Specimens	WD1	WD2	WD3	WD4	WD5	WD6	WD7
Test	314	360	628	417	314	634	702
ABAQUS	349	415	412	299	129	490	500
Method 1	382	456	456	326	-	553	567
Method 2	199	248	248	163	-	316	327
Method 3	150	188	188	122	-	242	251
Method 4	385	472	472	319	-	591	609
Method 5	319	399	399	261	-	513	531

3.3.2 Nonlinear Behavior

3.3.2.1 Introduction

The nonlinear model uses plastic and elastic material properties for the steel frame and infill. The model uses an elastic-plastic material model for the steel frame. The

ABAQUS concrete model is used to define the masonry properties beyond the elastic range. A softened interface model is used for the wall-frame boundary. This accounts for the localized mortar crushing that tends to occur at the corners of infilled frames.

3.3.2.2 Concrete Model

The ABAQUS concrete option describes the infill behavior beyond the elastic range. This option defines the uniaxial compressive stress and plastic strain relationship. As many points as necessary can be used to define the uniaxial stress-strain curve. Figure 3.11 shows the simplified proposed stress-strain curve that was used. The figure also shows Atkinson and Yan's (1990) proposed stress-strain curve for ungrouted masonry. Infilled frames were analyzed with both stress-strain curves and the resultant load-displacement curves are identical with either stress-strain curve. Therefore, the simplified stress-strain curve is adopted.

Three sub-options may follow the concrete option. These include failure ratios, shear retention, and tension stiffening.

Failure ratios define the shape of the failure surface. Figure 3.12 shows the ABAQUS failure surface in the principal stress plane, σ_1 and σ_2. The failure ratios are proposed as the following:

Ratio of biaxial to uniaxial compression yield stress:	1.16
Ratio of biaxial to uniaxial compression failure stress:	1.16
Ratio of uniaxial tensile to compressive failure stress:	0.05

These proposed values give comparable results to experimental test results.

The tension stiffening sub-option defines the relationship between the retained

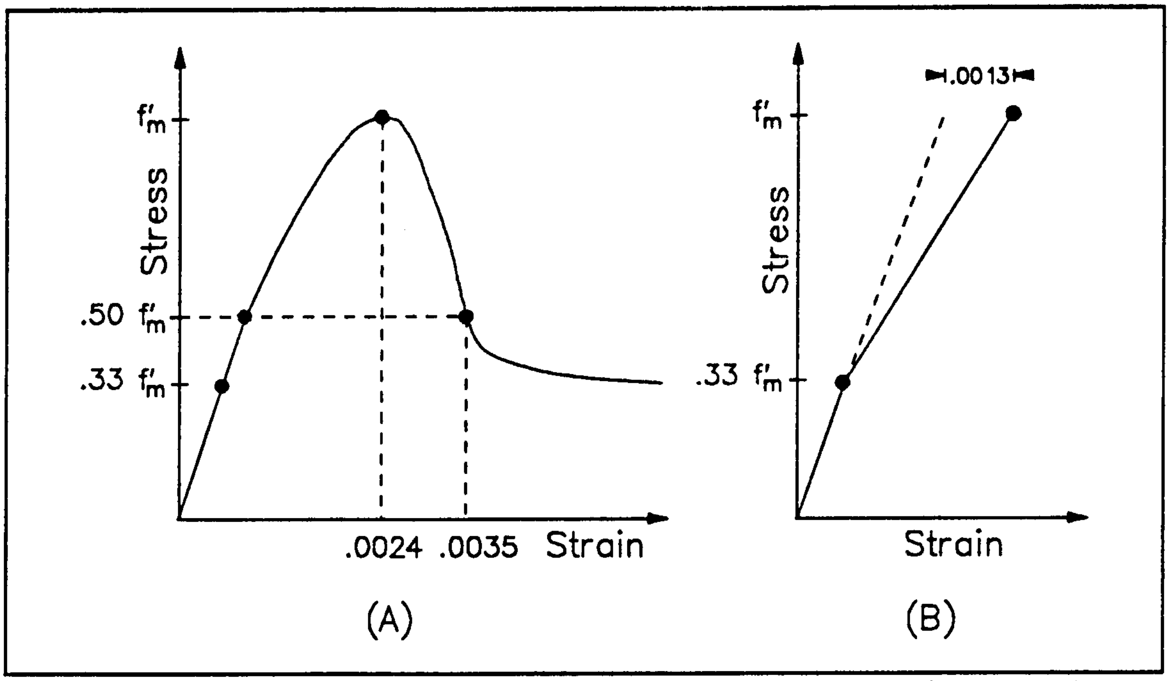

Figure 3.11. Stress-strain curves for masonry; (A) Atkinson and Yan's proposed curve (1990); (B) ABAQUS simplified curve.

tensile stress normal to a crack and the strain in the same direction. For this option, the remaining stress, and the absolute value of the direct strain minus the direct strain at cracking are assumed zero and 0.0005 respectively.

The shear retention sub-option defines the shear-stiffness and the tensile-strain relationship across a crack. This option is omitted because the necessary parameters for this option are not available, e.g., the maximum strain for dry and wet concrete. Assigning the default values is identical with omitting the option (ABAQUS manual).

3.3.2.3 Nonlinear model

Figure 3.13 shows the ABAQUS finite element model for WD1 infilled frame. This model uses gap elements to model the steel-tile interface. It also uses CPS4, solid elements, to model the steel frame. The steel yield stress is taken to be 31.9 ksi (220

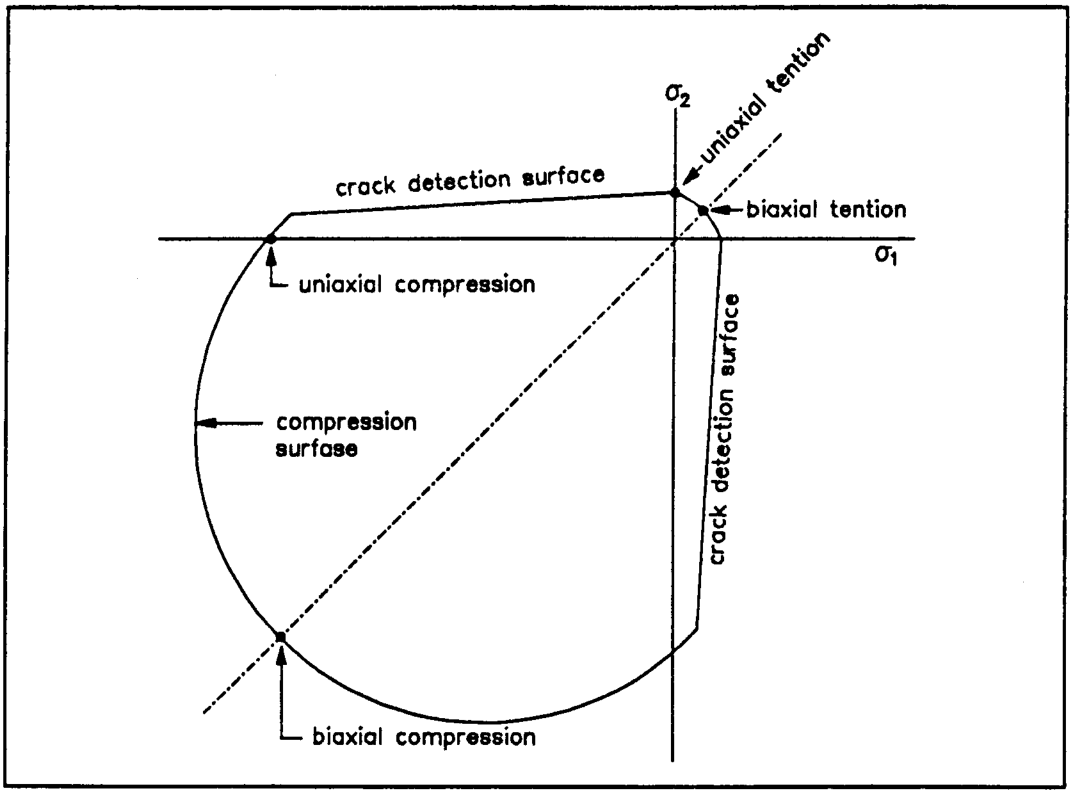

Figure 3.12. The ABAQUS concrete failure surfaces in plane stress.

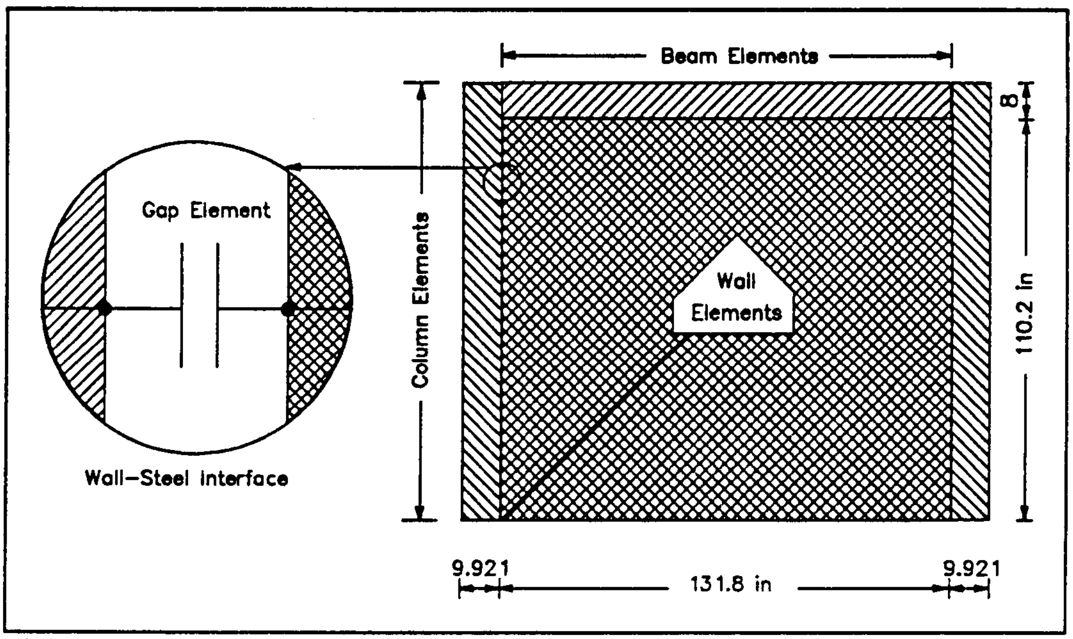

Figure 3.13. WD1 finite element model.

MPa). The steel frame loaded corner is kept elastic to avoid local yielding under the concentrated load. Table 3.6 shows the average compressive strength of the infills (Richardson, 1986). The infill yield compressive stress is taken to be one third of the compressive strength (Atkinson and Yan, 1990).

Table 3.6. Compressive strength for WD specimens.

Specimen	WD1	WD2	WD3	WD4	WD5	WD6	WD7
Compressive Strength (ksi)	3.76	3.60	3.35	3.28	4.26	3.81	3.68

Figure 3.14 shows the resultant load-deflection curves for WD1 using the ABAQUS model as well as the experimental curve. As a first approximation, these results are reasonable.

3.3.2.4 Softened Interface

Inter1 elements are two node interface elements. These elements provide the basic characteristic of gap elements, but also may provide softened pressure-clearance behavior. This behavior can be used to describe the localized mortar crushing that often occurs at the infilled frame corners. Inter1 elements, when used without the softened option, give identical results to gap elements. Figure 3.15 shows the default and softened pressure relationship. The softened behavior option does not affect the ultimate strength, but it does affect the infilled frame stiffness. Table 3.7 shows the resultant secant stiffness, at 45. kips (200 kN), for the ABAQUS model with and without the softened option and the

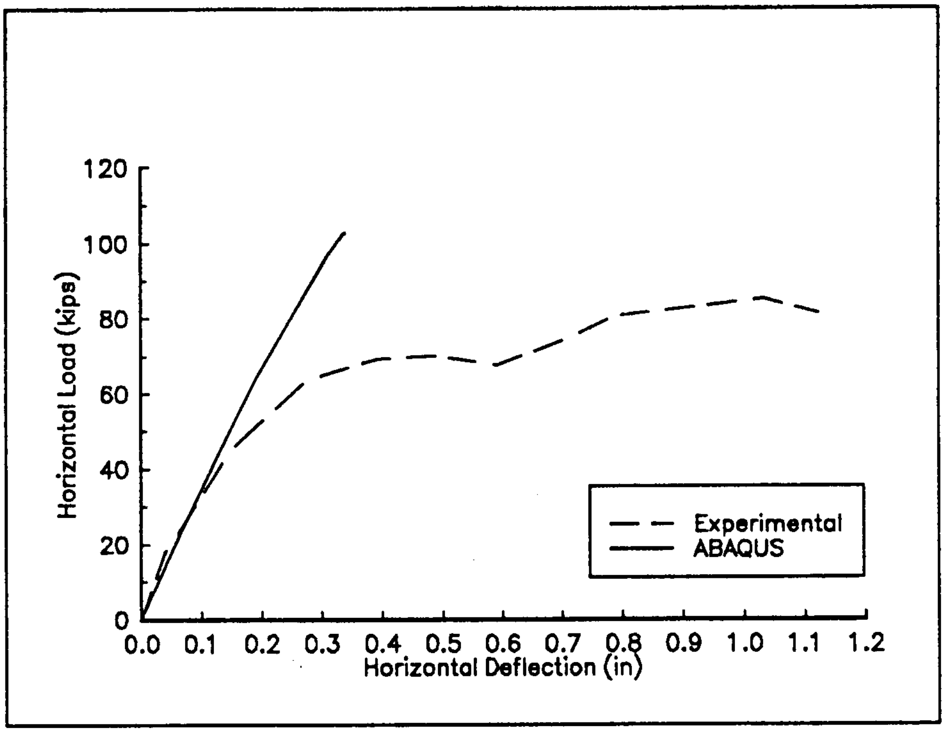

Figure 3.14. ABAQUS and experimental test load-deflection curves for WD1.

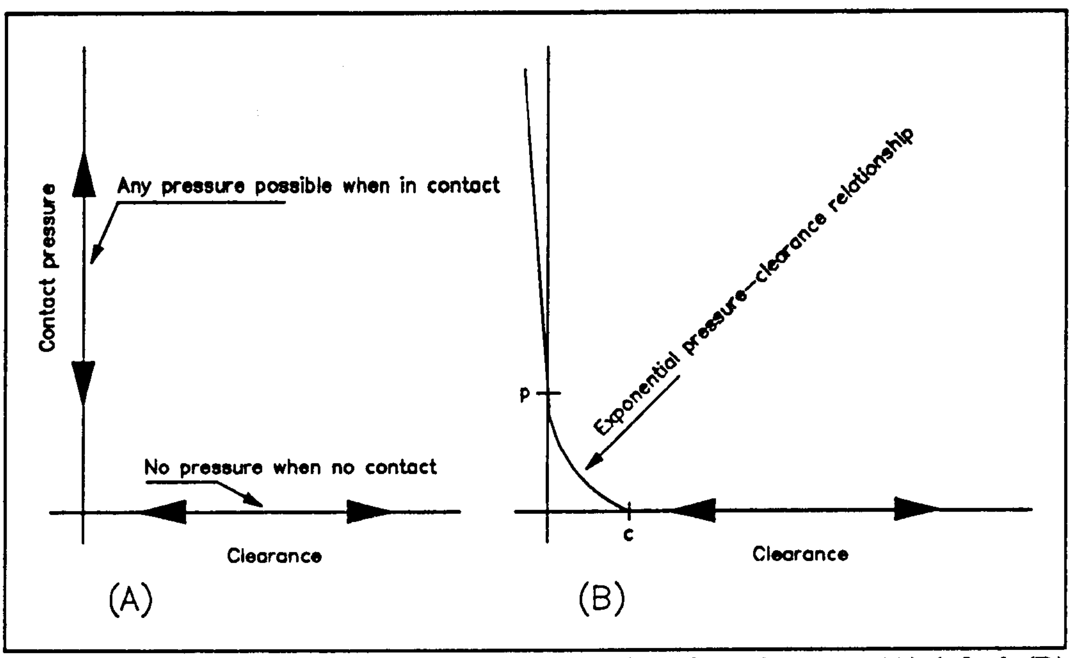

Figure 3.15. Pressure-clearance relationship for interface elements; (A) default (B) softened. (after ABAQUS).

Table 3.7. Secant stiffness at 45. kips load for WD specimens.

	Secant stiffness at a 45. kips horizontal load (k/in)						
Specimens	WD1	WD2	WD3	WD4	WD5	WD6	WD7
Test	303	251	177	246	126	371	320
ABAQUS-Default	344	405	399	295	* 113	473	480
ABAQUS-Softened	256	287	284	230	* 82	317	319
Method 2	199	248	248	163	-	316	327
Method 3	150	188	188	122	-	242	251

* The model diverged before reaching the 45. k load level.

experimental results (Richardson, 1986). The analytical methods 2 and 3 are based on equivalent strut formulations using Equations 2.4 (Klingner, 1980), and 2.5 and 2.7 (Chrysostomou et al., 1988) respectively. The softened option results in a closer prediction of the secant stiffness, Figure 3.16.

3.3.2.5 Failure Loads

Table 3.8 shows the failure loads from ABAQUS models, experimental tests, and the plastic collapse theory (Liauw and Kwan, 1983) applying Wood's (1978) penalty factor. These results show good agreement among ABAQUS, tests, and the plastic theory results.

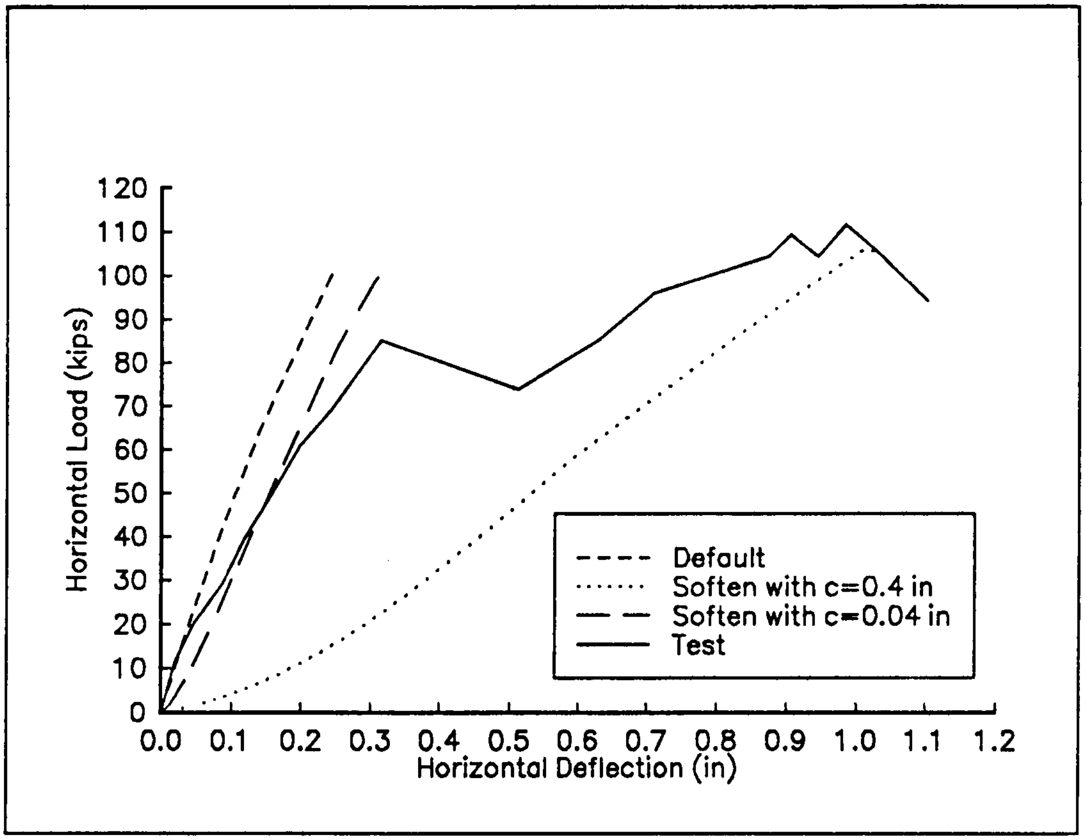

Figure 3.16. Load-deflection curves for WD7 using the default, soften option with clearance of 0.4 in and 0.04 in, and tests (Richardson, 1986).

Table 3.8. Collapse shear for WD specimens.

	Collapse Shear (kips)						
Specimen	WD1	WD2	WD3	WD4	WD5	WD6	WD7
Tests	85	100	80	105	75	140	111
ABAQUS def	103	98	91	91	20	105	101
ABAQUS soften	105	101	93	93	16	105	102
Plastic theories	74	72	70	69	-	74	73

CHAPTER 4

INITIAL STIFFNESS PARAMETRIC STUDY

4.1 Introduction

The initial stiffness parametric study is preformed for one, two, and three bay infilled frames. The case of vertical loads is also investigated to determine whether the equivalent strut method holds. Infill variables include net thickness, Young's modulus, height, and diagonal and horizontal angle. Steel frame variables include frame length and height, Young's modulus, and column and beam moment of inertia.

4.2 One Bay Infilled Frames

A typical infilled frame model has a net thickness, t, of 4.0 in (102 mm), a Young's modulus, E_c, of 1500 ksi (10340 MPa), and height, h', of 110.2 in (2800 mm). The steel frame has a Young's modulus, E_s, of 30,000 ksi (205500 MPa), length, L, of 141.7 in (3600 mm), and height, h, of 114.2 in (2901 mm). The column moment of inertia , I_h, is 45.16 in^4 (18.8X10^6 mm^4) and the beam moment of inertia, I_b, is 109.7 in^4 (45.66X10^6 mm^4). The diagonal horizontal angle, θ, is 37.87°. Only one infilled frame parameter changes at a time. In each investigation, ABAQUS results are compared with equivalent strut methods 1, 4, and 5. Method 1 uses Equation 2.1 (Stafford-Smith and Carter 1969); method 4 uses Equation 2.8 (Liauw and Kwan 1984); method 5 calculates the stiffness directly and uses Equation 2.3 (Barua and Mallick 1977).

Figures 4.1 to 4.4 show the results for rigidly connected steel frames. Figure 4.1

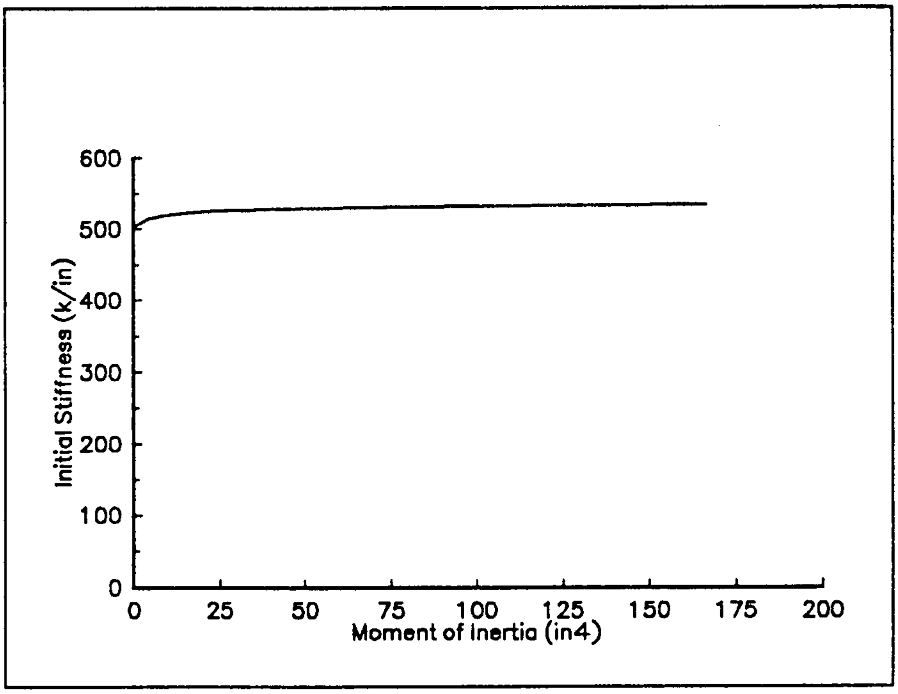

Figure 4.1. Initial stiffness versus frame-beam moment of inertia (ABAQUS models).

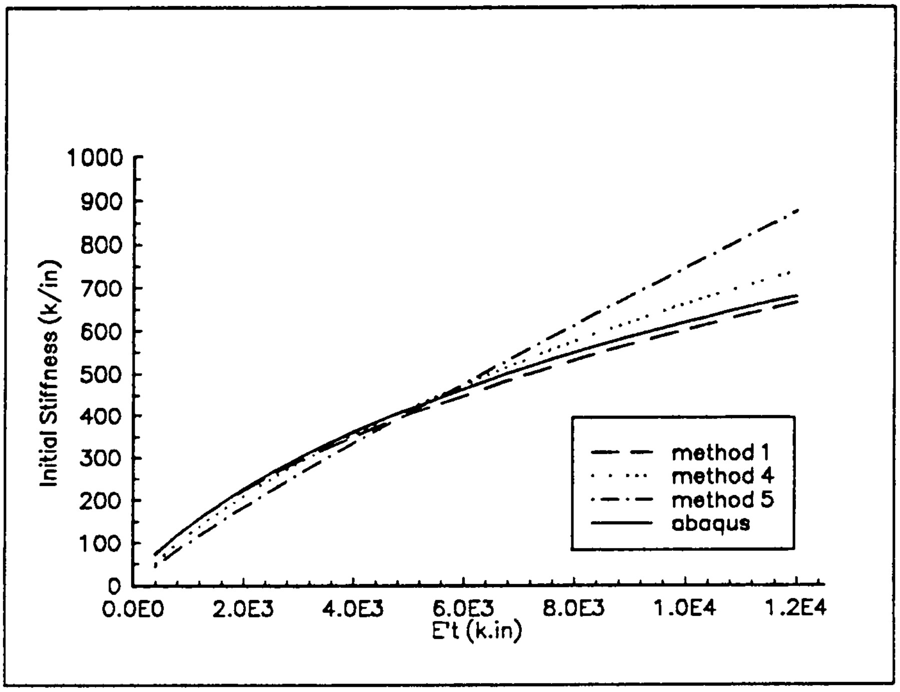

Figure 4.2. Initial stiffness versus the infill Young's modulus times net thickness.

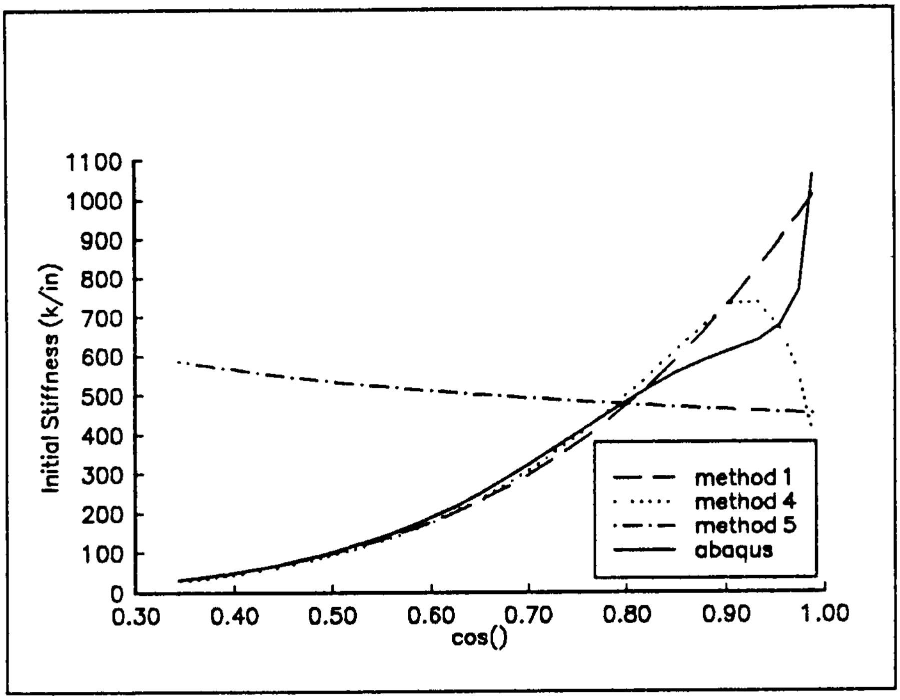

Figure 4.3. Initial stiffness versus the horizontal diagonal angle.

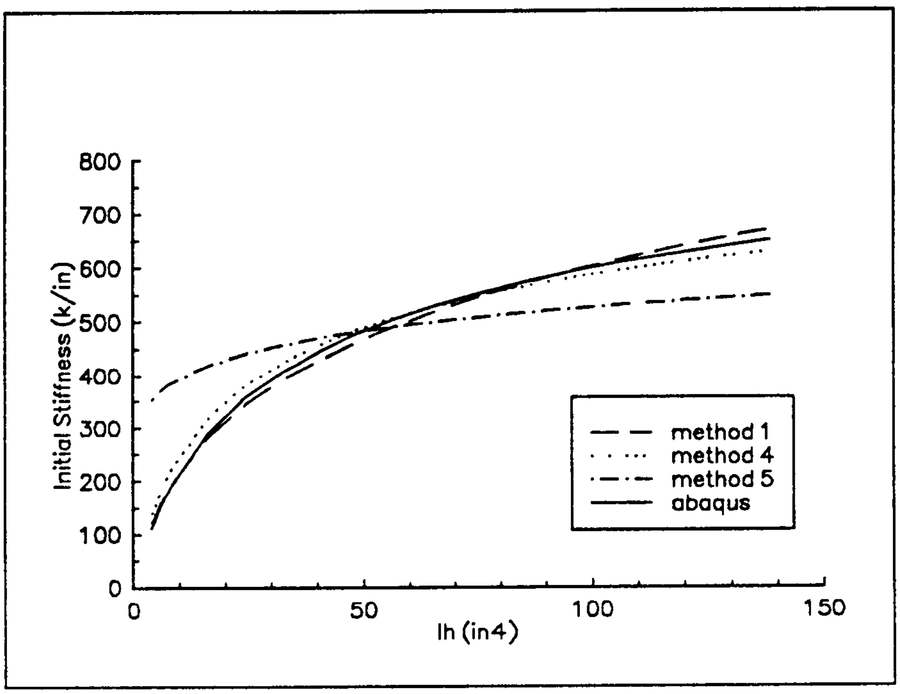

Figure 4.4. Initial stiffness versus the frame column moment of inertia.

shows that the beam moment of inertia has almost no effect on the initial stiffness. Thus, the beam moment of inertia can rightfully be neglected in equivalent strut formulations. Figure 4.2 shows that the infill Young's modulus times net thickness significantly affects the initial stiffness. Doubling the infill Young's modulus times the infill net thickness increases the frame initial stiffness by more than 50%. The cosine(θ), Figure 4.3, is varied by changing the frame height but keeping all the other parameters constant. Figure 4.4 shows initial stiffness versus the moment of inertia of the frame for identical columns. For the case when the frame columns are different, Figures 4.5 and 4.6, the average column moment of inertia is used to calculate the relative stiffness, λ (Equation 2.2). Note that with different columns, the initial stiffness will depend on the direction of the load. The leeward column has almost no effect on the stiffness since it is virtually stress free. The horizontal diagonal angle, θ, is kept constant, Figure 4.7, by changing both the frame

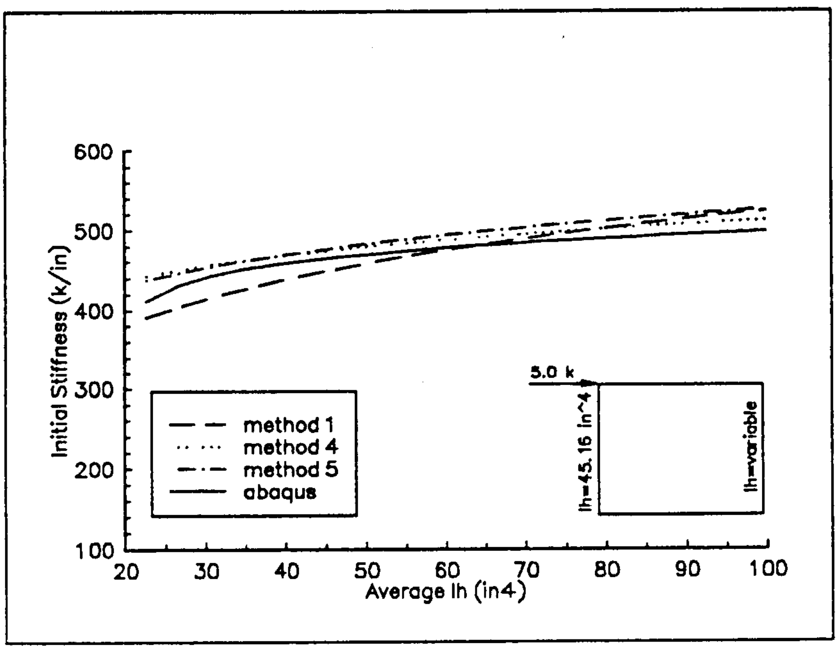

Figure 4.5. Initial stiffness versus the frame column average moment of inertia.

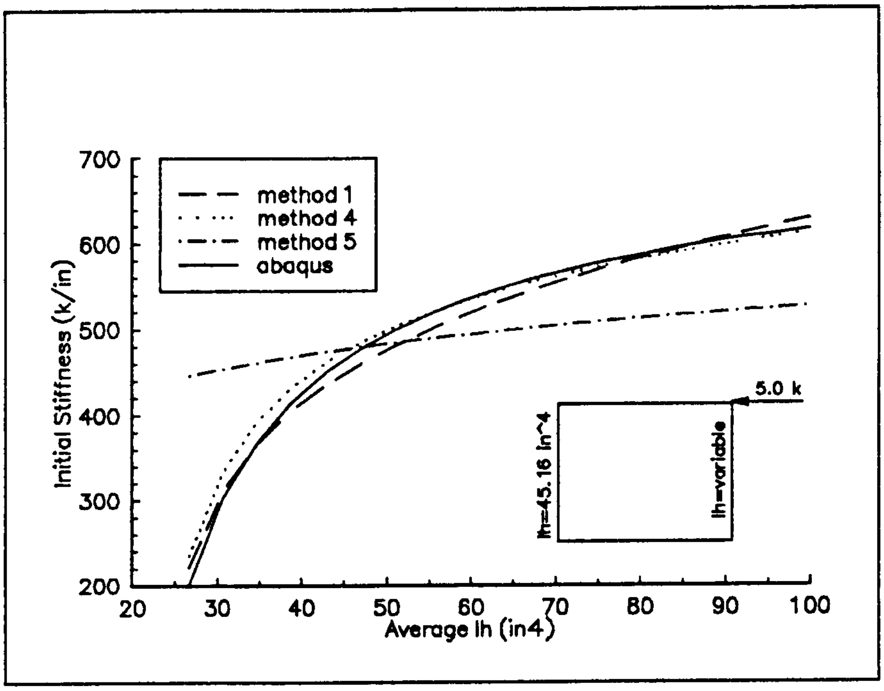

Figure 4.6. Initial stiffness versus the frame column average moment of inertia.

length and height. Figure 4.7 shows that the initial stiffness decreases with an increase of the frame length. This observation indicates that the frame height increase has greater effect on the initial stiffness.

Figures 4.1 to 4.7 show good agreement between the ABAQUS model and the three examined stiffness method results. Among these methods, method 1 (Stafford-Smith and Carter 1969) consistently matches the ABAQUS results.

The results for hinged connected frames are shown in Figures 4.8 to 4.11. It was found that a reduced stiffness obtained by omitting the 4 in the denominator for the relative stiffness parameter λ (Equation 2.2) resulted in a better match with ABAQUS values. The infill net thickness, Figure 4.8, drastically affects the initial stiffness. Figure 4.9 shoes the effect of diagonal horizontal angle on the initial stiffness. The angle varies

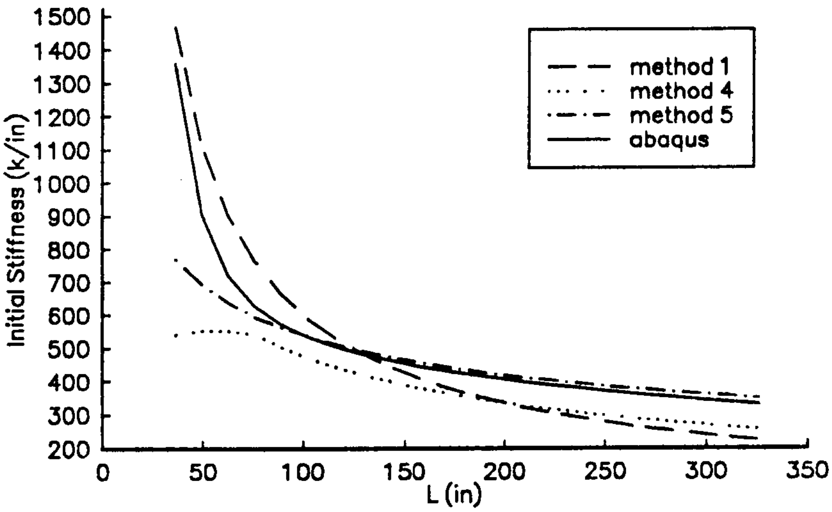

Figure 4.7. Initial stiffness versus the frame length.

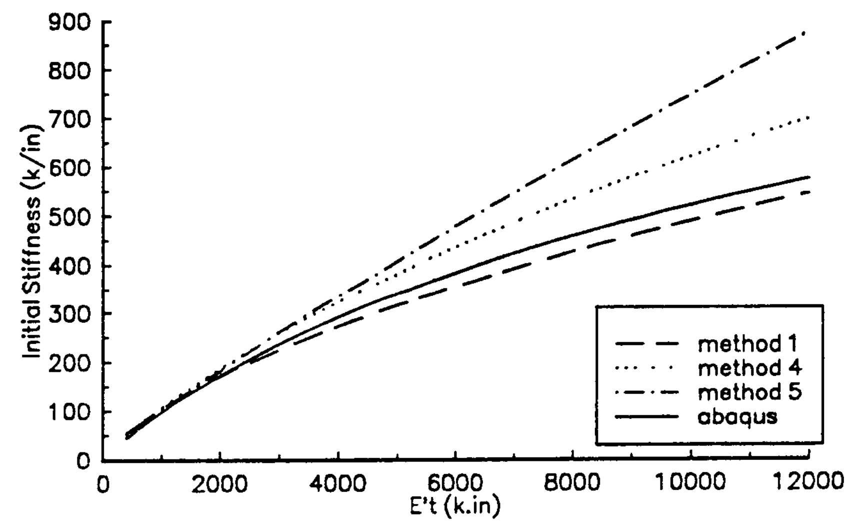

Figure 4.8. Initial stiffness versus the infill Young's modulus times net thickness.

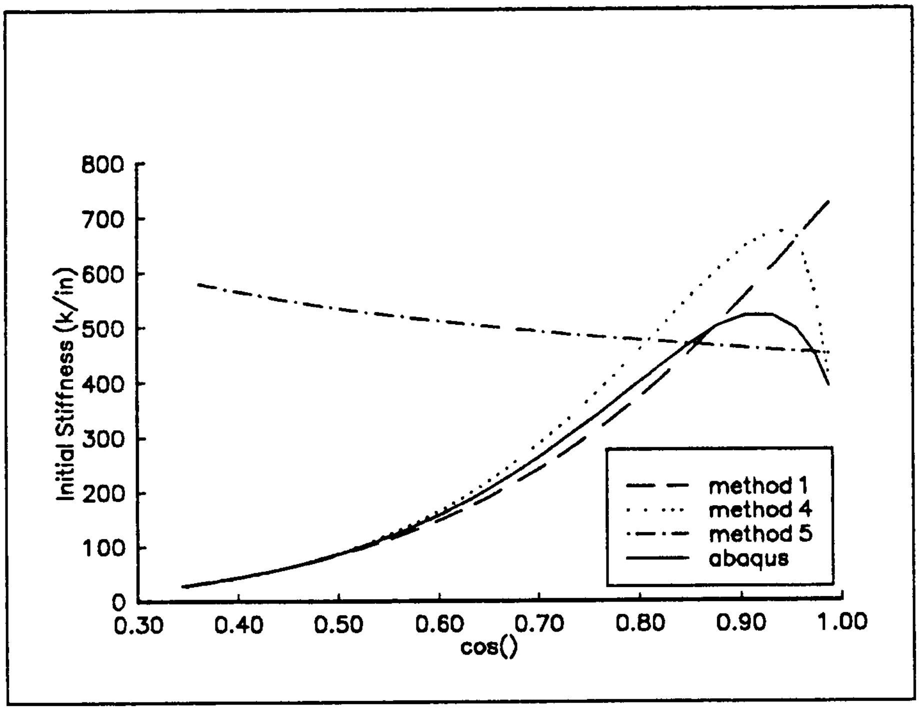

Figure 4.9. Initial stiffness versus the horizontal diagonal angle.

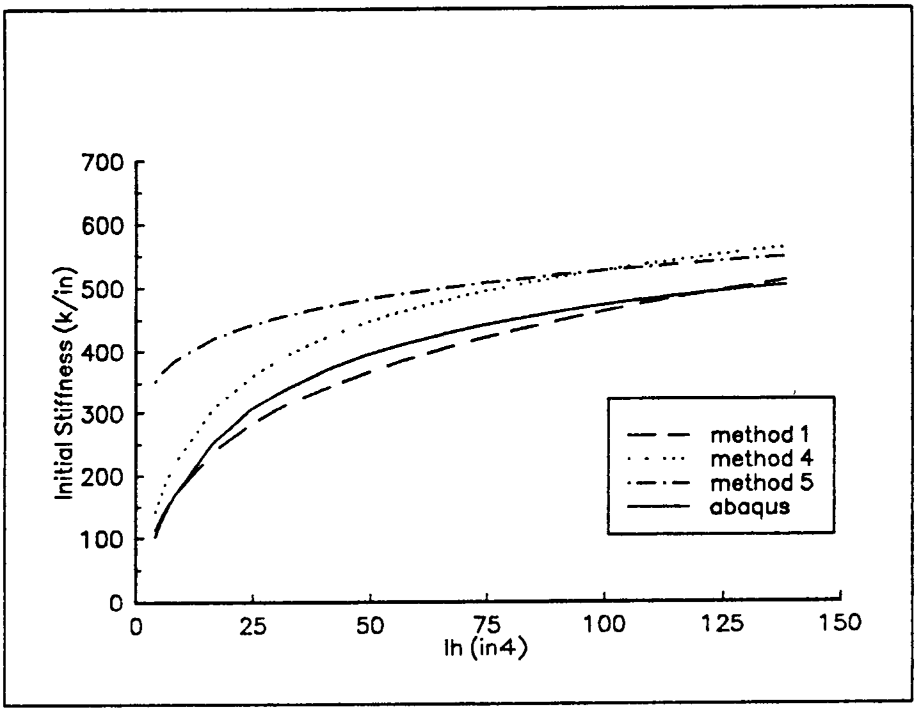

Figure 4.10. Initial stiffness versus the frame column moment of inertia.

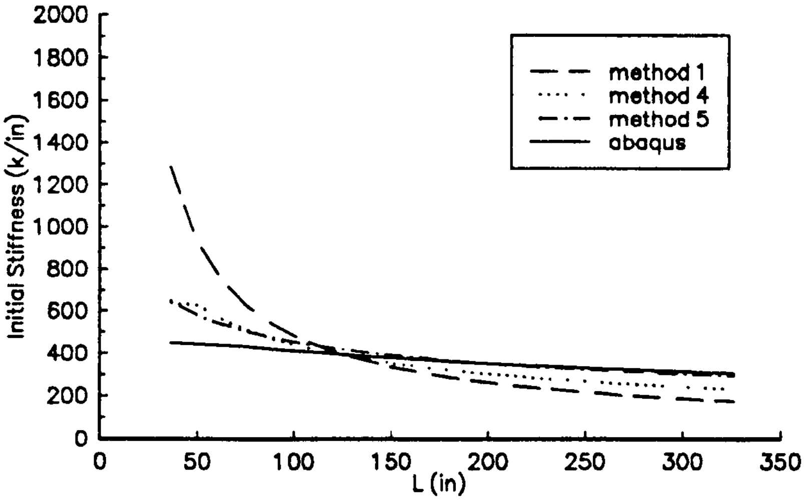

Figure 4.11. Initial stiffness versus the frame length.

by changing the infill height and keeping the other parameters constant. The column moment of inertia affects the initial stiffness, Figure 4.10, less than it does when frames are rigidly connected. The frame length and height are changed so that the diagonal horizontal angle is constant, Figure 4.11. Figures 4.8 to 4.11 show reduction of the initial stiffness due to the frame pinned connections. They also show that method 1 (Stafford-Smith and Carter 1969) reasonably matched the ABAQUS results, although not as well as with rigid connections. It is recommended that in order to be consistent and keep the same relative stiffness parameter λ, (Equation 2.2), Equation 2.1 be changed to Equation 4.1 for hinged frames.

$$a = \frac{\pi}{2\sqrt{2}\ \lambda} \tag{4.1}$$

4.3 Two Bay Infilled Frames

A rigidly connected infilled frame model is constructed of two bays, each identical to those of the one bay study. The lateral load pushes at the left or right corner. The middle column has equal or twice the moment of inertia of an external column. The left bay infill net thickness varies, while that of the right bay is constant, 4.0 in (102 mm). Method 1 (Stafford-Smith and Carter, 1969) is used to calculate the equivalent strut width. The moment of inertia of the middle column is divided equally between the two bays and for each bay, the average moment of inertia of the two columns is used in the calculation for the relative stiffness. Then, the simple structure consisting of a pinned two bay frame and the two calculated struts is analyzed using GTSTRUDL, a general structural analysis program. Tables 4.1 and 4.2 show the ABAQUS model results and equivalent strut results. Note the closeness of the results.

4.4 Three Bay Infilled Frames

The model is extended by adding a third bay. The middle columns have twice the moment of inertia of an exterior column. Method 1 (Stafford-Smith and Carter, 1969) is used to calculate the equivalent strut width. The moment of inertia of each middle column is divided equally between the two adjacent bays. For each bay, the average moment of inertia of the two columns is used in obtaining the relative stiffness. Then, the simple structure consisting of a pinned three bay frame braced by the three struts is analyzed using GTSTRUDL. Table 4.3 gives the results for varying infill thickness. In Table 4.4, the outer bay infill thicknesses vary, while that of the middle bay is constant, 4.0 in (102 mm). The lateral load is applied at the left corner.

Table 4.1. ABAQUS and method 1 initial stiffness for two bay infilled frames (the lateral load is applied at the left corner).

Left bay infill thickness (in)	Initial stiffness (k/in)					
	Middle column has 1I			Middle column has 2I		
	Equ. Strut	ABAQUS	Dif%	Equ. Strut	ABAQUS	Dif%
.2	440.	476.	8.	506.	535.	6.
.4	475.	504.	6.	543.	564.	4.
.6	505.	531.	5.	575.	591.	3.
.8	532.	555.	4.	604.	616.	2.
1.0	557.	578.	4.	630.	639.	1.
1.2	580.	600.	4.	654.	661.	1.
1.4	601.	621.	3.	677.	681.	1.
1.6	621.	640.	3.	699.	701.	0.
1.8	641.	659.	3.	719.	720.	0.
2.0	659.	677.	3.	738.	738.	0.
2.2	676.	694.	3.	757.	756.	0.
2.4	693.	711.	2.	775.	772.	0.
2.6	710.	727.	2.	792.	788.	0.
2.8	725.	742.	2.	808.	804.	1.
3.0	740.	757.	2.	824.	818.	1.
3.2	755.	771.	2.	839.	833.	1.
3.4	769.	785.	2.	854.	847.	1.
3.6	783.	798.	2.	869.	860.	1.
3.8	797.	811.	2.	883.	873.	1.
4.0	810.	824.	2.	896.	886.	1.
4.2	822.	836.	2.	910.	898.	1.
4.4	835.	848.	2.	923.	910.	1.
4.6	847.	859.	1.	935.	921.	1.
4.8	858.	870.	1.	947.	933.	2.
5.0	870.	881.	1.	959.	944.	2.
5.2	881.	892.	1.	971.	954.	2.

Table 4.2. ABAQUS and method 1 initial stiffness for two bay infilled frames (the lateral load is applied at the right corner).

Left bay infill thickness (in)	Initial stiffness (k/in)					
	Middle column has 1I			Middle column has 2I		
	Equ. Strut	ABAQUS	Dif%	Equ. Strut	ABAQUS	Dif%
.2	477.	515.	8.	507.	535.	6.
.4	511.	544.	6.	544.	566.	4.
.6	540.	570.	6.	576.	593.	3.
.8	565.	593.	5.	605.	619.	2.
1.0	588.	615.	5.	631.	642.	2.
1.2	609.	635.	4.	655.	664.	1.
1.4	628.	654.	4.	678.	685.	1.
1.6	647.	671.	4.	699.	705.	1.
1.8	664.	688.	4.	720.	724.	1.
2.0	680.	703.	3.	739.	742.	0.
2.2	696.	718.	3.	757.	759.	0.
2.4	711.	732.	3.	775.	775.	0.
2.6	725.	745.	3.	792.	791.	0.
2.8	738.	758.	3.	809.	806.	0.
3.0	751.	770.	3.	824.	821.	0.
3.2	764.	782.	2.	840.	835.	1.
3.4	776.	793.	2.	855.	848.	1.
3.6	787.	804.	2.	869.	861.	1.
3.8	799.	814.	2.	883.	874.	1.
4.0	810.	824.	2.	896.	886.	1.
4.2	820.	833.	2.	910.	898.	1.
4.4	830.	842.	1.	923.	909.	1.
4.6	840.	851.	1.	935.	920.	2.
4.8	850.	859.	1.	947.	931.	2.
5.0	859.	868.	1.	959.	941.	2.
5.2	868.	876.	1.	971.	951.	2.

Table 4.3. ABAQUS and method 1 initial stiffness for three identical bay infilled frames.

Infill net thickness (in)			Initial stiffness (k/in)		
Left bay	Middle bay	Right bay	Equivalent strut	ABAQUS	Dif. %
.2	.2	.2	171.	186.	8.
.4	.4	.4	281.	283.	1.
.6	.6	.6	372.	369.	1.
.8	.8	.8	453.	445.	2.
1.0	1.0	1.0	526.	514.	2.
1.2	1.2	1.2	592.	577.	3.
1.4	1.4	1.4	654.	634.	3.
1.6	1.6	1.6	712.	688.	3.
1.8	1.8	1.8	767.	737.	4.
2.0	2.0	2.0	819.	783.	4.
2.2	2.2	2.2	868.	827.	5.
2.4	2.4	2.4	914.	868.	5.
2.6	2.6	2.6	959.	906.	6.
2.8	2.8	2.8	1002.	942.	6.
3.0	3.0	3.0	1043.	977.	6.
3.2	3.2	3.2	1082.	1009.	7.
3.4	3.4	3.4	1120.	1040.	7.
3.6	3.6	3.6	1157.	1070.	8.
3.8	3.8	3.8	1192.	1098.	8.
4.0	4.0	4.0	1226.	1125.	8.
4.2	4.2	4.2	1260.	1151.	9.
4.4	4.4	4.4	1292.	1176.	9.
4.6	4.6	4.6	1323.	1200.	9.
4.8	4.8	4.8	1353.	1223.	10
5.0	5.0	5.0	1383.	1245.	10
5.2	5.2	5.2	1411.	1267.	10

Table 4.4. ABAQUS and method 1 initial stiffness for three different bay infilled frames.

Infill net thickness (in)			Initial stiffness (k/in)		
Left bay	Middle bay	Right bay	Equivalent strut	ABAQUS	Dif. %
.2	4.0	5.2	885.	847.	4.
.4	4.0	5.0	915.	867.	5.
.6	4.0	4.8	939.	885.	6.
.8	4.0	4.6	960.	901.	6.
1.0	4.0	4.4	978.	915.	6.
1.2	4.0	4.2	993.	928.	7.
1.4	4.0	4.0	1007.	940.	7.
1.6	4.0	3.8	1019.	951.	7.
1.8	4.0	3.6	1030.	961.	7.
2.0	4.0	3.4	1040.	970.	7.
2.2	4.0	3.2	1048.	979.	7.
2.4	4.0	3.0	1055.	986.	7.
2.6	4.0	2.8	1061.	993.	6.
2.8	4.0	2.6	1066.	998.	6.
3.0	4.0	2.4	1070.	1003.	6.
3.2	4.0	2.2	1073.	1008.	6.
3.4	4.0	2.0	1075.	1011.	6.
3.6	4.0	1.8	1075.	1013.	6.
3.8	4.0	1.6	1075.	1015.	6.
4.0	4.0	1.4	1073.	1016.	5.
4.2	4.0	1.2	1069.	1016.	5.
4.4	4.0	1.0	1064.	1014.	5.
4.6	4.0	.8	1057.	1012.	4.
4.8	4.0	.6	1048.	1008.	4.
5.0	4.0	.4	1035.	1003.	3.
5.2	4.0	.2	1017.	995.	2.

4.5 Vertical Loads

Most infilled frames support a variety of loading conditions. Combinations of gravity and lateral loads are common. The diagonal strut analogy has its limitation (King and Pandey, 1978), therefore, the validity of the equivalent strut concept for a combination of vertical and lateral loads is examined. Two cases, one and two bay infilled frames, are considered in this study.

For the one bay infilled frame case, method 1, (Stafford-Smith and Carter 1969) is used to calculate the equivalent strut width. The pinned frame braced with the diagonal strut is analyzed with GTSTRUDL. Figure 4.12 shows the initial stiffness from ABAQUS and the equivalent strut method with varying vertical loads. It is clear that the equivalent strut method is applicable in this case. Note the increase in stiffness provided by the vertical loads.

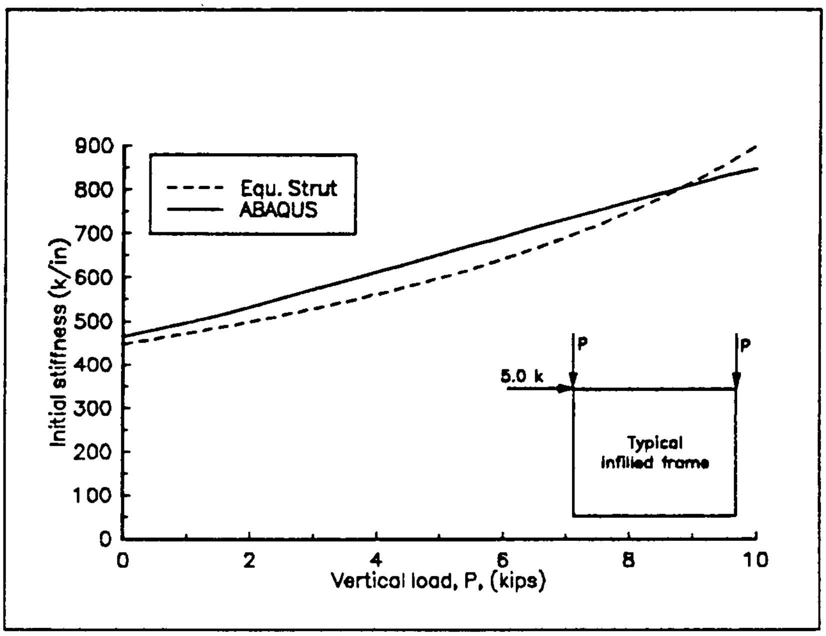

Figure 4.12. Initial stiffness for one bay infilled frames under vertical and lateral loads.

When a typical two bay model was examined in the same manner as without vertical loads, the results of equivalent strut method did not agree with that of ABAQUS models. This discrepancy led to rethinking about the whole equivalent strut analogy. There is a major difference between ABAQUS and equivalent strut models. The dissimilarity is that even for a symmetrical infilled frame, the diagonal strut model is not symmetrical. Therefore, under a symmetrical vertical loading, the diagonal braced frame moves laterally without lateral loadings, unlike ABAQUS models. A simple solution is to make strut structures symmetrical by bracing the frame with two diagonal struts, compressional and tensional. Applying this idea on one bay infilled frames led to discouraging results, Figure 4.13. Therefore, the concept of splitting the diagonal strut into two is omitted.

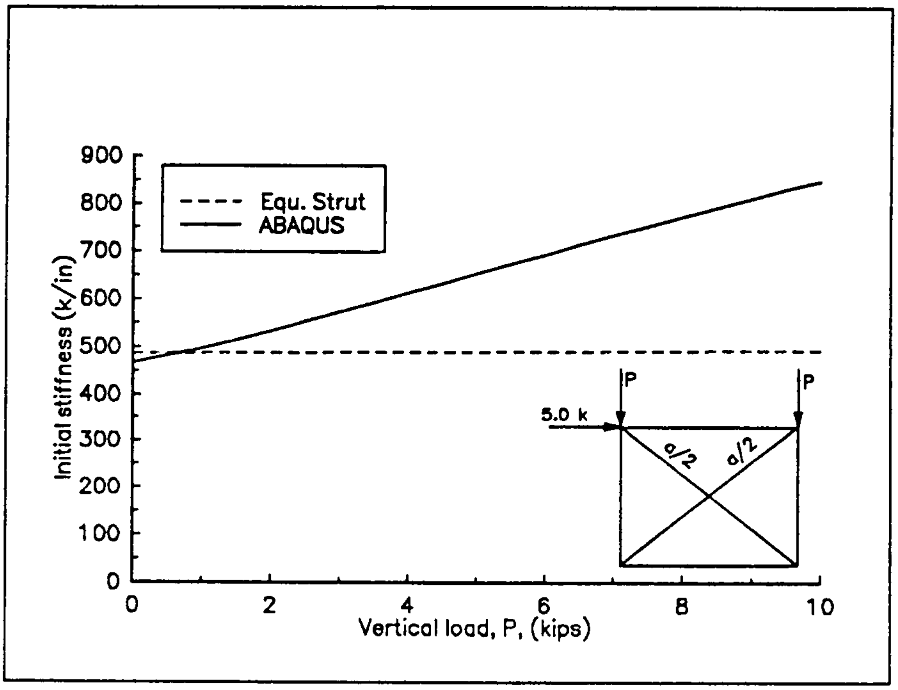

Figure 4.13. Initial stiffness for one bay infilled frames under vertical and lateral loads using two diagonal struts instead of one.

Another thought is to apply the lateral load at each corner instead of at one corner. The idea is tried on two bay infilled frame models. The left bay infill net thickness varies, while that of the right bay is constant, 4.0 in (102 mm). The middle column has twice the moment of inertia of an exterior column. Method 1 (Stafford-Smith and Carter, 1969) is used to calculate the equivalent strut width. The moment of inertia of the middle column is divided equally between the two bays. For each bay, the average moment of inertia of the two columns is used to calculate the relative stiffness. Then, the simple structure, a two bay braced pinned frame, is analyzed using GTSTRUDL. Figure 4.14 shows the loading condition and the resultant initial stiffness. The closeness of the results shows that splitting the lateral loads at each corner is a promising idea. The idea is valid even when there is no vertical load, Table 4.5.

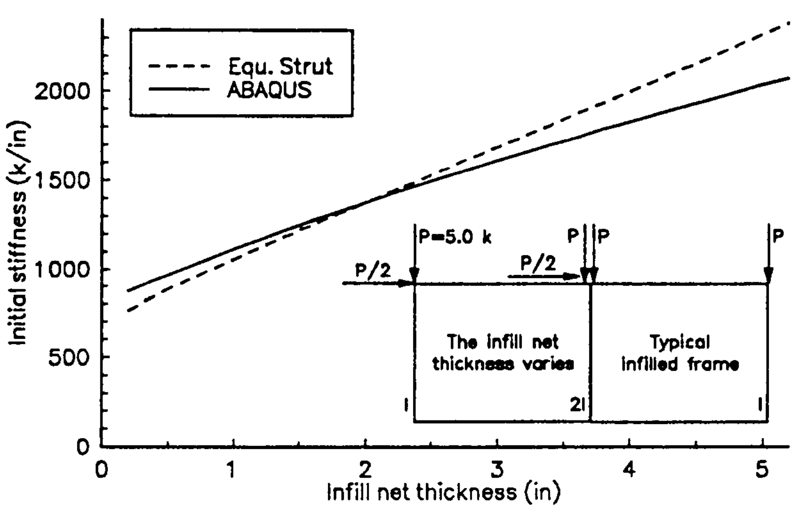

Figure 4.14. Initial stiffness for two bay infilled frames under vertical and lateral loads.

Table 4.5. ABAQUS and method 1 initial stiffness for three bay infilled frames (lateral loads are applied at each corner).

Infill net thickness (in)			Initial stiffness (k/in)		
Left bay	Middle bay	Right bay	Equivalent strut	ABAQUS	Dif. %
.2	.2	.2	175.	198.	13
.4	.4	.4	291.	309.	6.
.6	.6	.6	390.	412.	6.
.8	.8	.8	480.	508.	6.
1.0	1.0	1.0	562.	597.	6.
1.2	1.2	1.2	639.	682.	7.
1.4	1.4	1.4	712.	762.	7.
1.6	1.6	1.6	781.	839.	7.
1.8	1.8	1.8	847.	912.	8.
2.0	2.0	2.0	910.	982.	8.
2.2	2.2	2.2	971.	1049.	8.
2.4	2.4	2.4	1029.	1113.	8.
2.6	2.6	2.6	1086.	1175.	8.
2.8	2.8	2.8	1141.	1235.	8.
3.0	3.0	3.0	1194.	1293.	8.
3.2	3.2	3.2	1245.	1349.	8.
3.4	3.4	3.4	1295.	1403.	8.
3.6	3.6	3.6	1344.	1455.	8.
3.8	3.8	3.8	1392.	1506.	8.
4.0	4.0	4.0	1438.	1556.	8.
4.2	4.2	4.2	1484.	1604.	8.
4.4	4.4	4.4	1528.	1650.	8.
4.6	4.6	4.6	1571.	1695.	8.
4.8	4.8	4.8	1613.	1739.	8.
5.0	5.0	5.0	1655.	1782.	8.
5.2	5.2	5.2	1696.	1823.	8.

CHAPTER 5

ULTIMATE LOAD PARAMETRIC STUDY

5.1 Introduction

The ultimate load parametric study analyzes one, two, and three bay infilled frames. The study also investigates the case of vertical loads to determine their effects on the ultimate load. Infill variables include net thickness and height. Steel frame variables include frame height, joint connections, and column and beam moments of inertia.

5.2 One Bay Rigid Connection Infilled Frames

A typical infilled frame model has a net thickness, t, of 4.0 in (102 mm), a Young's modulus, E_c, of 1500 ksi (10340 MPa), and height, h', of 110.2 in (2800 mm). The model uses the concrete option to define the infill properties beyond the elastic range. The infill ultimate stress is 3.75 ksi (25.855 MPa) with a plastic strain of 0.0013. The infill plastic behavior starts at 1/3 of the ultimate stress, Figure 3.11. The finite element model uses the softened interface behavior option to describe the localized mortar crushing that tends to occur at the infill corners. The clearance, c, at which the steel-infill contact pressure starts is set to 0.04 in (1 mm). At zero clearance, the pressure, p, is set to 3.0 ksi (20.684 MPa) which represents the mortar ultimate stress, Figure 3.15. The steel frame has a Young's modulus, E_s, of 30,000 ksi (205500 MPa), yield stress of 36 ksi (248.2 MPa), length, L, of 141.7 in (3600 mm), and height, h, of 114.2 in (2901 mm). The column moment of inertia, I_h, is 45.16 in^4 ($18.8X10^6$ mm^4) and the beam moment of inertia, I_b, is 109.7 in^4 ($45.66X10^6$ mm^4). The diagonal horizontal angle, θ, is 37.87°.

Only one infilled frame parameter (the infill thickness or height, or the moment of inertia of column or beam) changes at a time. In each investigation, ABAQUS results are compared with analytical methods. These methods include plastic theories (Liauw and Kwan, 1983), the upper and lower bounds for the ultimate load (Wood, 1978), and equivalent strut models. A penalty factor is applied to account for the imperfect plasticity of the infill.

5.2.1 Plastic theories

The plastic collapse theories developed by Liauw and Kwan (1983) use Equations 2.30, 2.34, and 2.37 or 2.38 depending on the failure mode to determine the infill ultimate strength. A penalty factor is applied to reduce the infill compressive strength. The penalty factor, ν_p, Equation 2.22 (Wood, 1978) was introduced for brickwork rather than concrete block infill. Therefore, it was necessary to develop a suitable penalty factor formula for block infill. The penalty factors are obtained by equating ABAQUS ultimate load results to those from plastic collapse theories. The best fit quadratic formula is obtained using the penalty points as a function of nominal m, Equation 2.16. Using different upper limits for ν_p produces different penalty factor equations. These upper limits are 0.60, 0.70, and 0.80 giving Equations 5.1, 5.2, and 5.3 respectively.

$$\nu_p = 12.2\ m^2 - 5.08\ m + 0.589 \ \leq 0.60 \tag{5.1}$$

$$\nu_p = 20.0\ m^2 - 7.37\ m + 0.678 \ \leq 0.70 \tag{5.2}$$

$$\nu_p = 27.0\ m^2 - 9.42\ m + 0.756 \ \leq 0.80 \tag{5.3}$$

Figures 5.1 to 5.4 show ABAQUS results and those predicted by plastic theories (Liauw and Kwan, 1983). Different equations for the penalty factor, v_p, are used. The penalty factor Equation 2.22 (Wood, 1978) is also used as a reference. Figure 5.1 shows that the column moment of inertia has no effect on the ultimate strength after exceeding the beam moment of inertia. Likewise, the beam moment of inertia does not affect the ultimate strength after exceeding the column moment of inertia, Figure 5.2. For very low values of the beam moment of inertia, the plastic collapse theories tend to underestimate the ultimate load. Figure 5.3 shows that the infill net thickness significantly affects the ultimate load. Figure 5.4 demonstrates the effect the frame height has on the ultimate strength. The figure reveals that square infilled frames have the highest ultimate strength.

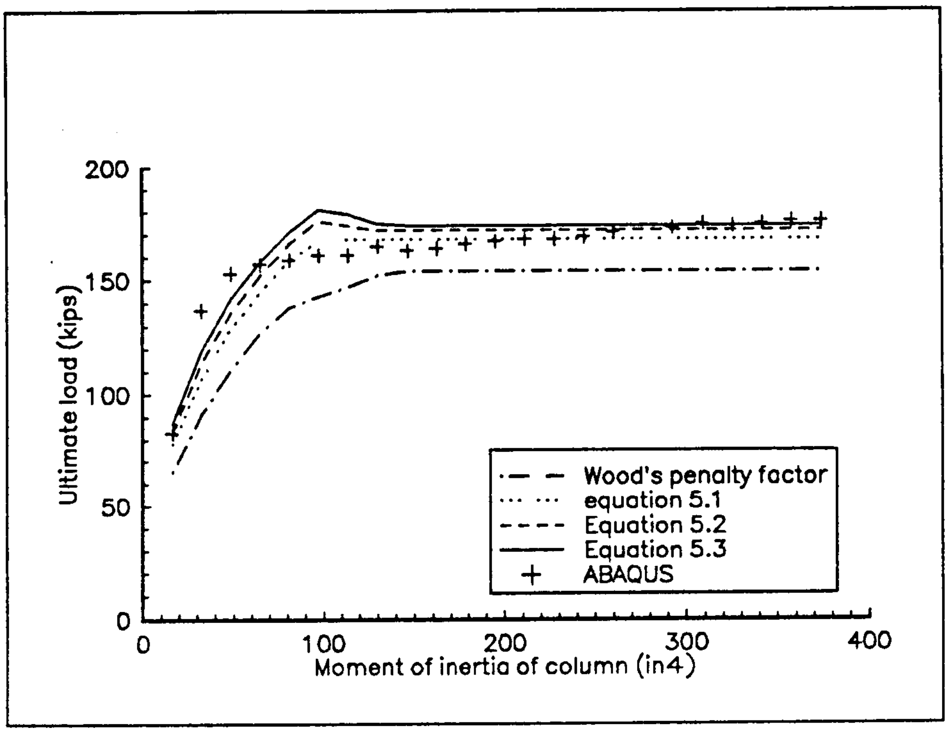

Figure 5.1. Ultimate load versus frame column moment of inertia using ABAQUS and plastic theories (Liauw and Kwan, 1983) applying different penalty factors.

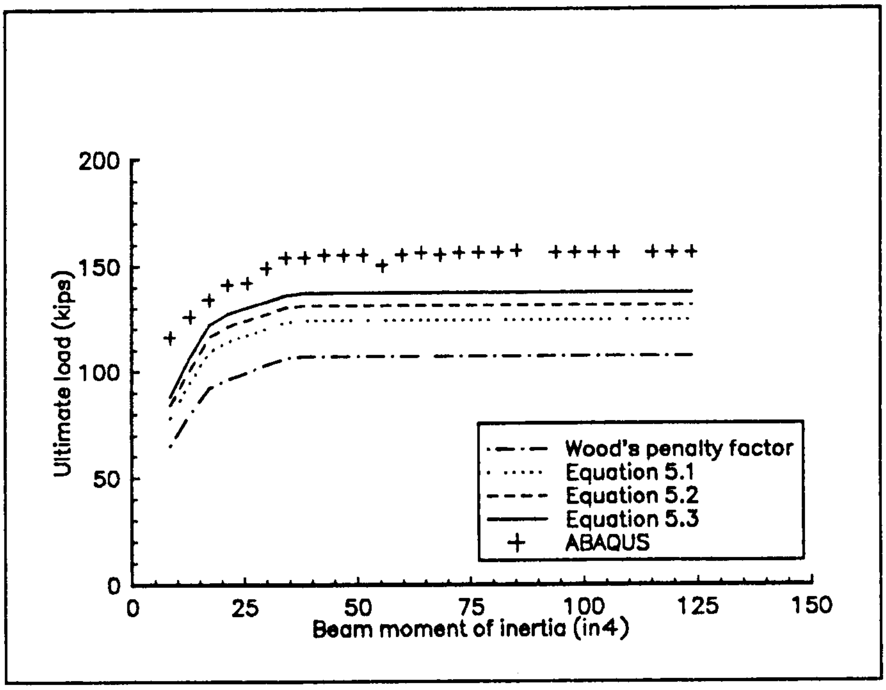

Figure 5.2. Ultimate load versus frame top beam moment of inertia using ABAQUS and plastic theories (Liauw and Kwan, 1983) applying different penalty factors.

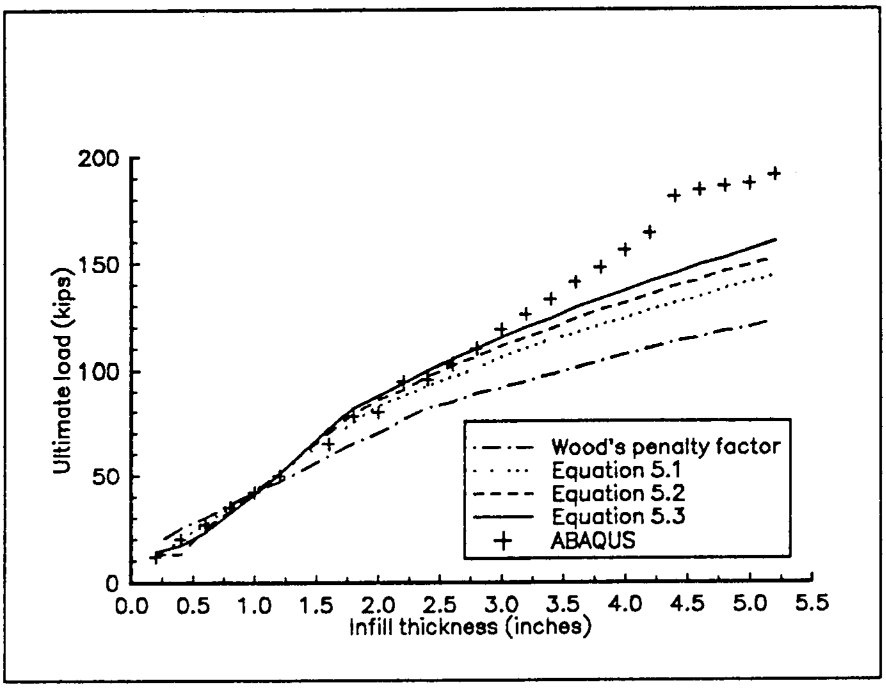

Figure 5.3. Ultimate load versus infill net thickness using ABAQUS and plastic theories (Liauw and Kwan, 1983) applying different penalty factors.

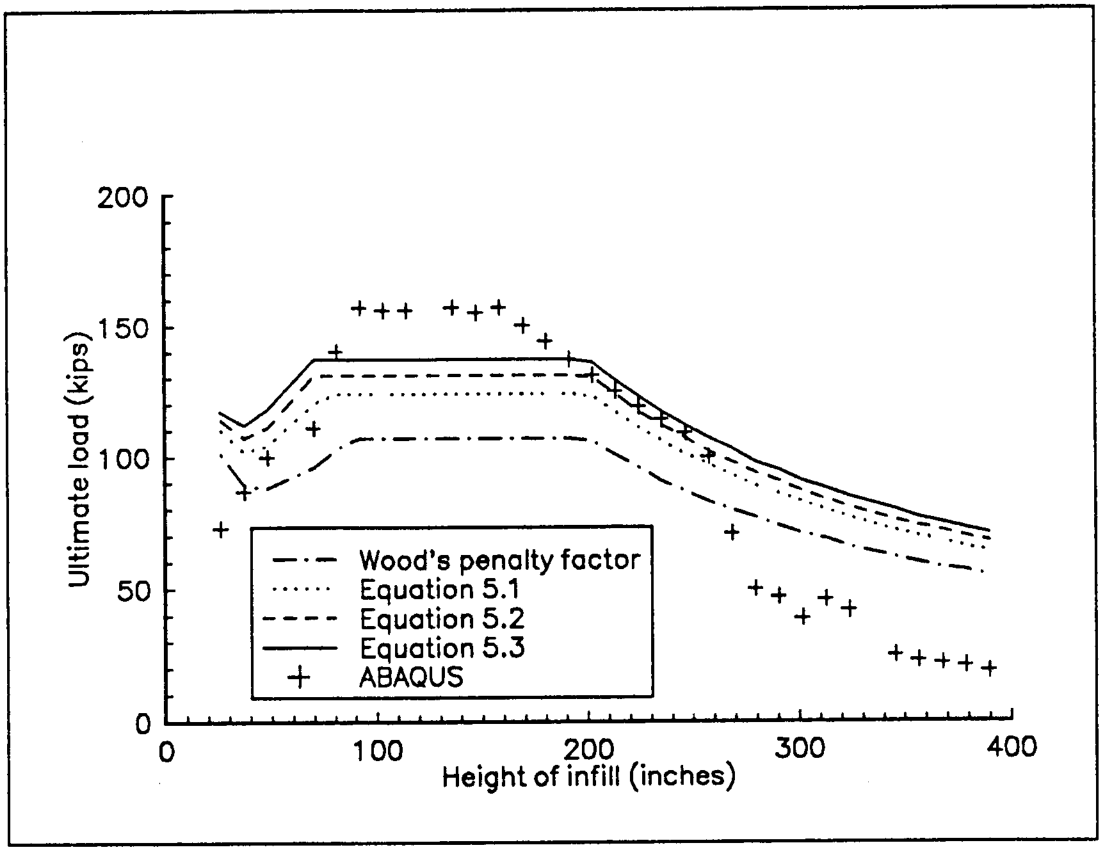

Figure 5.4. Ultimate load versus frame height using ABAQUS and plastic theories (Liauw and Kwan, 1983) applying different penalty factors.

5.2.2 Upper and Lower Bounds for Ultimate Loads

Wood's analyses (1978) give upper and lower bounds for the infilled frame ultimate loads. Using the same manner with Wood's formulations (1978) and ABAQUS results, penalty factor equations are obtained. Equation 5.4 uses 0.80 as an upper limit for the penalty factor and Equation 5.5 is for an upper limit of 1.00. Figures 5.5 to 5.8 show ABAQUS results and those given by upper and lower bound formulations (Wood, 1978). Different penalty factors are applied, Equation 2.22 (Wood, 1978), Equation 5.4, or Equation 5.5.

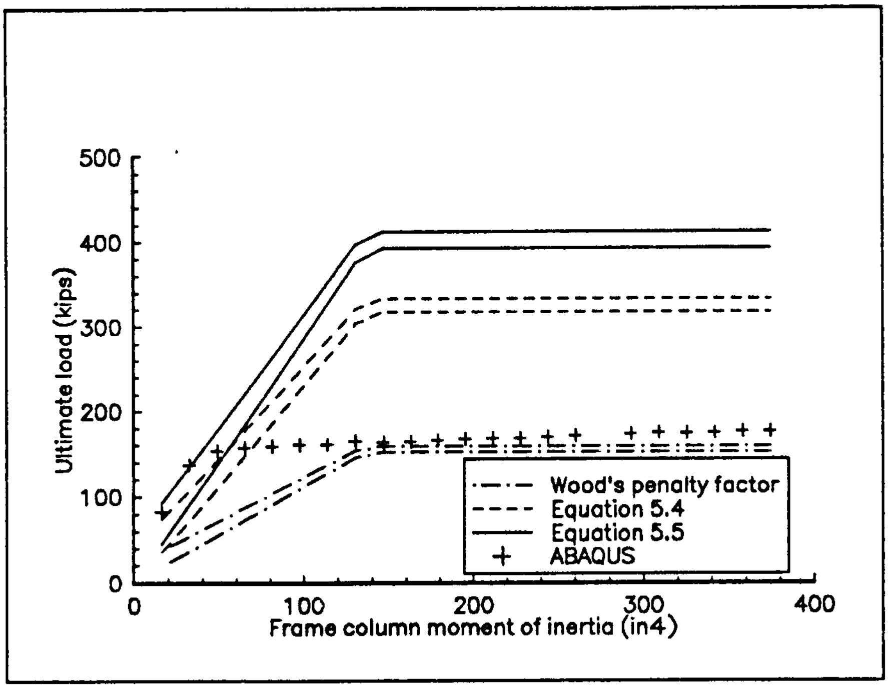

Figure 5.5. Ultimate load versus frame column moment of inertia using ABAQUS and upper and lower bound solutions (Wood, 1978) applying different penalty factors.

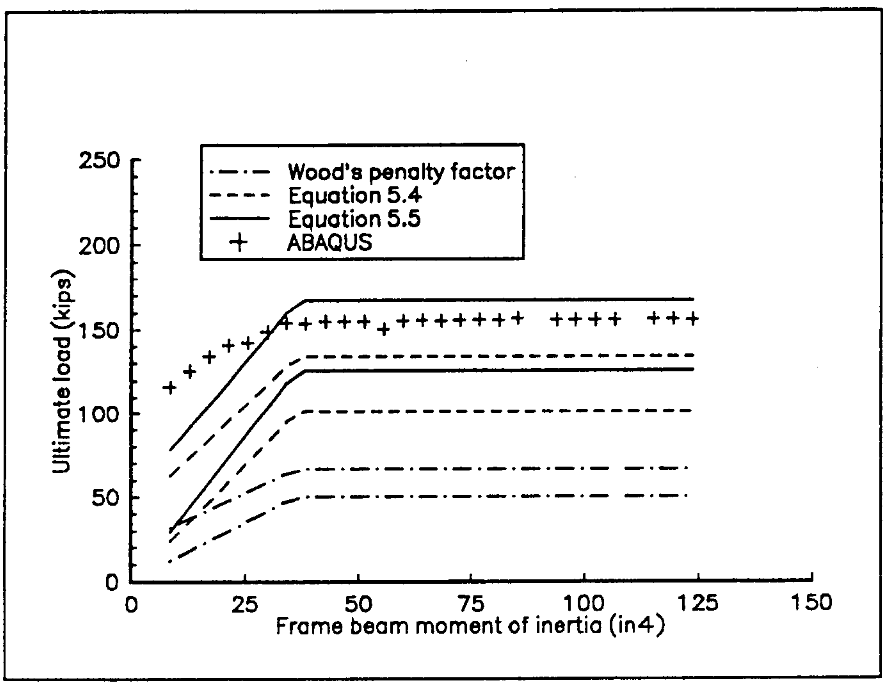

Figure 5.6. Ultimate load versus frame top beam moment of inertia using ABAQUS and upper and lower bound solutions (Wood, 1978) applying different penalty factors.

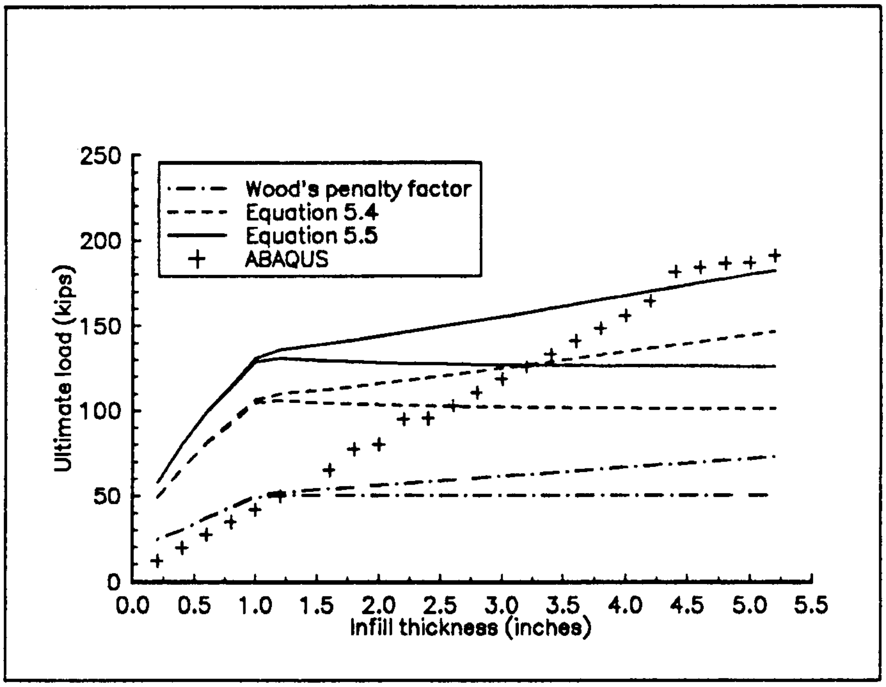

Figure 5.7. Ultimate load versus infill net thickness using ABAQUS and upper and lower bound solutions (Wood, 1978) applying different penalty factors.

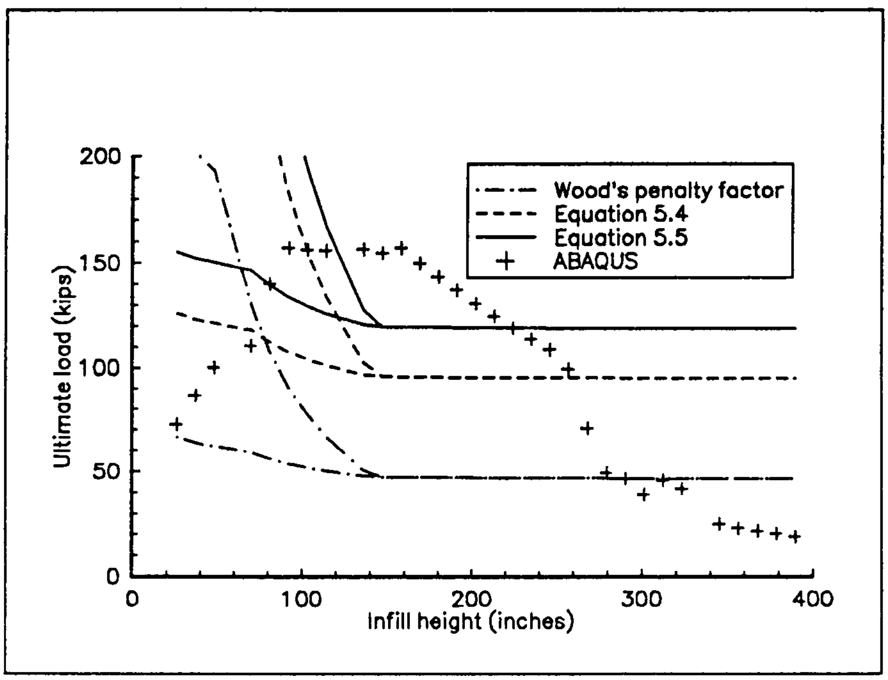

Figure 5.8. Ultimate load versus frame height using ABAQUS and upper and lower bound solutions (Wood, 1978) applying different penalty factors.

$$\nu_p = 29.6\ m^2 - 9.89\ m + 0.815 \le 0.80 \tag{5.4}$$

$$\nu_p = 46.4\ m^2 - 14.8\ m + 1.0 \le 1.00 \tag{5.5}$$

5.2.3 Equivalent Strut Model

The equivalent strut analogy is to replace the infill by a diagonal strut. Equation 2.1 (Stafford-Smith and Carter, 1969) gives the diagonal strut net effective thickness. This model was intended to estimate the infill stiffness rather than the failure load. The simplicity of the model causes one to investigate whether the model has the ability to determine the infilled frame ultimate strength. The diagonal strut compressive strength or windward column ultimate tensile strength governs the model ultimate load. The model ultimate load is the minimum of the collapse shear, H_u, given by Equation 5.6 (infill) or 5.7 (steel), where A_s and F_Y are the windward column area and yield stress; σ_c and t are the infill compressive strength and net thickness; α_c is the strut effective width, Figure 5.9. ABAQUS results are compared to the model ultimate loads to obtain the penalty factors. Equation 5.8 is the best fit quadratic formula using the penalty factor points as a function of nominal m, Equation 2.16. Equation 5.9 does not depend on m since it is the best fit constant formula for the penalty factor points. Figures 5.10 to 5.13 show ABAQUS and equivalent strut model ultimate strength applying different penalty factors.

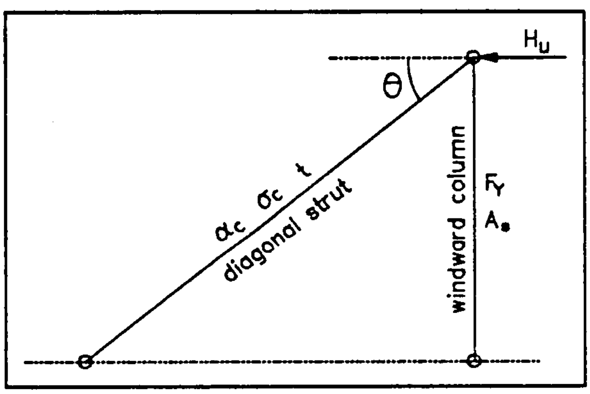

Figure 5.9. Ultimate strength strut model.

Equation 5.8, Equation 5.9, and Wood's (1978) penalty factor formula, which is used as a reference, are used. The figures reveal that equivalent strut model and ABAQUS results are comparable. The difference between using Equation 5.8 or 5.9 to estimate the penalty factor is negligible. Thus, it is recommended to use the simple formula 5.9 to estimate the penalty factor.

$$H_u = \sigma_c \, t \, \alpha_c \, \nu_p \cos(\theta) \tag{5.6}$$

$$H_u = F_Y A_s \cot(\theta) \tag{5.7}$$

$$\nu_p = 4.56 \, m^2 - 1.44 \, m + 0.414 \leq 0.45 \tag{5.8}$$

$$\nu_p = 0.387 \tag{5.9}$$

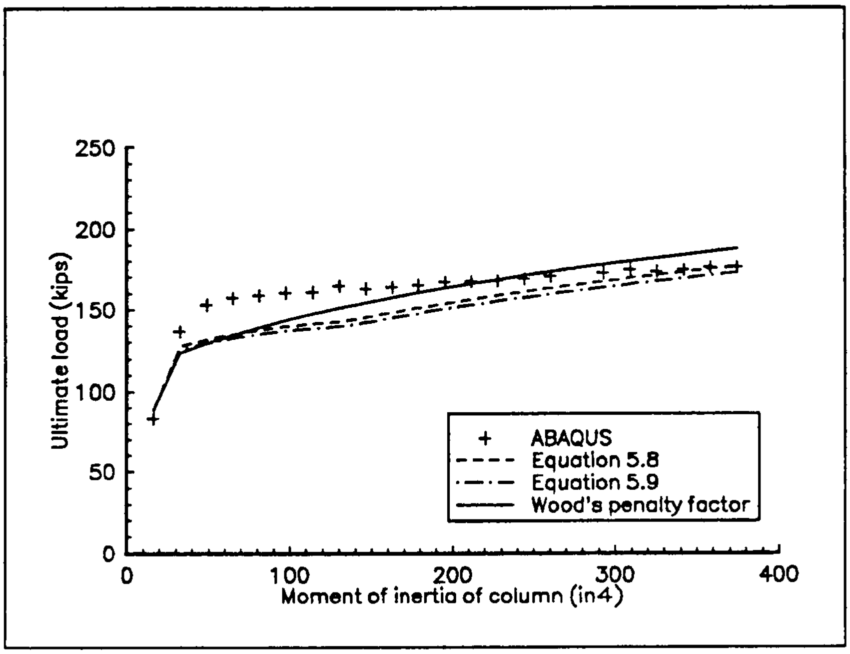

Figure 5.10. Ultimate load versus frame column moment of inertia using ABAQUS and equivalent strut models (Stafford-Smith and Carter, 1969) applying different penalty factors.

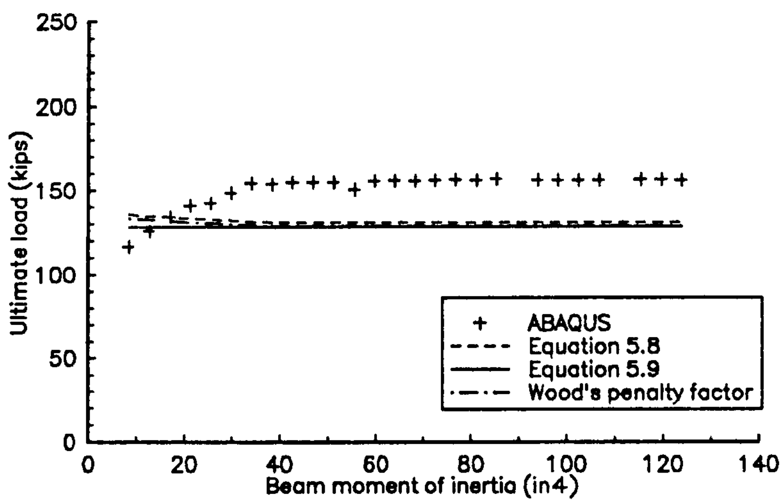

Figure 5.11. Ultimate load versus frame top beam moment of inertia using ABAQUS and equivalent strut models (Stafford-Smith, and Carter, 1969) applying different penalty factors.

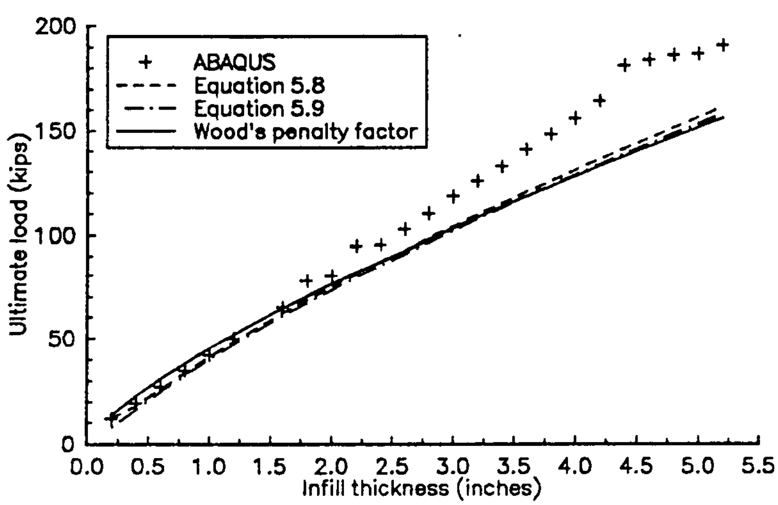

Figure 5.12. Ultimate load versus infill net thickness using ABAQUS and equivalent strut models (Stafford-Smith and Carter, 1969) applying different penalty factors.

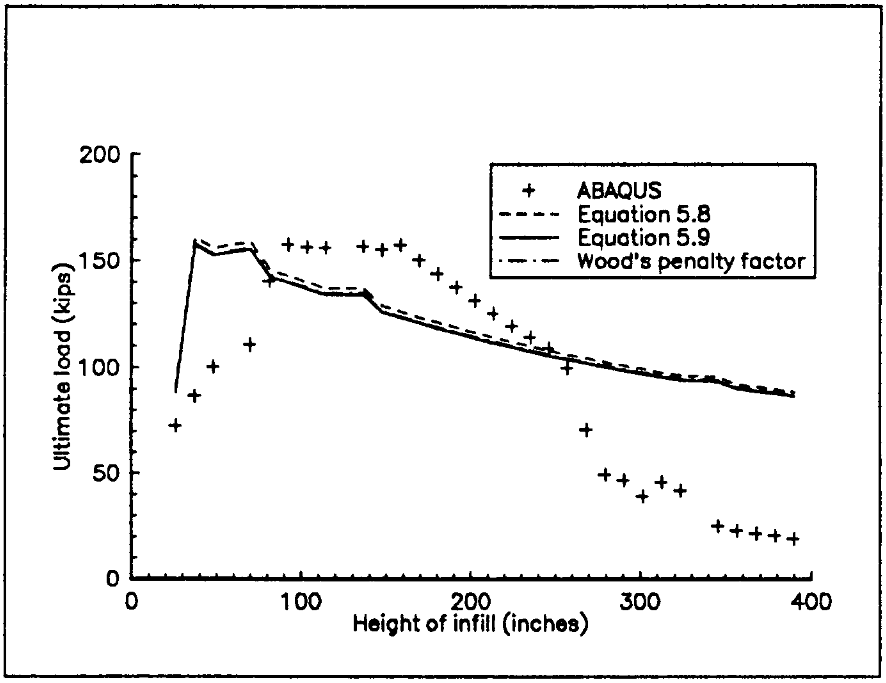

Figure 5.13. Ultimate load versus frame height using ABAQUS and equivalent strut models (Stafford-Smith and Carter, 1969) applying different penalty factors.

5.2.4 One Bay Rigidly Connected Infilled Frame Summary

The analytical method results were reasonably comparable to ABAQUS results. These methods included plastic theories (Liauw and Kwan, 1983), upper and lower bound solutions (Wood, 1978), and an equivalent strut analogy. Equation 2.1 (Stafford-Smith and Carter, 1969) was used to estimate the diagonal strut effective width. The simple infill representation is vital in analyzing complicated structures which may include many infilled frames.

5.3 One Bay Hinge Connection Infilled Frames

This section uses a typical one bay hinged connection infilled frame model with the same characteristics of a rigidly connected model. The four surrounding steel frame connections are hinged rather than rigid. The infill net thickness, t, varies to determine its effects for hinged connected frames. The frame columns can be identical or different. ABAQUS results are compared to those given by numerical methods.

5.3.1 Identical Column Infilled Frames

Only the infill net thickness varies for models with identical frame columns. ABAQUS ultimate loads are compared to those estimated by plastic theories (Liauw and Kwan, 1983), upper and lower bound solutions (Wood, 1978), and equivalent strut models, Figures 5.14 to 5.16. Note that lower bound solutions, Figure 5.15, coincide with the x-axis, and therefore, they do not appear. The modified formula for hinged connected frames, Equation 4.1, estimates the diagonal strut effective width. The model results are comparable to ABAQUS results. The closeness in the results, Figure 5.16, confirms that Equation 4.1 can reasonably estimate the model strut effective width for hinged connection frames. Equation 2.1 (Stafford-Smith and Carter, 1969) is meant for rigid connection frames rather than hinged connection frames.

5.3.2 Different Column Infilled Frames

It is common for the surrounding frame to have different columns. The study uses two sets of models to study the effect of different columns on the infilled ultimate strength. The models are typical infilled frames with a variable moment of inertia of one column. The ultimate load, as obtained from ABAQUS, differs depending on the direction of the load. Plastic theories (Liauw and Kwan, 1983) results are compared to ABAQUS results, Figures 5.18 and 5.19. Upper and lower bound solutions (Wood, 1978) are compared to ABAQUS, Figures 5.20 and 5.21. The lower bound solution coincides with

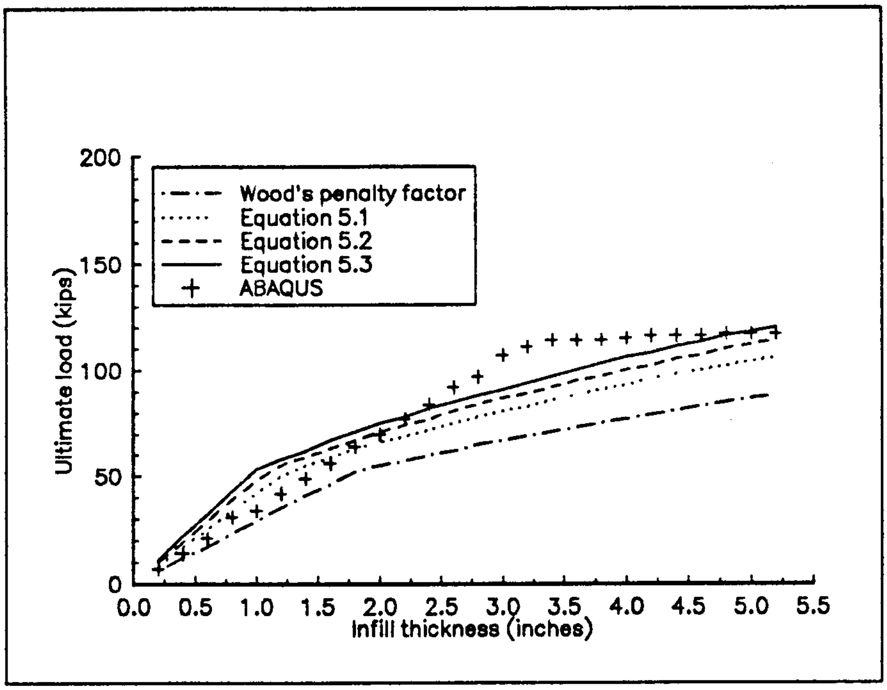

Figure 5.14. Ultimate load versus infill net thickness using ABAQUS and plastic theories (Liauw and Kwan, 1983) applying different penalty factors.

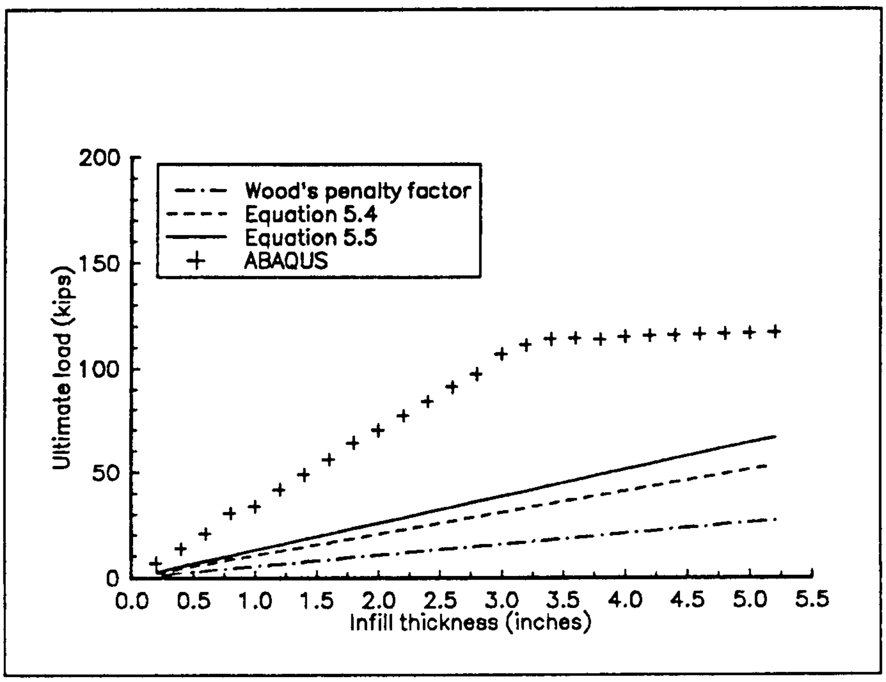

Figure 5.15. Ultimate load versus infill net thickness using ABAQUS and upper and lower bond solutions (Wood, 1978) applying different penalty factors.

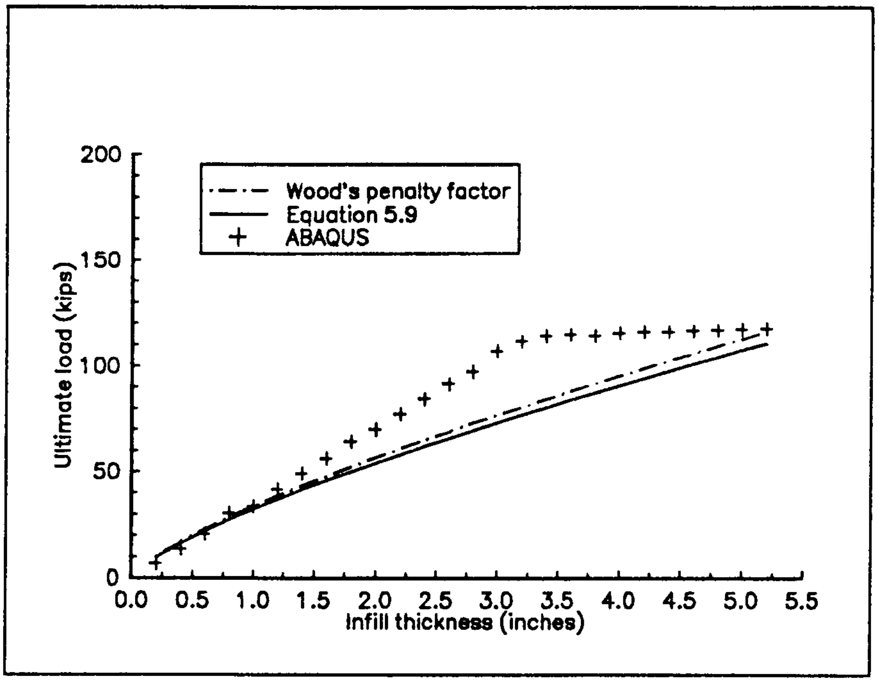

Figure 5.16. Ultimate load versus infill net thickness using ABAQUS and equivalent strut models, Equation 4.1, applying different penalty factors.

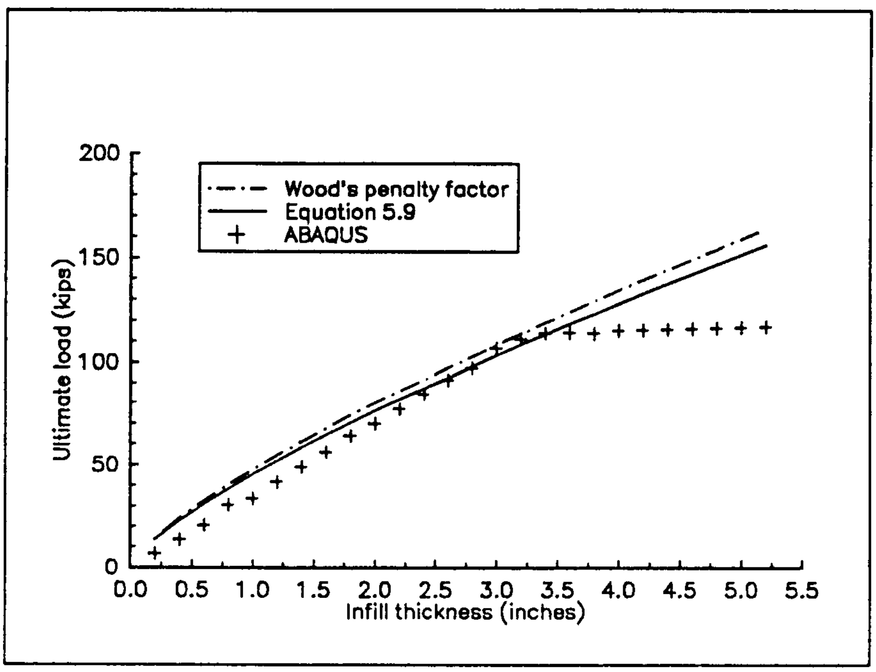

Figure 5.17. Ultimate load versus infill net thickness using ABAQUS and equivalent strut models (Stafford-Smith and Carter, 1969) applying different penalty factors.

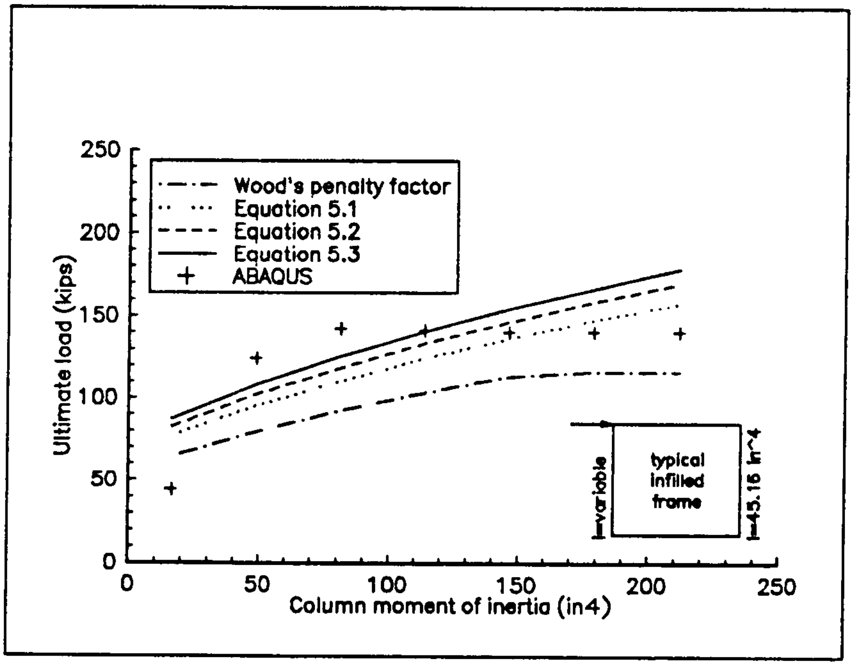

Figure 5.18. Ultimate load versus infill net thickness using ABAQUS and plastic theories (Liauw and Kwan, 1983) applying different penalty factors for different column models.

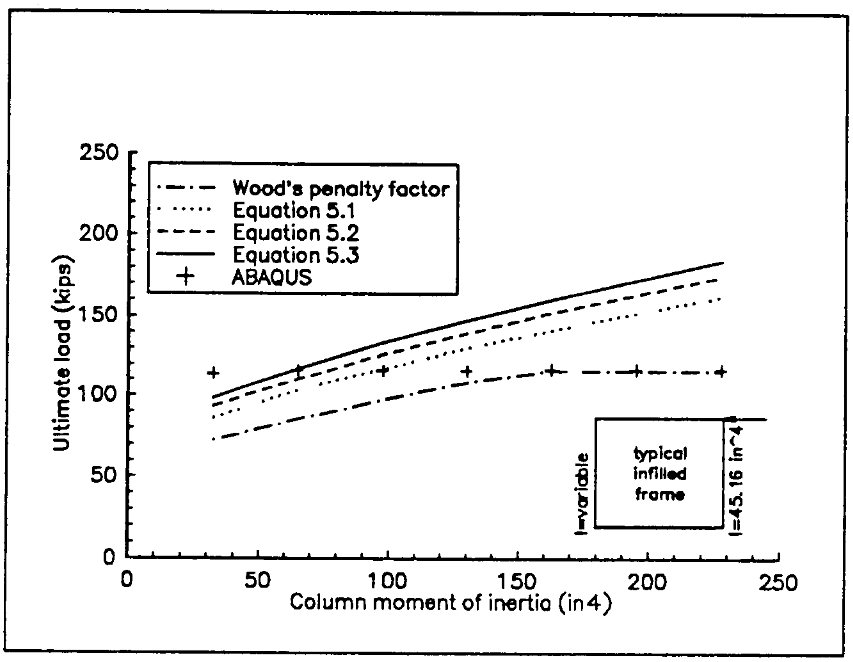

Figure 5.19. Ultimate load versus infill net thickness using ABAQUS and plastic theories (Liauw and Kwan, 1983) applying different penalty factors for different column models.

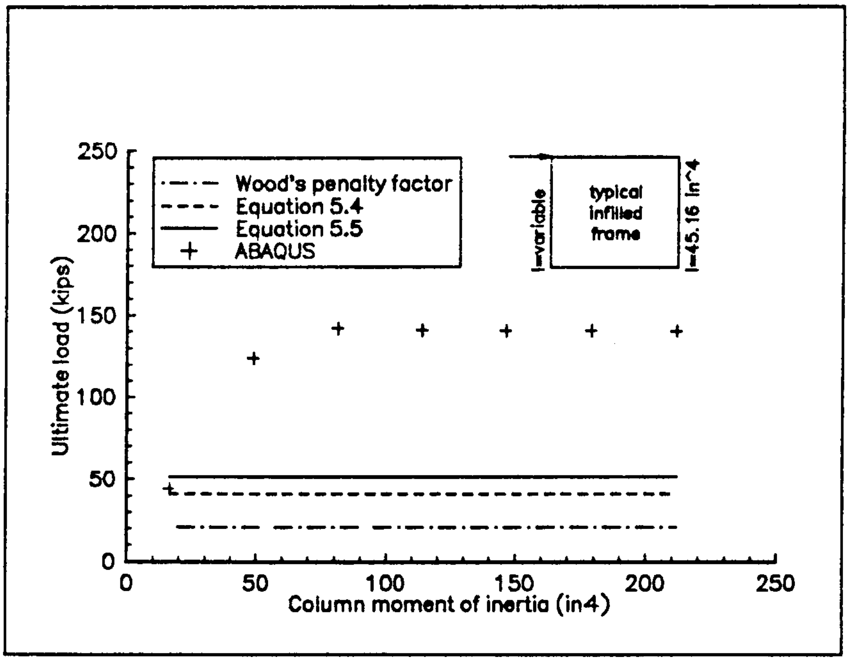

Figure 5.20. Ultimate load versus infill net thickness using ABAQUS and upper and lower bound solutions (Wood, 1978) applying different penalty factors for different column models.

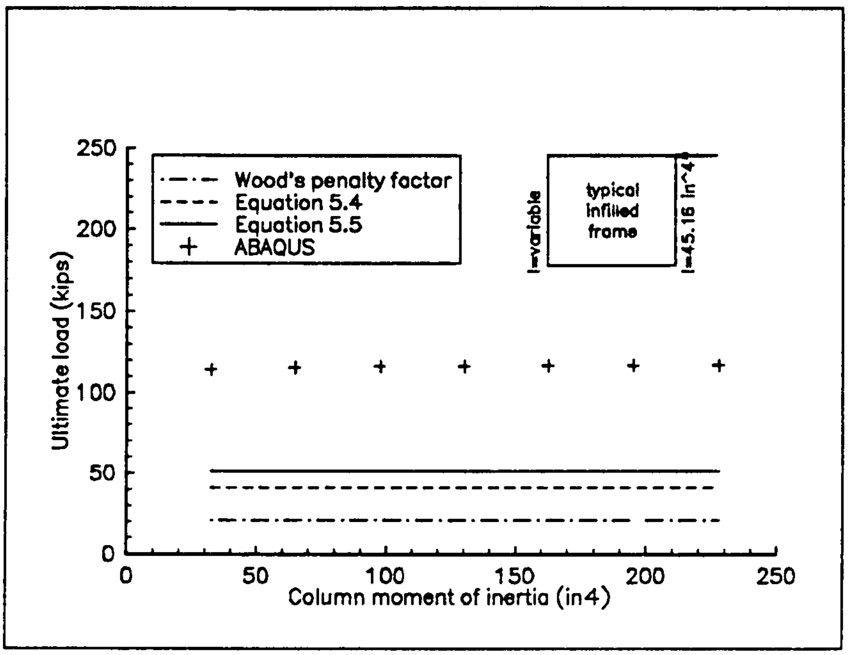

Figure 5.21. Ultimate load versus infill net thickness using ABAQUS and upper and lower bound solutions (Wood, 1978) applying different penalty factors for different column models.

the x-axis. Finally, ABAQUS results are compared to equivalent strut models, Figures 5.22 and 5.23. The strut model uses Equation 4.1 to estimate the strut effective width.

5.3.3 One Bay Hinged Connection Conclusion

Unlike the other analytical methods, an equivalent strut model was successfully capable of predicting the ultimate lateral strength of one bay hinged connection infilled frames. The model uses Equation 4.1 to estimate the effective strut width. The model was successfully tested in identical or different frame column situations. When the frame columns differ, the average values of moment of inertia are used in the calculations to obtain the effective width. Note that the equivalent strut method makes the structural analysis easier by allowing the infill to be replaced by a strut. The resultant structure is a plane frame structure which is easier to analyze than the complicated infill modeling.

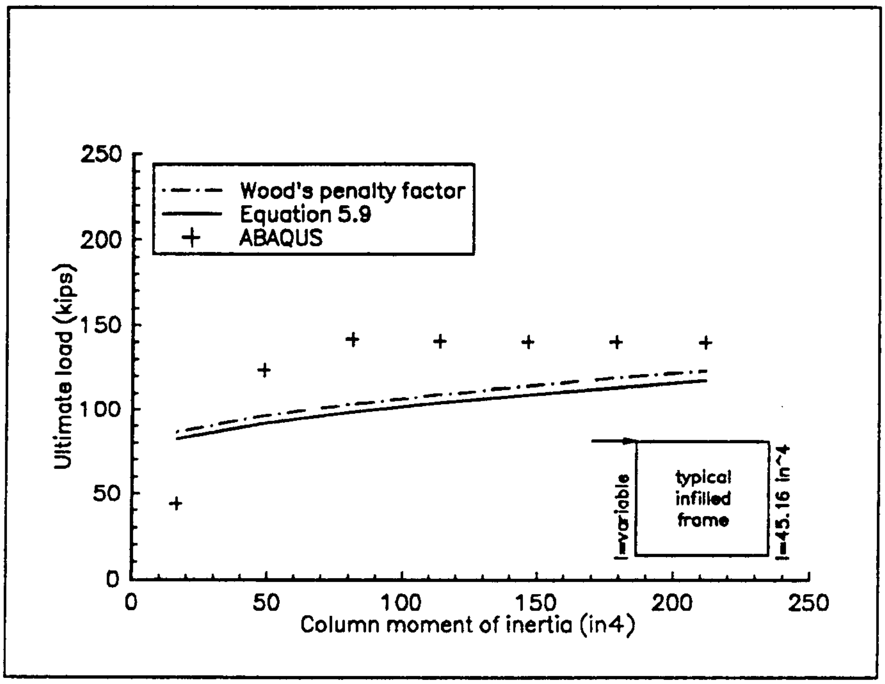

Figure 5.22. Ultimate load versus infill net thickness using ABAQUS and equivalent strut models, Equation 4.1, applying different penalty factors for different column models.

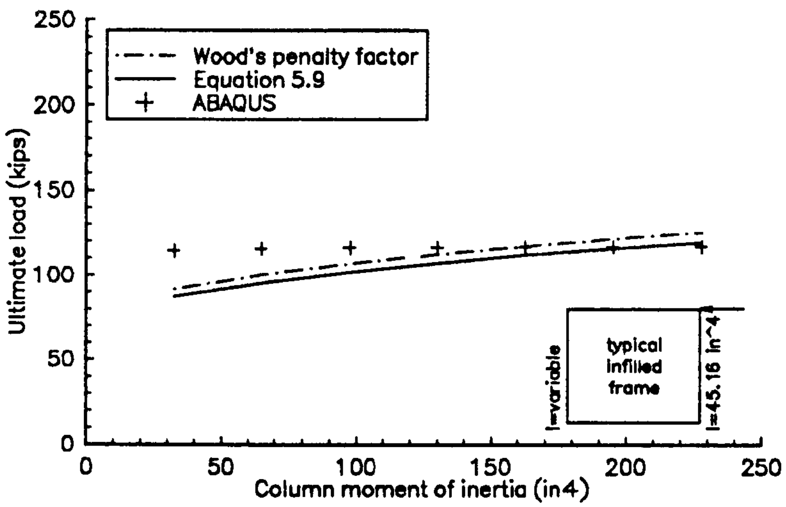

Figure 5.23. Ultimate load versus infill net thickness using ABAQUS and equivalent strut models, Equation 4.1, applying different penalty factors for different column models.

5.4 Two Bay Infilled Frames

A rigidly connected infilled frame model is constructed of two typical bays each identical to those of the one bay study. The middle column moment of inertia is twice that of an external column. The infill net thickness varies in both bays. The other infilled frame parameters are kept constant. ABAQUS model lateral loads are applied in two different ways. A single increasing load is applied at the top corner or two equal increasing loads are applied at the top first and middle columns. The two load models are more realistic since the floor system distributes the lateral load among the infilled frames in that floor. The ABAQUS run shows that applying one or two loads does not make a significant difference in the results, Figure 5.24. The figure also shows the equivalent strut

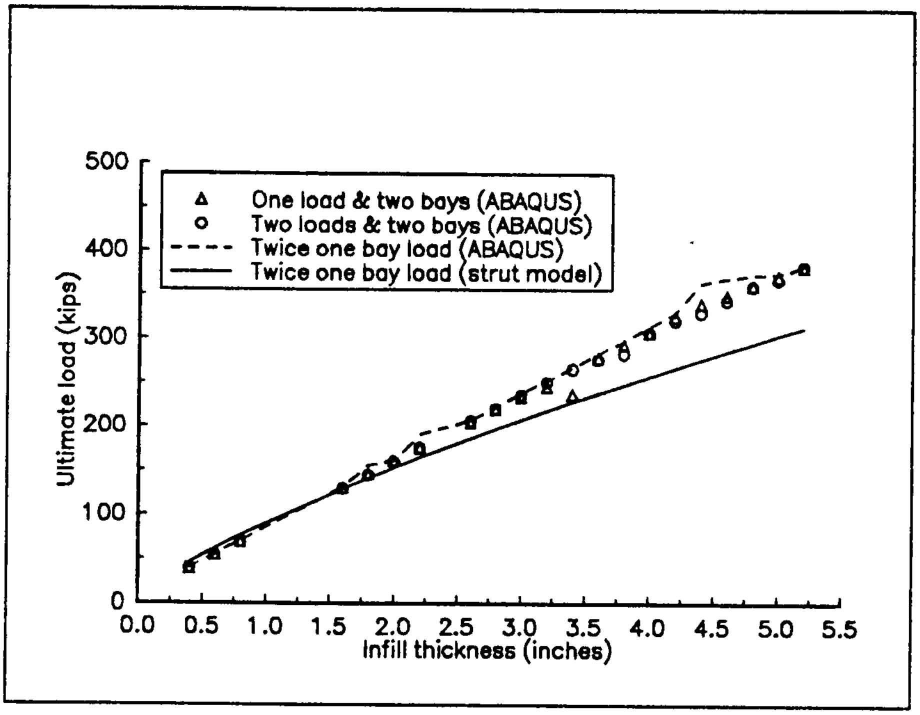

Figure 5.24. ABAQUS and equivalent strut model ultimate loads for two bay infilled frames.

model ultimate loads. The middle column thickness is divided between the two identical one bay infilled frames. Therefore, the equivalent strut model is identical for both bays. Figure 5.24 shows that the equivalent strut model failure load of a two bay infilled frame is obtained by adding the failure loads of both bays.

5.5 Three Bay Infilled Frames

This section investigates rigidly connected three bay infilled frames. The model consists of three identical typical bays. The only variable is the infill net thickness. The moment of inertia of an interior column is twice that of a typical column. Three identical lateral load are applied at the infilled frame corners. ABAQUS results for three bay frames are comparable to three-times the ultimate load of a one bay infilled frame. The

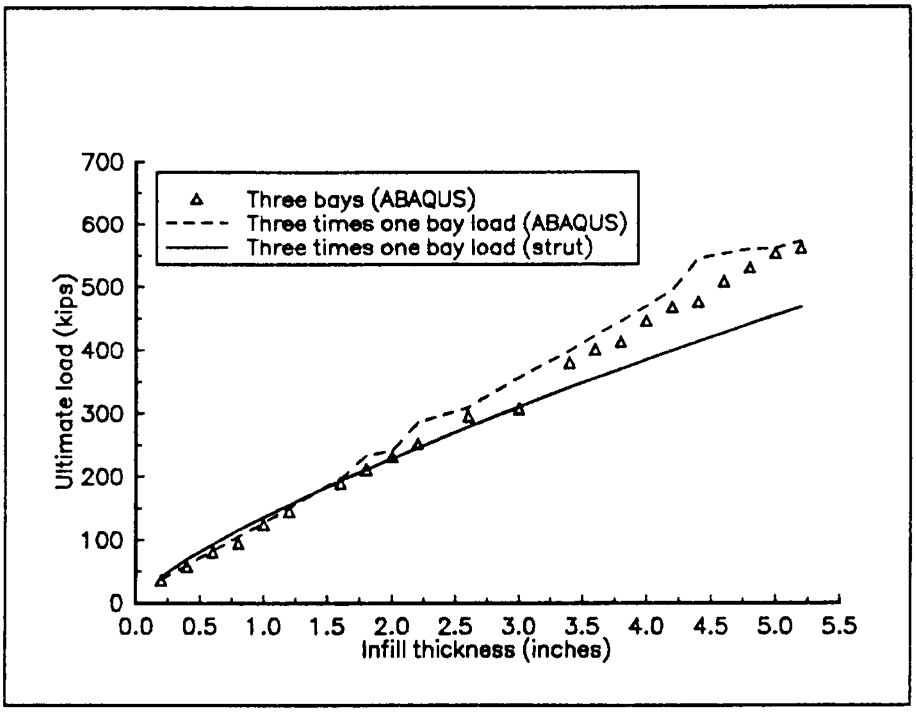

Figure 5.25. ABAQUS and equivalent strut model ultimate loads for three bay infilled frames.

figure also shows equivalent strut model estimated ultimate loads. A conclusion can be drawn that the ultimate load of a three bay infilled frame is about three times the ultimate load of a one bay infilled frame.

5.6 Vertical Loads

Infilled frames usually support not only lateral, but also gravity loads. Therefore, it is important to investigate the effects of vertical loads on the infilled frame ultimate loads. This section uses a typical one bay infilled frame with rigid connections. The only infilled variable parameter is the infill net thickness. Several vertical loads are examined for each infill net thickness. Two increasing identical concentrated vertical loads are applied at the frame top corners. An increasing lateral load is applied at the frame top corner up to failure. The vertical to lateral load ratio is kept constant. Table 5.2 shows ABAQUS results for different infill net thicknesses and different vertical loads. The vertical load is expressed as a fraction of horizontal load, and the vertical load tabulated is the total vertical load (sum of two loads). For considerably weak infills, the vertical loads do not significantly influence the ultimate load. For more reasonable infill strengths, the effect of the vertical load changes with differing vertical to horizontal load ratios. At moderate vertical to lateral load ratios, the vertical loads have little effect on the lateral strength. As the ratio of vertical to horizontal load increases to more than 1.0, the vertical loads seem to negatively influence the infilled frame strength. The cause of the reduction is presumably due to the decrease in the infill capacity resisting lateral loads since it supports the increasing vertical loads as well. A compression failure will occur sooner. In order to investigate the vertical load effects more thoroughly, many different vertical to lateral load ratios are applied to two typical infilled frame models with 0.6 and 4.0 inch thick infills, Figures 5.26 and 5.27. The results support the previous findings.

Table 5.2. ABAQUS results for different infill net thicknesses and different vertical to lateral load ratios.

Infill Thick. (in)	Ultimate Horizontal Load (kips)				Vertical/Ultimate Load Ratios		
	No Vertical	Vertical I	Vertical II	Vertical III	I	II	III
0.2	12.0	11.8	11.8	11.6	0.5	1.0	2.0
0.4	19.5	19.6	19.4	19.3	0.5	1.0	2.0
0.6	27.1	27.1	27.1	26.8	0.5	1.0	2.0
0.8	34.7	34.5	34.4	34.2	0.5	1.0	2.0
1.0	42.2	42.5	42.5	42.0	0.5	1.0	2.0
1.2	50.0	49.7	49.6	49.2	0.5	1.0	2.0
1.4	-	57.3	57.3	57.3	0.5	1.0	2.0
1.6	65.1	65.0	64.7	64.2	0.5	1.0	2.0
1.8	77.5	72.6	72.2	72.1	0.5	1.0	2.0
2.0	80.1	80.1	79.8	78.9	0.5	1.0	2.0
2.2	94.9	87.5	87.5	86.2	0.5	1.0	2.0
2.4	95.5	95.3	95.3	93.5	0.5	1.0	2.0
2.6	103.0	103.1	102.1	101.3	0.5	1.0	2.0
2.8	110.4	110.4	109.6	107.9	0.5	1.0	2.0
3.0	118.5	118.1	117.3	115.2	0.5	1.0	2.0
3.2	125.7	125.3	124.4	122.5	0.5	1.0	2.0
3.4	132.7	133.1	131.9	130.1	0.5	1.0	2.0
3.6	140.8	140.4	139.7	137.3	0.5	1.0	2.0
3.8	148.2	148.6	146.8	144.0	0.5	1.0	2.0
4.0	156.0	155.9	154.5	149.5	0.5	1.0	2.0
4.2	164.3	162.8	162.2	148.9	0.5	1.0	2.0
4.4	181.3	171.4	169.4	148.9	0.5	1.0	2.0
4.6	184.0	178.8	177.2	148.9	0.5	1.0	2.0
4.8	186.3	187.2	184.8	148.9	0.5	1.0	2.0
5.0	186.7	194.9	192.5	145.8	0.5	1.0	2.0
5.2	190.8	207.7	199.3	145.8	0.5	1.0	2.0

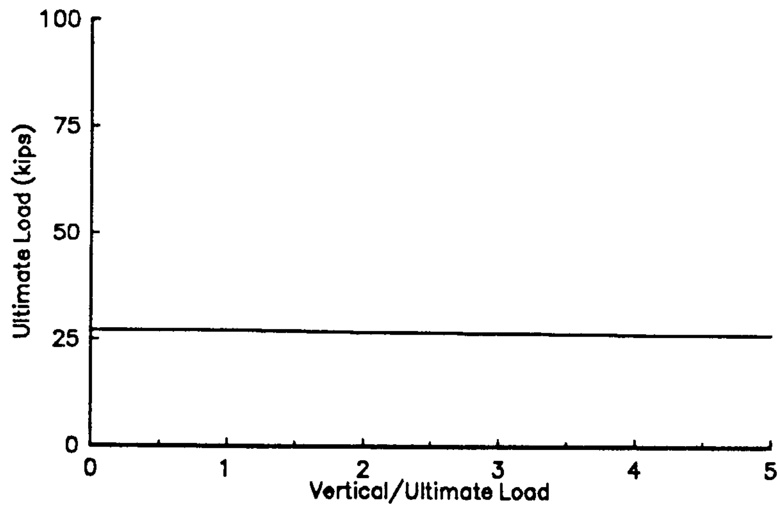

Figure 5.26. Ultimate load versus vertical to lateral load ratio for a 0.6 inch thick infill infilled frame model.

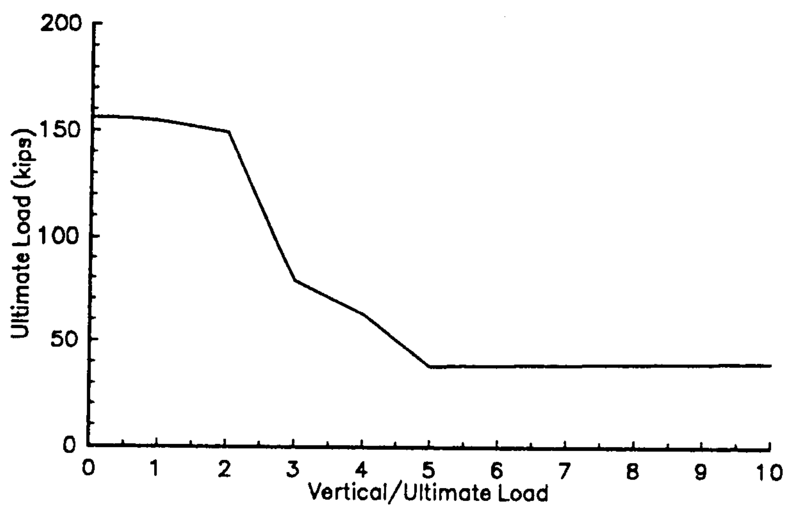

Figure 5.27. Ultimate load versus vertical to lateral load ratio for a 4.0 inch thick infill infilled frame model.

CHAPTER 6

SECANT STIFFNESS PARAMETRIC STUDY

6.1 Introduction

Stiffness is an important aspect of infilled frame structures. It defines the natural frequency of the building, and thus the response to an earthquake. The infill structure stiffness varies depending on the load history the structure experiences and therefore, the level of cracking of the structure. The initial stiffness is the elastic stiffness at low levels of lateral load. As the infill structure supports increasing lateral loads, its behavior changes. The level of applied load determines the infill cracking intensity. As the load progresses, the inelastic behavior dominates. Thus, the structural stiffness changes depending on the severity of the lateral load. Accordingly, it is necessary to define a loading level at which the stiffness is calculated. Two load levels are important, service and ultimate. Therefore, it is adequate to assume a load level at half of the ultimate. This level defines the secant stiffness.

This section performs a parametric study for secant stiffness on one, two, and three bay infilled frames. The case of vertical loads is also investigated to determine their effects. Infill variables include net thickness and height. Steel frame variables include frame height, and column and beam moment of inertia.

6.2 One Bay Infilled Frames

A typical infilled frame model has a net thickness, t, of 4.0 in (102 mm), a Young's modulus, E_c, of 1500 ksi (10340 MPa), and height, h', of 110.2 in (2800 mm). The model uses the concrete option to define the infill properties beyond the elastic range. The infill ultimate stress is 3.75 ksi (25.855 MPa) with a plastic strain of 0.0013. The infill plastic behavior starts at 1/3 of the ultimate stress, Figure 3.11. The finite element model uses the softened interface behavior option to describe the localized mortar crushing that tends to occur at the infill corners. The clearance, c, at which the steel-infill contact pressure starts is set to 0.04 in (1 mm). At zero clearance, the pressure, p, is set to 3.0 ksi (20.684 MPa) which represents the mortar ultimate stress, Figure 3.15. The steel frame has a Young's modulus, E_s, of 30,000 ksi (205500 MPa), yield stress of 36 ksi (248.2 MPa), length, L, of 141.7 in (3600 mm), and height, h, of 114.2 in (2901 mm). The column moment of inertia, I_h, is 45.16 in^4 (18.8X10^6 mm^4) and the beam moment of inertia, I_b, is 109.7 in^4 (45.66X10^6 mm^4). The diagonal horizontal angle, θ, is 37.87°.

Only one infilled frame parameter (the infill thickness or height, or the moment of inertia of a frame column or beam) changes at a time. In each investigation, ABAQUS results are compared with analytical equivalent strut methods, 1, 2, and 3. Method 1 uses Equation 2.1 (Stafford-Smith and Carter, 1969); method 2 uses Equation 2.4 (Klingner, 1980); method 3 uses Equations 2.5 and 2.7 (Chrysostomou et al., 1988).

6.2.1 One Bay Rigidly Connected Infilled Frames

It was suggested in chapter 3 that analytical methods 2 and 3 are to predict the infilled frame secant stiffness. It was proven in chapter 4 that methods 1, 4, and 5 can successfully estimate the infilled frame initial stiffness. Method 4 uses Equation 2.8 (Liauw and Kwan 1984); method 5 calculates the stiffness directly and uses Equation 2.3 (Barua and Mallick 1977). In order to thoroughly evaluate the ability of the different analytical methods to predict the secant stiffness, a typical infilled frame model is used. The only variable in the model is the infill net thickness. Figure 6.1 shows ABAQUS results and those given by various analytical methods, 1 to 5. The figure does not determine which method is the most capable of estimating the infilled frame secant stiffness at 50% of the ultimate loads. However, method 1 has successfully predicted the infilled frame initial stiffness and the ultimate load. Therefore, method 1 is the best

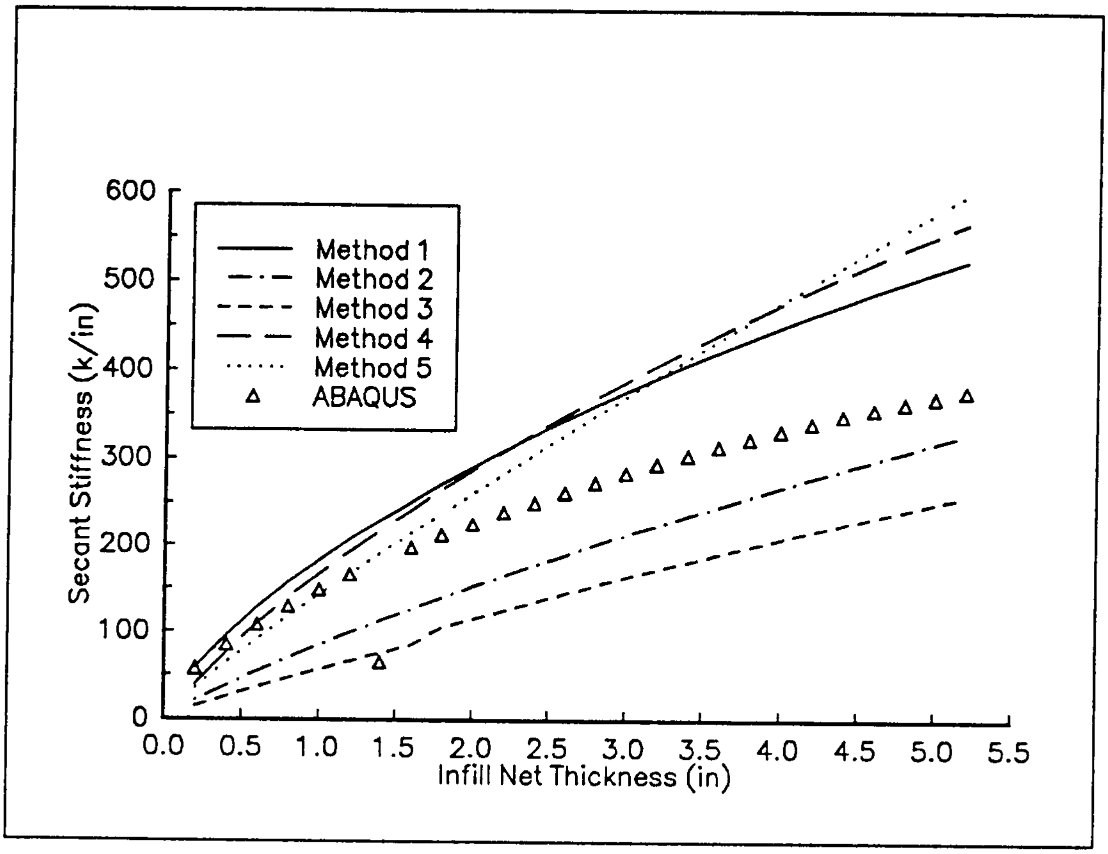

Figure 6.1. ABAQUS and analytical methods infilled frame secant stiffness.

candidate to use to predict the infill secant stiffness. In order to adopt method 1 to predict the secant stiffness, a penalty factor is applied. The penalty factor is to reflect the infilled frame stiffness reduction due to the infilled frame degrading behavior. The penalty factor is applied on the infill Young's modulus or the strut effective width. The penalty factor is obtained by equating ABAQUS secant stiffnesses to those given by method 1. The best fit quadratic formula, Equation 6.1, is obtained using the penalty factor points as a function of nominal m, Equation 2.16. In the same manner, a linear and a constant penalty factor, Equations 6.2 and 6.3 respectively, are obtained. One hundred twenty-four different infilled frame models are used to develop the penalty factor formulas.

$$\nu_p = 3.51\, m^2 + 0.474\, m + 0.646 \tag{6.1}$$

$$\nu_p = 1.23\, m + 0.633 \tag{6.2}$$

$$\nu_p = 0.662 \tag{6.3}$$

Figure 6.2 shows the infilled frame secant stiffness at 50% of ultimate loads versus the infill net thickness. The figure shows that ABAQUS and equivalent strut model results are comparable. The equivalent strut model uses method 1 (Stafford-Smith and Carter, 1969) to estimate the effective strut width. The penalty factors applied on the infill Young's modulus are given by Equations 6.1, 6.2, and 6.3. The success of the equivalent strut prediction of the infill secant stiffness leads to try the method with other infilled frame variables. Figures 6.3 to 6.5 show ABAQUS and equivalent strut model results applying different penalty factors, Equations 6.1 to 6.3. Figure 6.3 shows secant stiffness versus the infilled frame height. The figure shows the close prediction of the equivalent

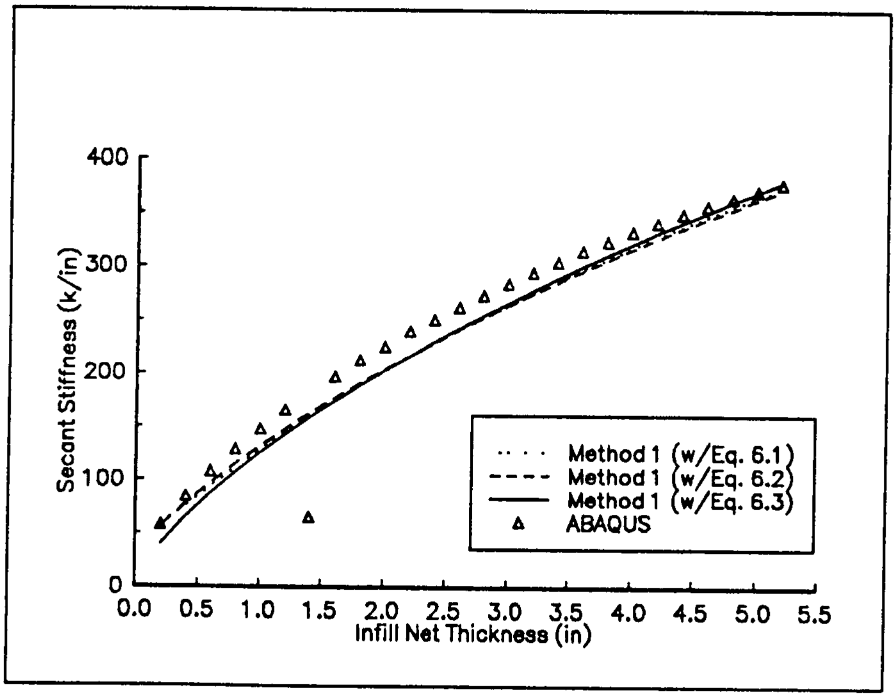

Figure 6.2. ABAQUS and method 1 secant stiffness versus infill net thickness using different penalty factors, Equations 6.1, 6.2, and 6.3.

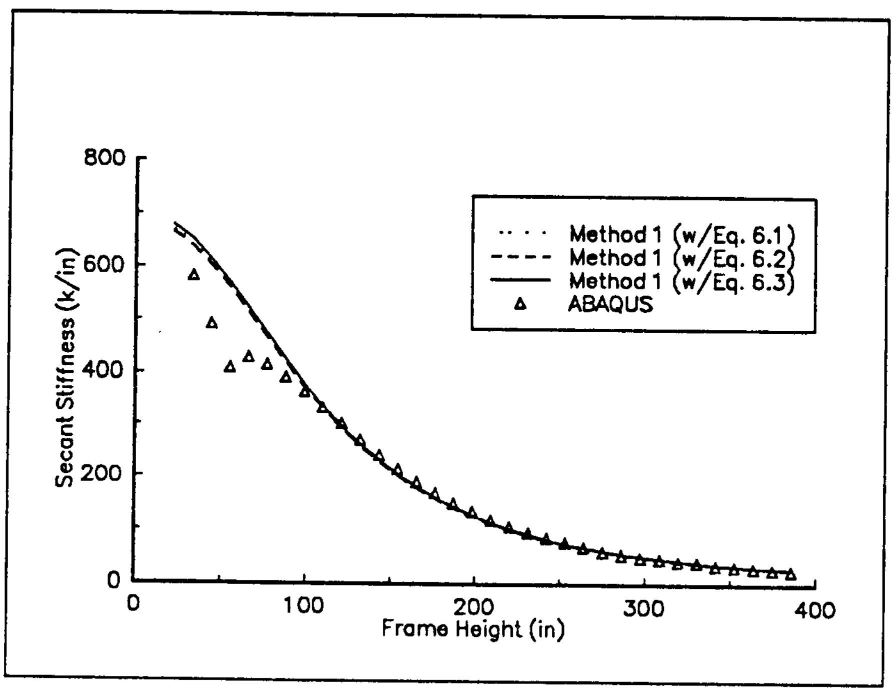

Figure 6.3. ABAQUS and method 1 secant stiffness versus frame height using different penalty factors, Equations 6.1, 6.2, and 6.3.

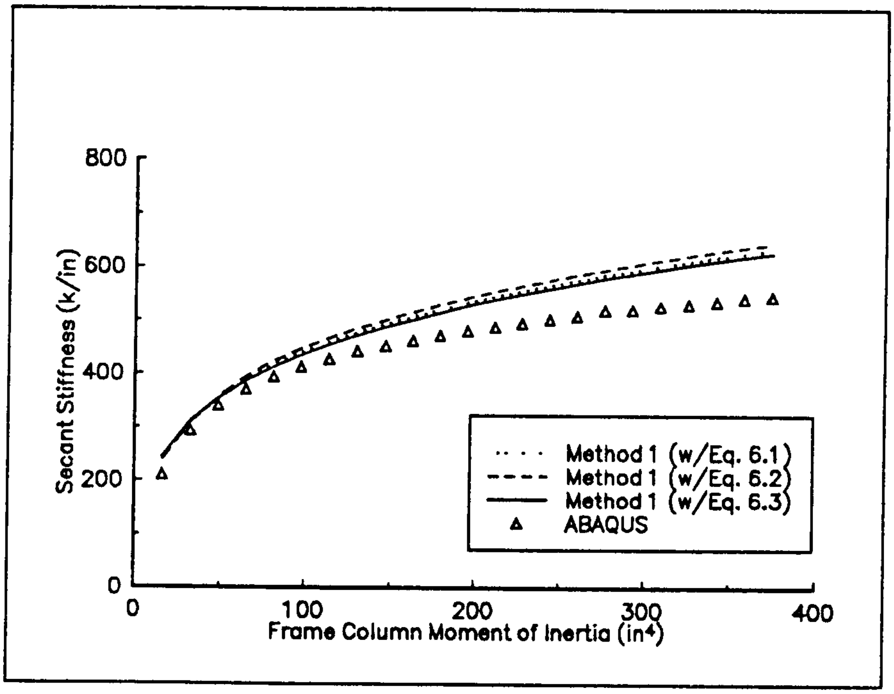

Figure 6.4. ABAQUS and method 1 secant stiffness versus frame column moment of inertia using different penalty factors, Equations 6.1, 6.2, and 6.3.

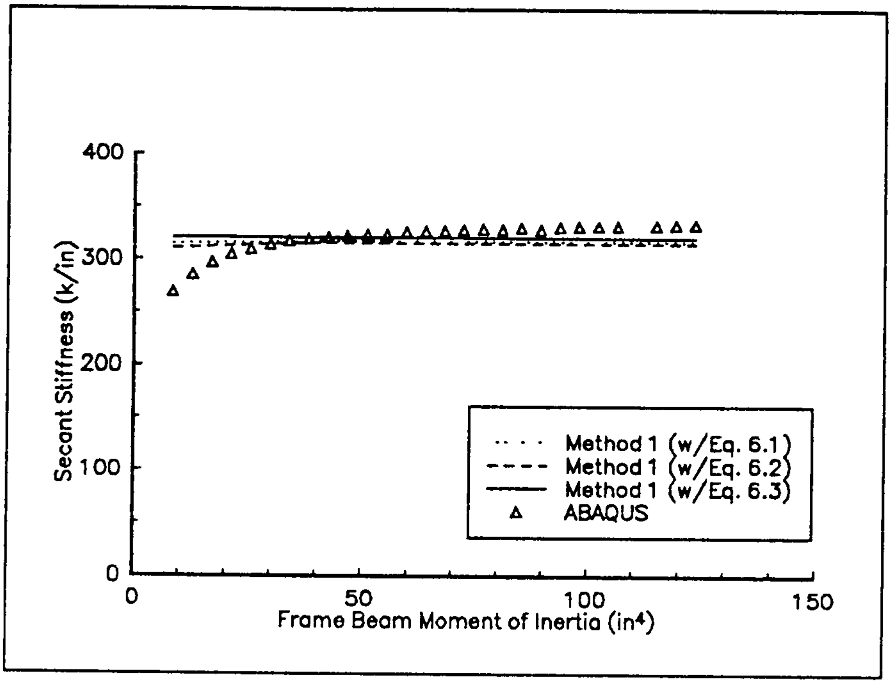

Figure 6.5. ABAQUS and method 1 secant stiffness versus frame beam moment of inertia using different penalty factors, Equations 6.1, 6.2, and 6.3.

strut model. Figure 6.4 shows secant stiffness versus the frame column moment of inertia. The figure shows that ABAQUS results are fairly close to those given by the equivalent strut method (Stafford-Smith and Carter, 1969) applying different penalty factors, Equations 6.1 and 6.2. Figure 6.5 shows secant stiffness versus the frame beam moment of inertia. The figure shows that the equivalent strut method are comparable to ABAQUS results. The figure also indicates the same finding from initial stiffness that the beam moment of inertia does not affect the stiffness after a moderate value. Figures 6.2 to 6.5 reveal that applying either penalty factor given by Equation 6.1 or 6.2 gives identical results. Thus the quadratic, Equation 6.1, is no longer considered. There is no significant difference between the penalty factor formulas, 6.2 and 6.3. Equation 6.3 is the best to calculate the penalty factor since it is the simplest, but more cases need be studied before accepting that conclusion. These cases include one bay hinge connection and multiple bay infilled frames.

6.2.2 One Bay Hinge Connection Infilled Frames

This section uses a typical one bay hinged connected infilled frame model with the same characteristics of a rigidly connected model. The four surrounding steel frame connections are hinged rather than rigid. The infill net thickness, t, is the only variable. As for rigid connection infilled frames, secant stiffnesses are calculated at 50% of the ultimate loads. ABAQUS results are compared to those given by an equivalent strut analogy. Equation 4.1 estimates the effective equivalent strut width. Equation 4.1 was introduced in chapter 4 to reflect the reduction in stiffness due to the frame hinge connections. Equation 4.1 is a modified form of Equation 2.1 (Stafford-Smith and Carter, 1969). A penalty factor, Equation 6.2 or 6.3, is applied on the infill Young's modulus to reduce the strut stiffness to reflect the infill degrading behavior. The penalty factor can applied on the strut effective width keeping the same infill Young's modulus. ABAQUS and equivalent strut model results compare well, Figure 6.6. The difference between Equations 6.2 and 6.3 is negligible.

6.3 Two Bay Infilled Frames

The infilled frame model in this section is constructed of two one bay infilled frames identical to those in the one bay study. The middle column has twice the area and moment of inertia of a typical column. Exterior columns are typical and identical to one bay frame columns. The only variable in this model is the infill net thickness, which varies in both bays. The failure load and thereafter the secant stiffness at 50% of the

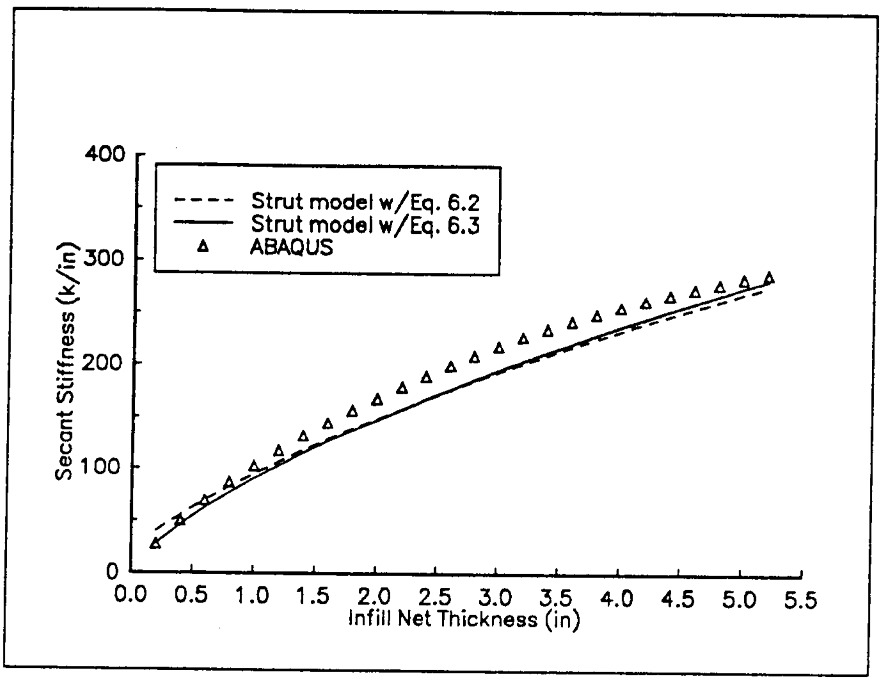

Figure 6.6. ABAQUS and equivalent strut method secant stiffness versus infill net thickness for hinge connection infilled frames. Equation 4.1 estimates the effective equivalent strut width applying a penalty factor, Equation 6.2 or 6.3.

ultimate depend on how and where the lateral loads are applied. The floor system distributes the load among the infilled frames. Therefore, it is realistic to apply the lateral loads equally at the infilled frame corners. Two increasing identical lateral loads are applied at the corners of the ABAQUS models. The equivalent strut model consists of two identical frames with diagonal struts. The strut model beams and columns are identical to those in the ABAQUS models. Equation 2.1 (Stafford-Smith and Carter, 1969) estimates the effective width of the struts. A penalty factor, Equation 6.2 or 6.3, is applied on the infill Young's modulus to reflect the degrading behavior of infilled frames. GTSTRUDL is used to analyze the equivalent strut model. Two lateral loads are applied at the strut model corners, exactly as in ABAQUS models. Figure 6.7 shows that ABAQUS and strut model results are comparable. The figure also indicates that Equation 6.3 is accurate enough in calculating the penalty factor.

6.4 Three Bay Infilled Frames

The infilled frame model is extended by adding a third bay. The three bays are identical to those in the one bay study. The infill net thickness in the three bays varies simultaneously. The other infilled frame parameters are kept constant. The middle columns have twice the area and the moment of inertia of an exterior column. The exterior columns are identical to those in one bay infilled frames. Three identical increasing lateral loads are applied at the frame corners. The load is applied in the same manner for ABAQUS and strut models. The equivalent strut model consists of three bays with the same beams and columns as the ABAQUS models. Equation 2.1 (Stafford-Smith and Carter, 1969) estimates the effective width of the diagonal struts. A penalty factor,

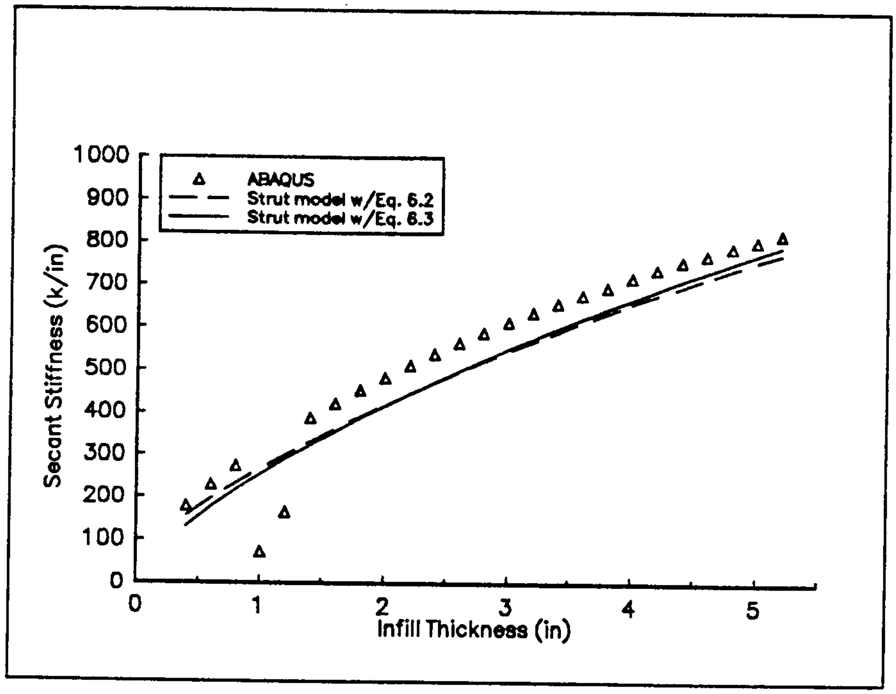

Figure 6.7. Scant stiffness versus infill net thickness for two bay infilled frames.

Equation 6.2 or 6.3, is applied on the infill Young's modulus to reflect the degrading behavior of infilled frames. GTSTRUDL is used to analyze the equivalent strut model. ABAQUS and strut model results are comparable, Figure 6.8. The figure also supports that Equation 6.3 is adequate to calculate the penalty factor. Thus, Equation 6.3 is adopted to compute the penalty factor.

6.5 Vertical Loads

Unlike lateral forces, from winds or earthquakes, gravity loads are constantly applied. Thus, infilled frames support both lateral and vertical loads simultaneously. This section studies the effect of vertical loads on the infilled frame secant stiffness. The secant stiffness is taken at 50% of the ultimate load. The analyses are performed for one bay infilled frames. The infilled frame model is a typical one with the infill thickness as

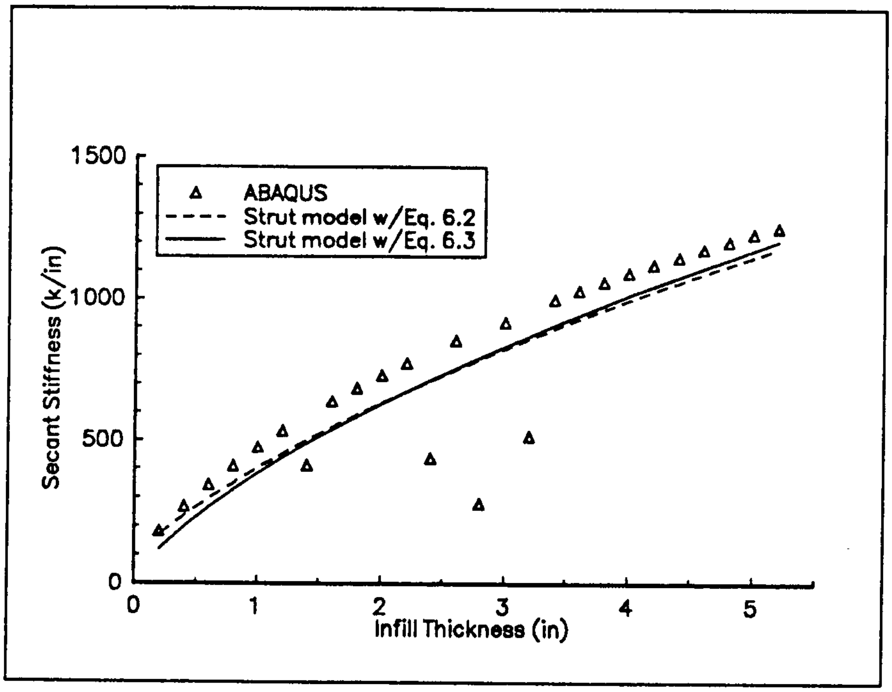

Figure 6.8. Scant stiffness versus infill net thickness for three bay infilled frames.

the only variable. Several vertical loads are examined for each infill net thickness. Two increasing identical concentrated vertical loads are applied at the frame top corners. One increasing lateral load is applied at the frame top corner up to failure. The vertical to lateral load ratio is kept constant up to failure. Table 6.1 shows ABAQUS results for different infill net thicknesses and different vertical to lateral load ratios. The vertical load is expressed as a fraction of the ultimate horizontal load, and the vertical load tabulated is the total vertical load (sum of two loads). The table reveals that vertical loads increase the infilled frame secant stiffness. In order to investigate the vertical load effects more thoroughly, two typical infilled frame models with 0.6 and 4.0 inch thick infills are examined. Many different vertical to lateral load ratios are applied on the two infilled frame models, Figures 6.9 and 6.10. The results support the previous findings.

Table 6.1. ABAQUS secant stiffness versus infill net thickness and vertical to lateral load ratio.

Infill Thick. (in)	Secant Stiffness (k/in)				Vertical/Lateral Load Ratios		
	No Vertical	Vertical I	Vertical II	Vertical III	I	II	III
0.2	57.2	57.6	58.1	59.0	0.50	1.00	2.00
0.4	84.4	85.6	86.7	89.1	0.50	1.00	2.00
0.6	107.8	109.8	111.8	116.2	0.50	1.00	2.00
0.8	128.7	131.6	134.6	140.9	0.50	1.00	2.00
1.0	147.7	151.6	155.7	164.4	0.50	1.00	2.00
1.2	165.3	170.1	175.2	186.3	0.50	1.00	2.00
1.4	64.9	187.5	193.7	207.7	0.50	1.00	2.00
1.6	196.9	203.7	211.0	227.6	0.50	1.00	2.00
1.8	212.2	219.2	227.8	247.4	0.50	1.00	2.00
2.0	224.6	233.8	243.6	265.7	0.50	1.00	2.00
2.2	239.3	247.8	258.9	284.0	0.50	1.00	2.00
2.4	249.9	261.2	273.7	301.7	0.50	1.00	2.00
2.6	261.6	274.4	287.7	319.1	0.50	1.00	2.00
2.8	272.9	286.6	301.5	335.7	0.50	1.00	2.00
3.0	283.9	298.5	314.5	352.1	0.50	1.00	2.00
3.2	294.2	310.0	327.2	368.2	0.50	1.00	2.00
3.4	304.1	321.2	339.7	384.0	0.50	1.00	2.00
3.6	314.0	331.5	351.4	398.0	0.50	1.00	2.00
3.8	322.8	341.7	362.5	410.9	0.50	1.00	2.00
4.0	332.0	352.6	375.1	426.9	0.50	1.00	2.00
4.2	340.3	361.6	385.3	437.9	0.50	1.00	2.00
4.4	349.0	370.5	394.8	449.0	0.50	1.00	2.00
4.6	356.4	379.2	404.4	459.4	0.50	1.00	2.00
4.8	363.6	387.9	414.1	469.4	0.50	1.00	2.00
5.0	370.2	396.7	427.4	476.2	0.50	1.00	2.00
5.2	377.2	404.2	433.4	485.2	0.50	1.00	2.00

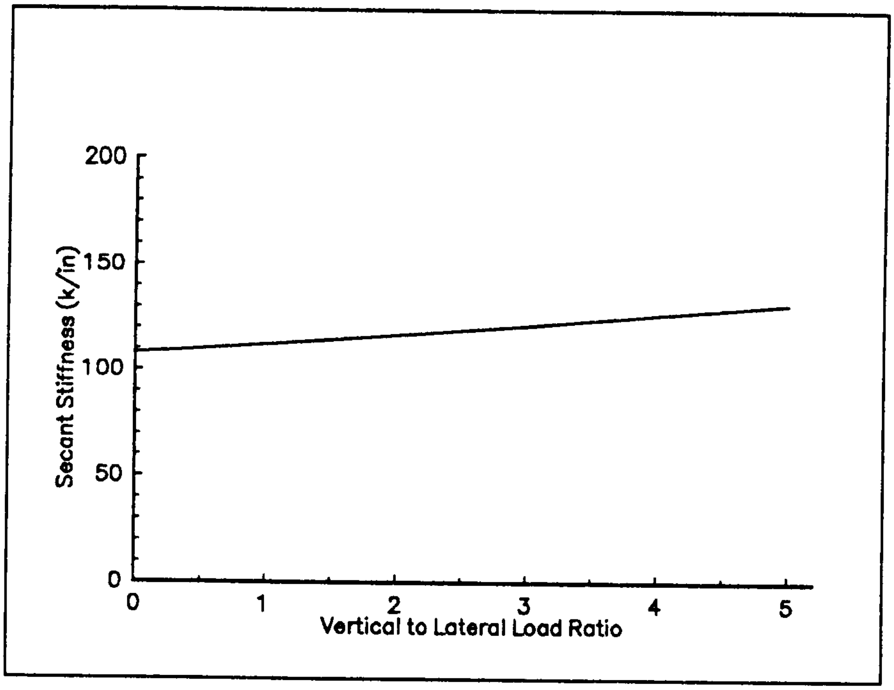

Figure 6.9. Secant stiffness versus vertical to lateral load ratio for a 0.6 inch thick infill infilled frame model.

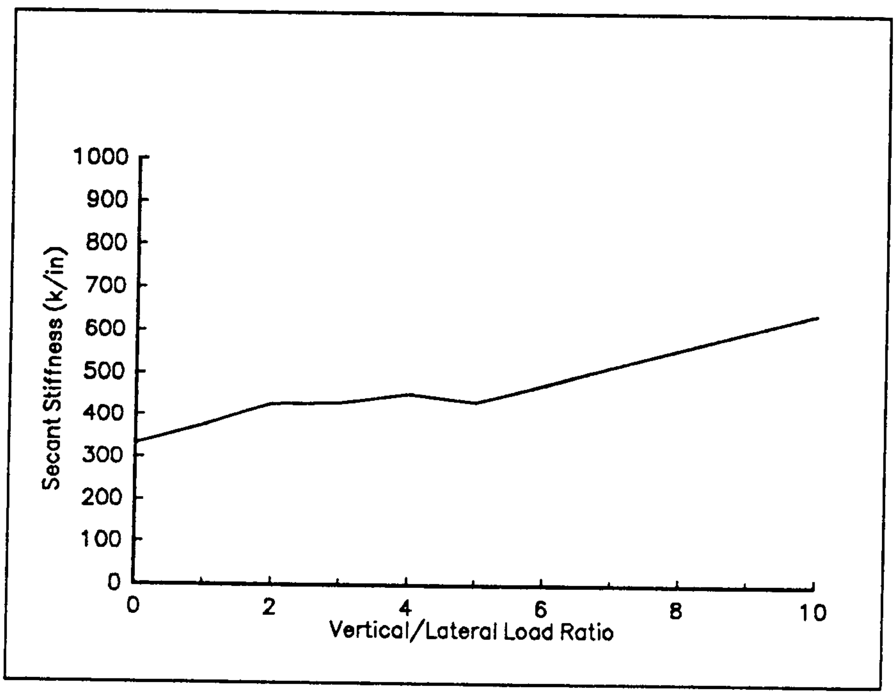

Figure 6.10. Secant stiffness versus vertical to lateral load ratio for a 4.0 inch thick infill infilled frame model.

Vertical loads have similar effects on the equivalent strut models. Vertical loads increase the strut model secant stiffness. However the vertical load affect is not as much as on the ABAQUS model. Figures 6.11, 6.12, and 6.13 show ABAQUS and equivalent strut model (Stafford-Smith and Carter, 1969) secant stiffness versus infill net thickness under vertical to lateral load ratio of 0.5, 1.0, and 2.0 respectively. The figures show that ABAQUS and strut model secant stiffness are reasonably comparable. Vertical to lateral load ratios represent total vertical loads to lateral load. Only one half of the total vertical load affects the equivalent strut model, the half on the windward column. The other half which acts on the leeward column does not affect the equivalent strut model behavior.

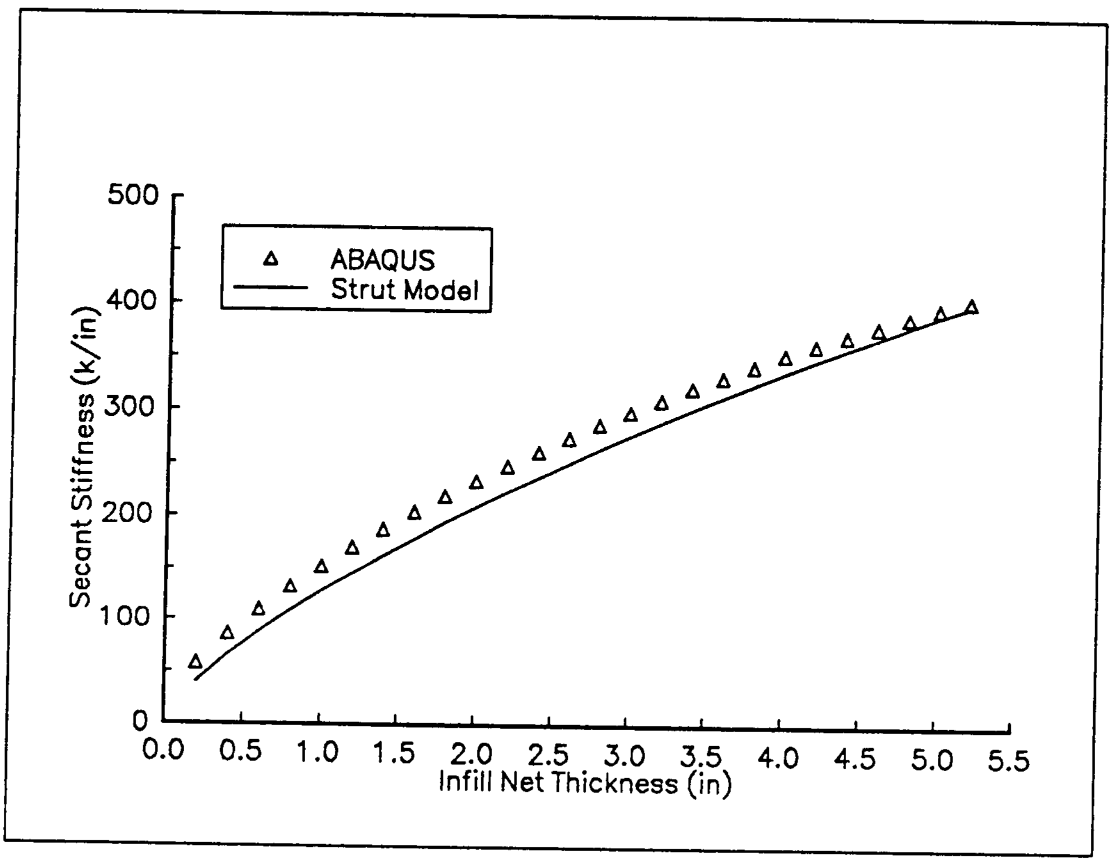

Figure 6.11. ABAQUS and strut model secant stiffness versus infill net thickness under vertical to lateral load ratio of 0.5.

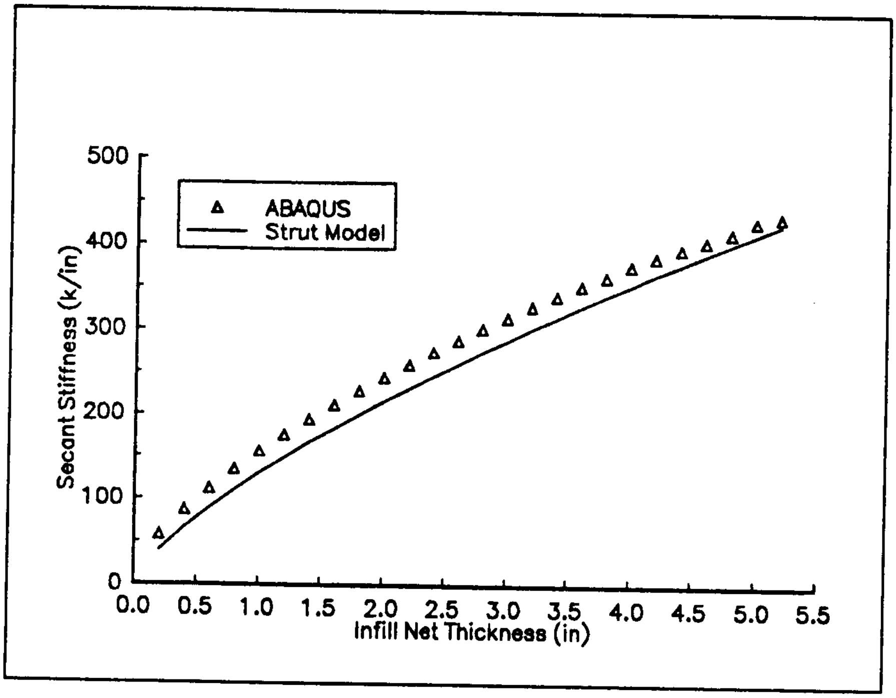

Figure 6.12. ABAQUS and strut model secant stiffness versus infill net thickness under vertical to lateral load ratio of 1.0.

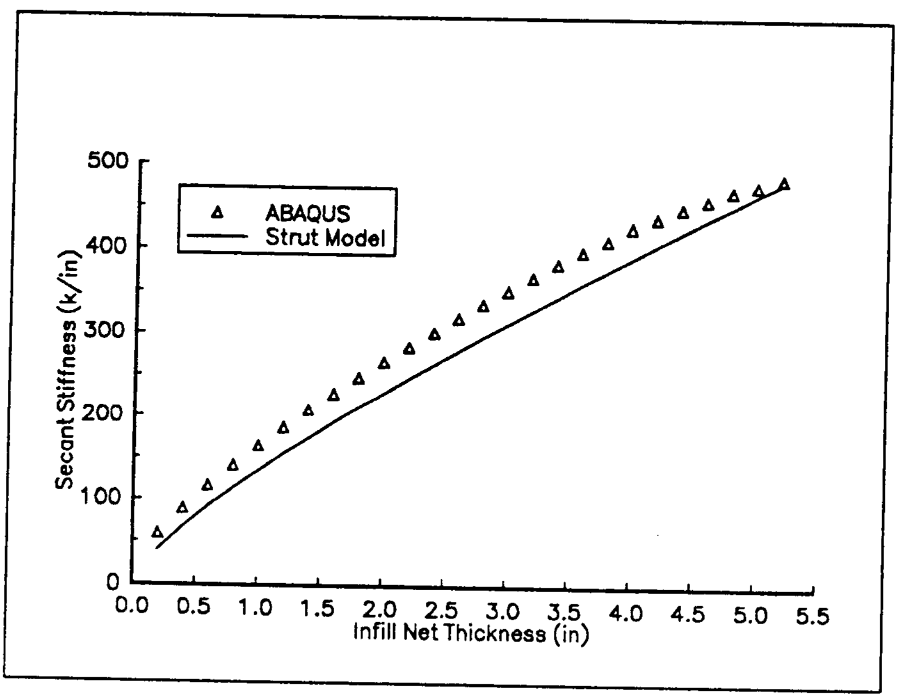

Figure 6.13. ABAQUS and strut model secant stiffness versus infill net thickness under vertical to lateral load ratio of 2.0.

CHAPTER 7

OTHER INFILLED FRAME PARAMETERS

7.1 Introduction

The parametric study in previous chapters considered unreinforced masonry infilled frames under monotonic lateral loads. These infilled frames were constructed of solid infills without door or window openings. No shear connectors were used at the frame infill boundary. The infill was assumed to perfectly fit the steel frame without any initial gaps. Infilled frames in general are not limited to these conditions and lateral loads can vary in magnitude and direction. Infilled frames may include panels with openings, frame top beam and infill initial gaps, reinforced infills, frame column and panel shear connectors, and load reversal. This chapter examines these various types and conditions of infilled frames.

The model used in this section is a typical infilled frame model with the necessary changes for each case. It has a net thickness, t, of 4.0 in (102 mm), a Young's modulus, E_c, of 1500 ksi (10340 MPa), and height, h', of 110.2 in (2800 mm). The model uses the concrete option to define the infill properties beyond the elastic range. The infill ultimate stress is 3.75 ksi (25.855 MPa) with a plastic strain of 0.0013. The infill plastic behavior starts at 1/3 of the ultimate stress, Figure 3.11. The finite element model uses the softened interface behavior option to describe the localized mortar crushing that tends to occur at the infill corners. The clearance, c, at which the steel-infill contact pressure starts is set to 0.04 in (1 mm). At zero clearance, the pressure, p, is set to 3.0 ksi (20.684 MPa) which represents the mortar ultimate stress, Figure 3.15. The steel frame has a Young's modulus, E_s, of 30,000 ksi (205500 MPa), yield stress of 36 ksi (248.2 MPa), length, L, of 141.7 in (3600 mm), and height, h, of 114.2 in (2901 mm). The column moment of inertia, I_h, is 45.16 in^4 ($18.8X10^6$ mm^4) and the beam moment of inertia, I_b, is 109.7 in^4 ($45.66X10^6$ mm^4). The diagonal horizontal angle, θ, is 37.87°.

7.2 Reinforced Infills

The behavior of the infill in this case may depend on the mode of failure. Therefore, two models with different modes of failure are used in this section. One model uses an infill net thickness of 4.0" which produces a corner crushing mode. The other model represents a diagonal failure mode with an infill net thickness of 1.2". Horizontal and vertical number 14 rebars are used. Horizontal rebars are spaced at 7.78" and vertical rebars at 7.32". Figure 7.1 shows the behavior of the 4.0" infill models with horizontal, vertical, both horizontal and vertical rebars, and no rebars. The figure reveals that reinforcements have no significant influence on the infilled frame behavior when corner crushing is the mode of failure. The 1.2" thick infill models also showed that the reinforcing had no effect, Figure 7.2. The finding is not conclusive since it may indicate a numerical problem. However, this result confirms the role that the infill plays as a compressive diagonal strut. Amos (1985) indicates that infill reinforcements do not noticeably effect the strength or stiffness of infilled frames. Recent experimental tests on panels with bed joint reinforcements (Hendry and Liauw, 1992) show that reinforcements

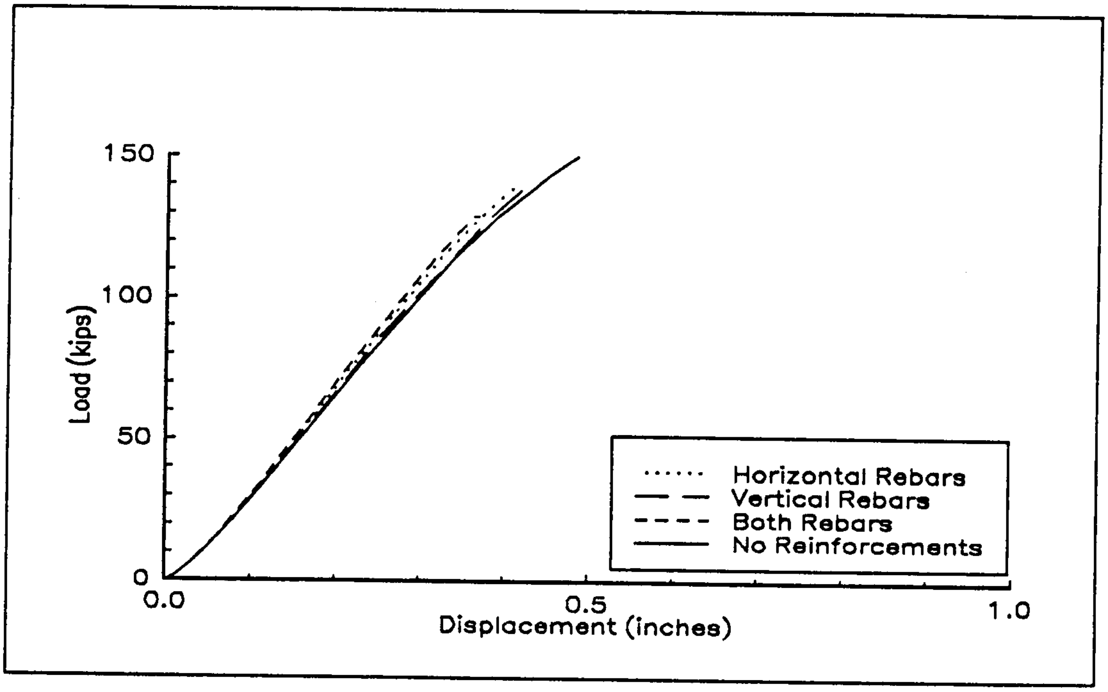

Figure 7.1. The effects of different infill reinforcements on the behavior of a corner crushing failure mode model.

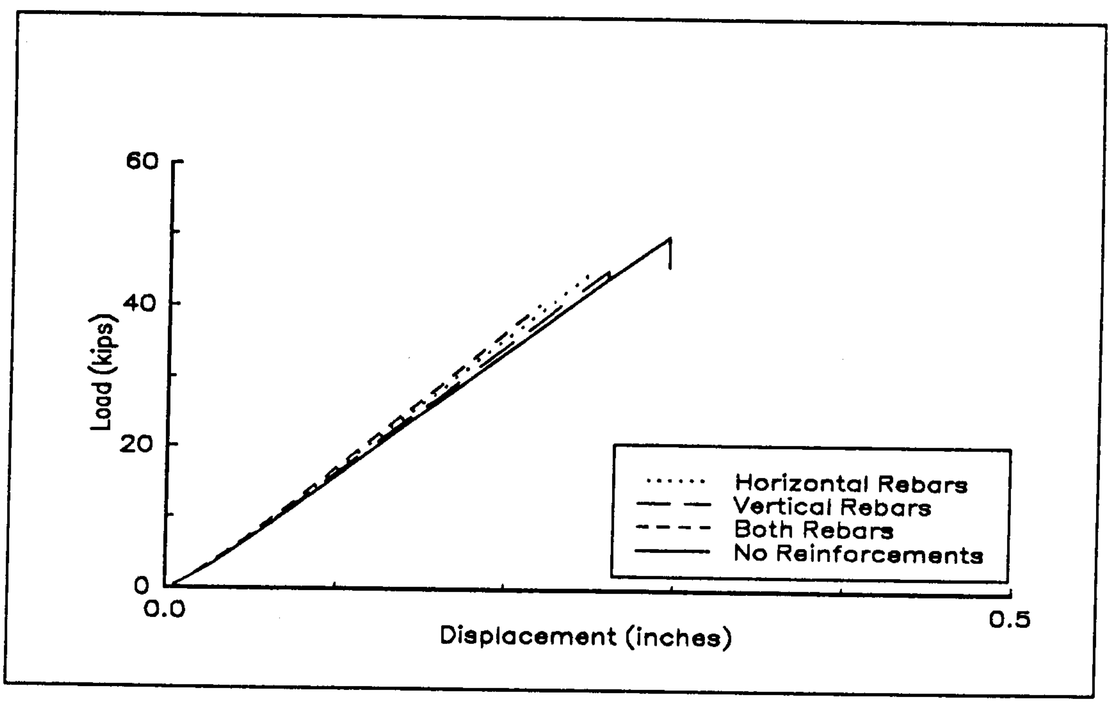

Figure 7.2. The effects of different infill reinforcements on the behavior of a diagonal crushing failure mode model.

do not significantly increase the strength. Thus, rebars do not contribute significantly to the infill stiffness or strength.

7.3 Shear Connectors

Shear connectors between the frame and infill are added to a typical model to examine their effects on the infilled frame behavior. Shear connectors are adopted by directly connecting the steel frame column and the infill, and therefore, eliminating the interface element at the frame columns and the infill boundary. The shear connectors significantly increase the infilled frame model initial and secant stiffness, Figure 7.3, as Liauw and Kwan (1982) concluded. However, the structure suffers a premature failure due to the shear and tensile stresses transferred to the infill through the shear connectors from the windward frame column. Thus, the infill does not fully develop a diagonal strut since it cannot freely assume a better equivalent strut position as Riddington (1984) describes, Figure 2.22. Yong (1984) found the same conclusion that panels without shear connectors can freely rotate and assume a better equivalent strut position, and consequently, they yield the highest ultimate strength.

To overcome the premature failure due to tensile and shear stress at the connectors, horizontal and vertical number 14 rebars are added to the model. The vertical and horizontal rebars are spaced at 7.87" and 7.32" respectively. Figure 7.3 shows that adding the rebars to the infill increases the infilled frame capacity and keeps the high stiffness. This finding leads to the conclusion that if high stiffnesses are required by using shear connectors, an adequate infill reinforcement is needed to keep the infilled frame full strength.

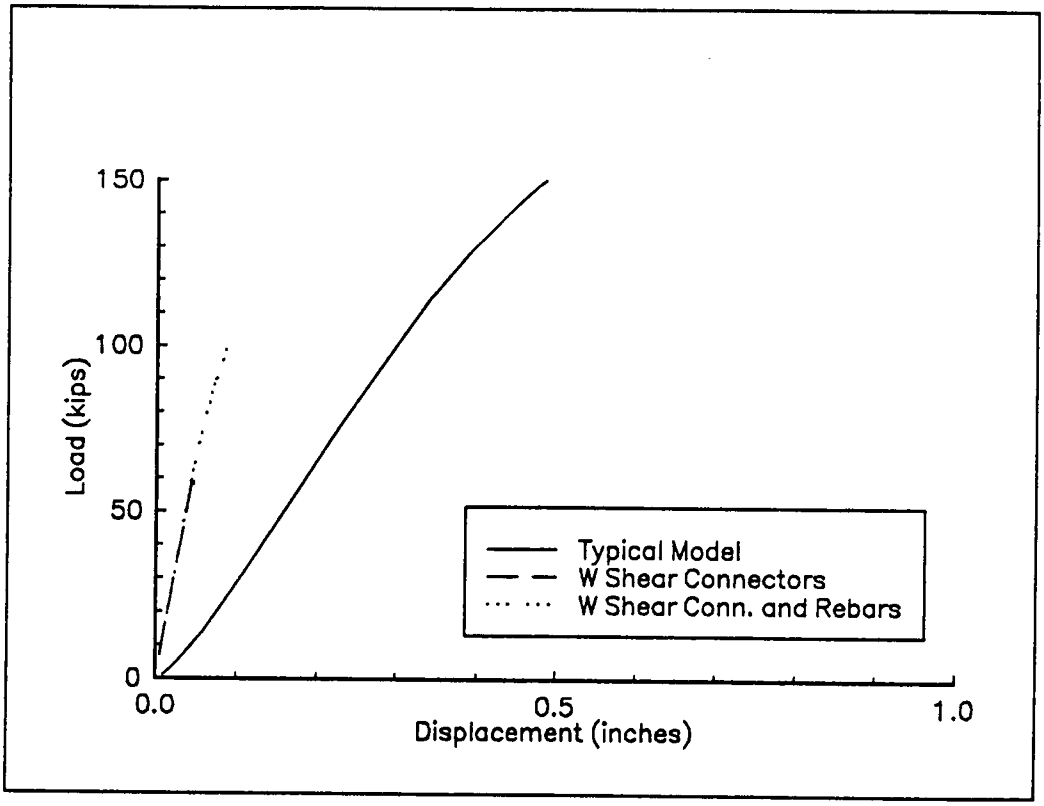

Figure 7.3. The effects of shear connectors with or without infill reinforcements on the infilled frame behavior.

7.4 Initial Gaps

Initial gaps are there for some reason, or they may result form shrinkage or poor construction. An initial gap with different sizes is added to a typical model to determine its effect on the infilled frame behavior. The gap is assumed to be between the frame top beam and the infill since that is the most likely place for the gap to occur. Figure 7.4 shows the load displacement curves for infilled frame models with different initial gap sizes, 0.0", 0.1", 0.2", and 0.3". The load deflection curve for the bare steel frame is used a reference. The figure reveals that even relatively small initial gaps significantly reduce the infilled frame racking stiffness, agreeing with Riddington's (1982) findings. Infills

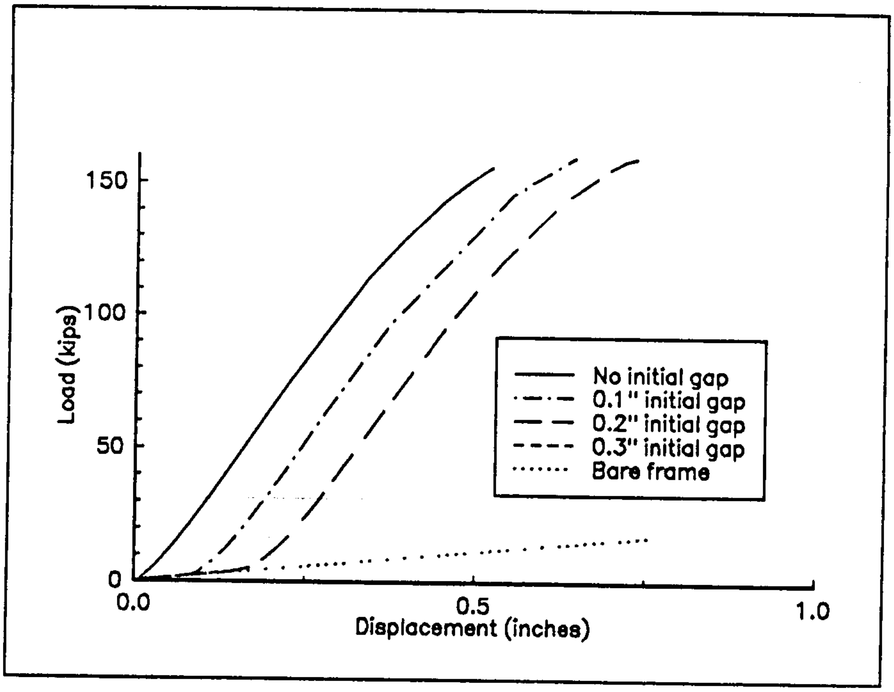

Figure 7.4. The effects of having initial gaps on the infilled frame behavior.

with very small initial gaps can successfully slip and lift to wedge into the loaded corners, and therefore, develop a diagonal strut. The infill with larger initial gaps dose not survive the large movement and thus prematurely fails. Consequently, the model behavior is reduced to that of a bare frame. Experimental tests (Young, 1984) reveal that initial gaps can substantially reduce the ultimate strength. It is recommended that serious efforts need to be made to avoid having initial gaps since they have an undesirable effect on the infilled frame stiffness and strength.

7.5 Infill Openings

Infills often have door, window, or ventilation openings. In order to study the effects openings have on the infilled frame behavior, a 78.7" high by 29.3" wide door opening is added to a typical infilled frame model. The door can be at the center or 29.3" off center toward or away from the loaded corner. Figure 7.5 shows the behavior of the infilled frame with the different opening positions. The figure reveals that the door opening, which only represents approximately 15% of the infill area, has a large effect on the infilled frame stiffness and ultimate strength. The reason for this is due to the tensile stresses in the infill along the leeward column and the top beam straight across from the door top right corner away from the load. Figure 7.6 shows the possible tensile stress concentration regions in an infill with an opening. Figures 7.7, 7.8, and 7.9 show the deformed shape of the infilled frames for central, off left, and off right door openings respectively. The deformed shapes indicate the regions where the tensile stress is the highest in the infill. Another way the opening position plays its role in the model behavior is by intercepting the diagonal strut formation. The farther the opening is from the diagonal strut, the lesser the effects are.

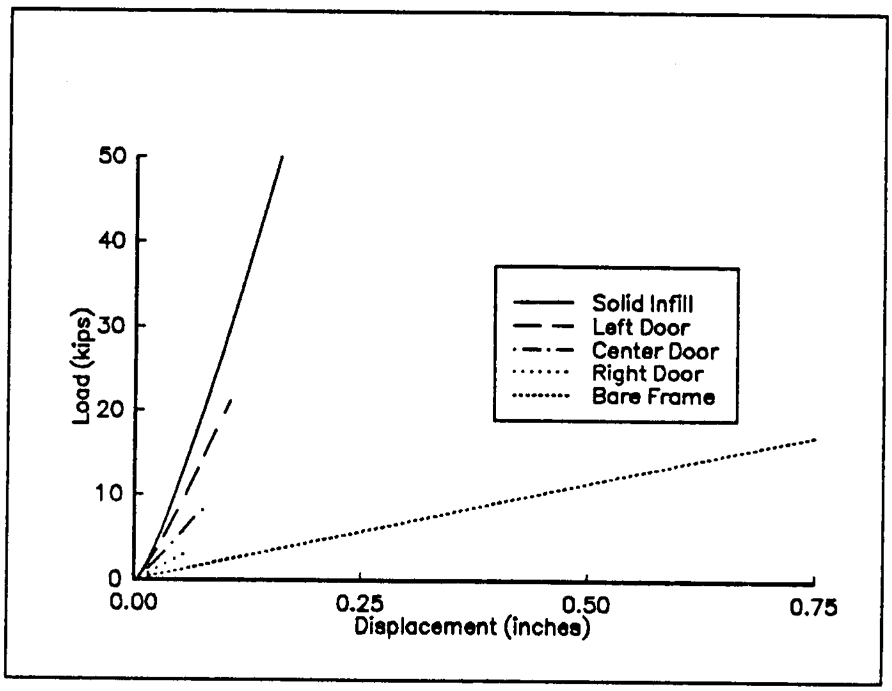

Figure 7.5. The effects of openings and their position on the infilled frame behavior.

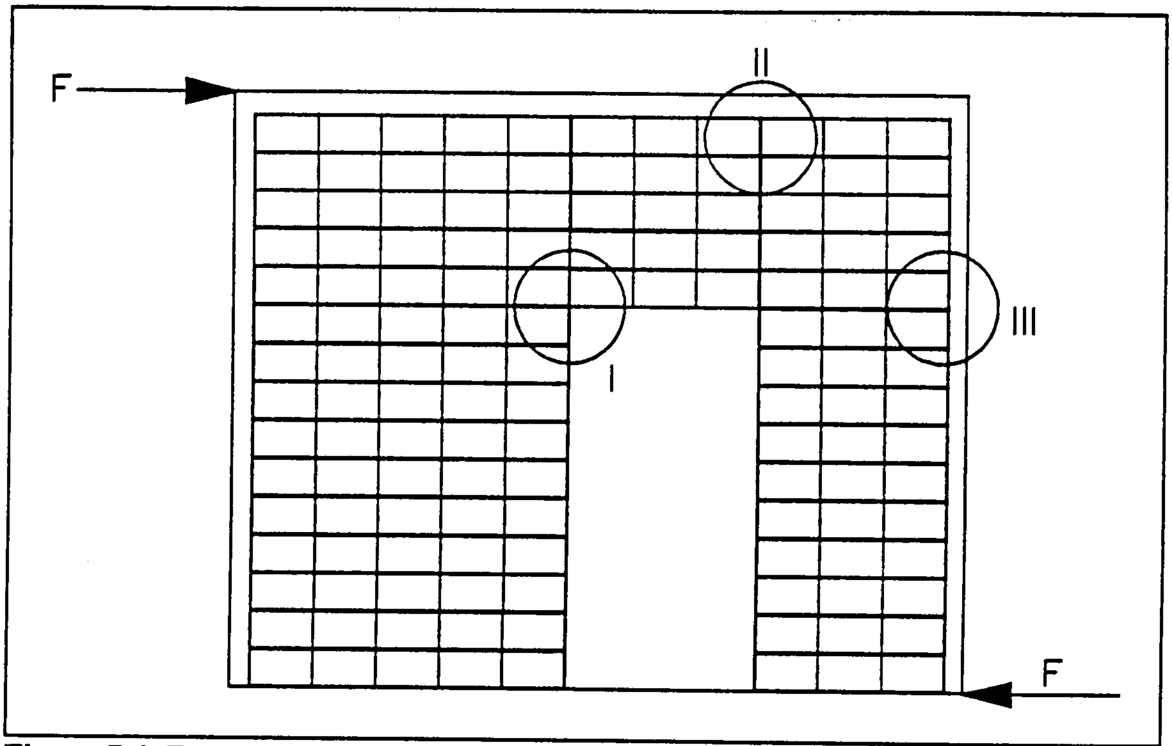

Figure 7.6. Tensile stress regions in the infill with an opening.

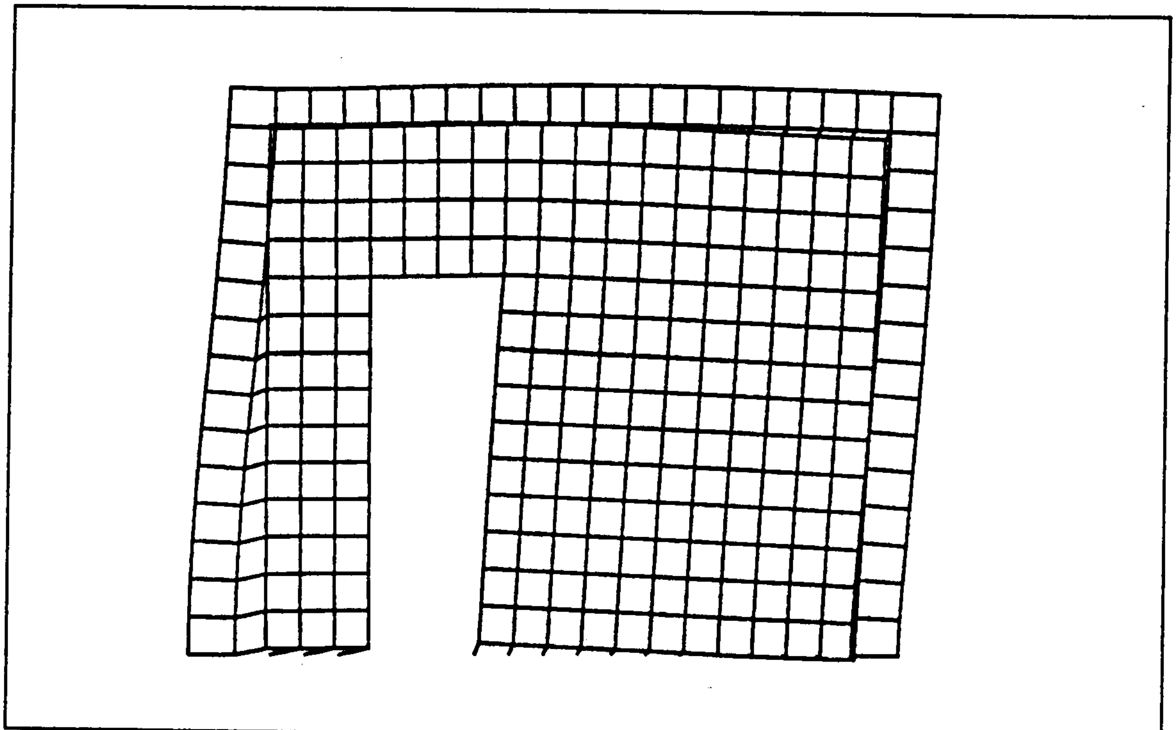

Figure 7.7. The deformed shape of the infilled frame with a left door opening.

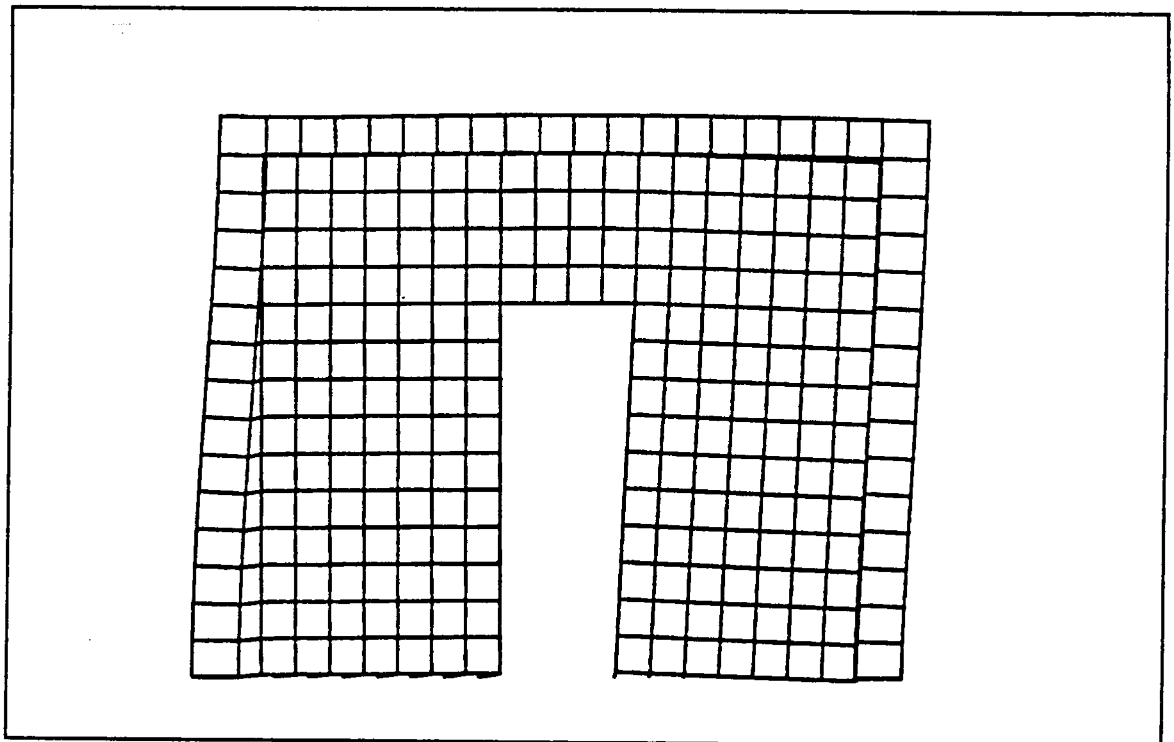

Figure 7.8. The deformed shape of the infilled frame with a central door opening.

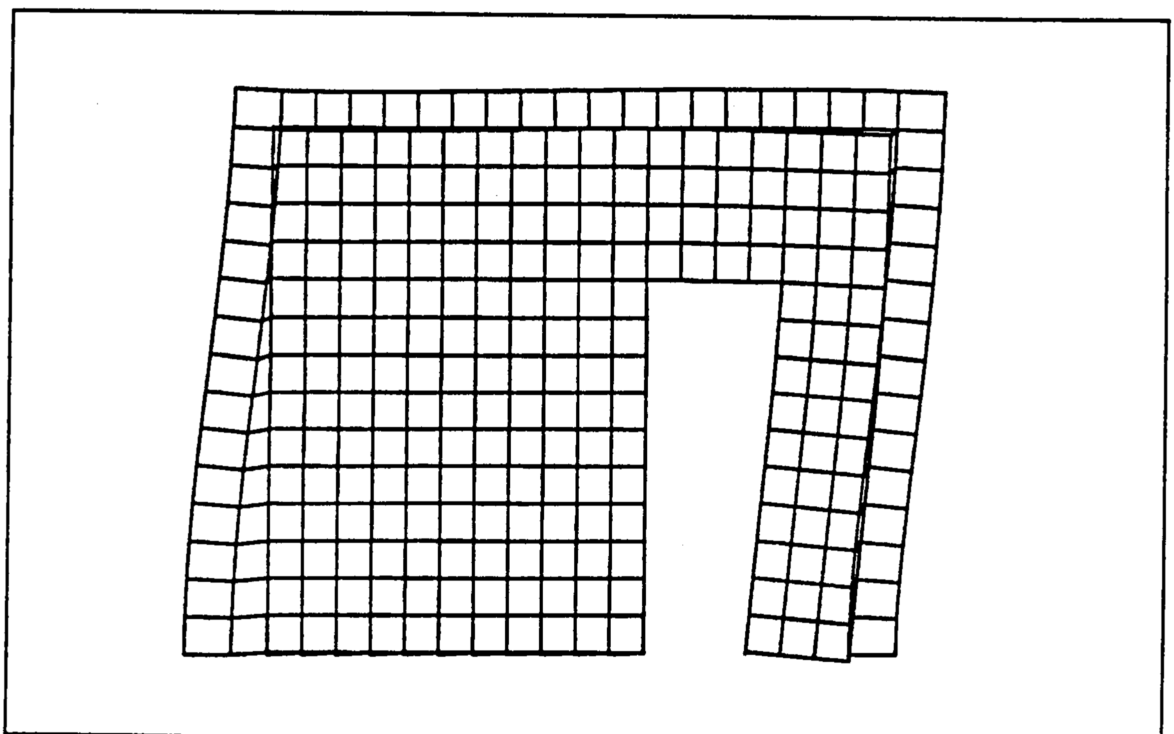

Figure 7.9. The deformed shape of the infilled frame with a right door opening.

The infill reinforcements may have a positive effect with openings by taking the tensile stresses. The elements around the opening are grouted, the infill net thickness is 8.0" instead of 4.0". They are reinforced with a single vertical and horizontal number 14 rebar along the sides and top of the opening respectively. Another way to strengthen the infilled frame is by reinforcing the whole infill with number 14 rebars. The rebars are spaced 7.32" horizontally and 7.78" vertically. Figures 7.10, 7.11, and 7.12 show the behavior of the infilled frame with no reinforcing, with reinforcing around the opening, and with reinforcing throughout the panel. The figures reveal that reinforcing the whole infill increases the ultimate strength more than reinforcing around only the opening.

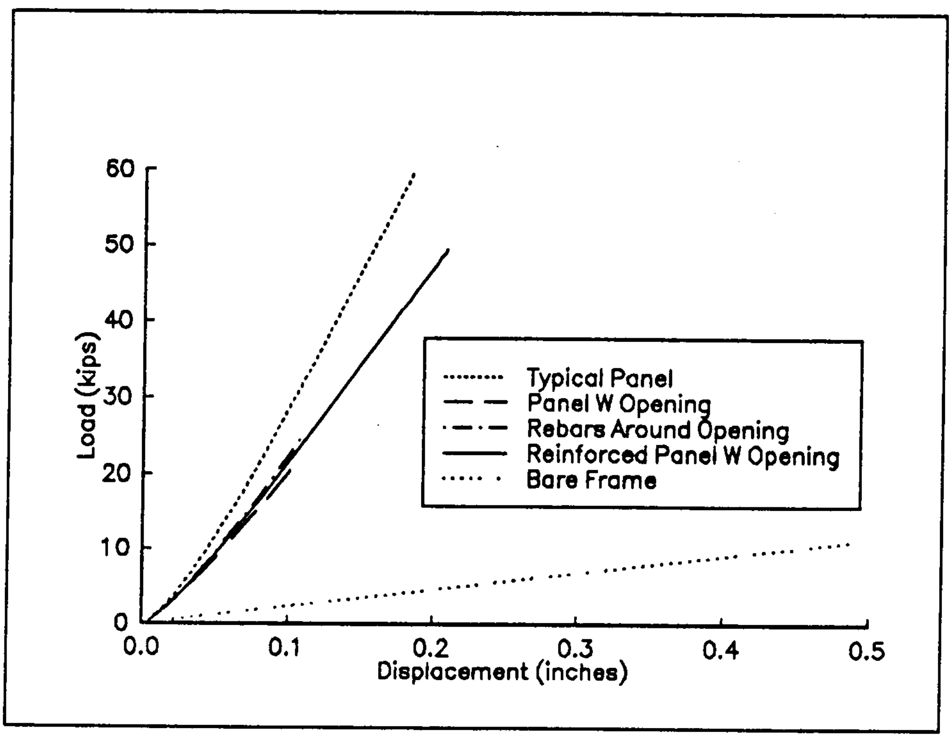

Figure 7.10. Left door infilled frame behavior with different reinforcements.

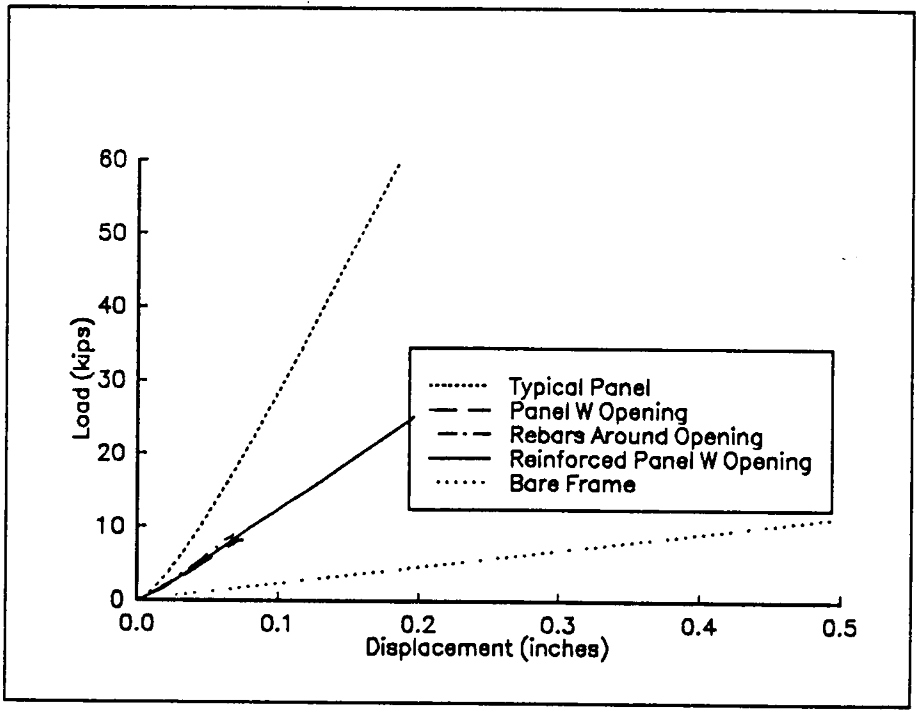

Figure 7.11. Central door infilled frame behavior with different reinforcements.

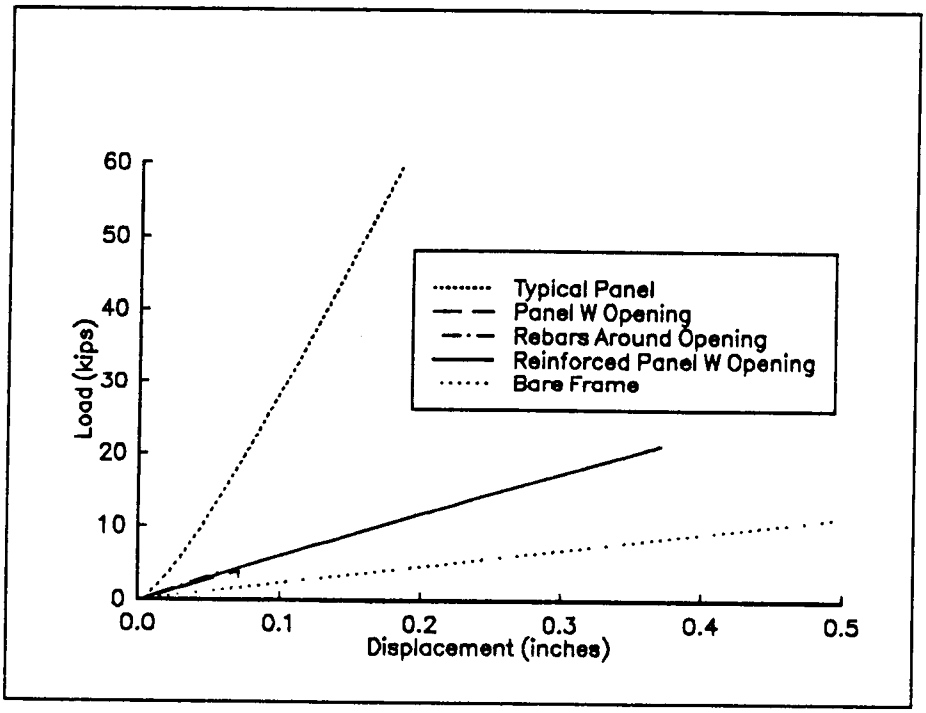

Figure 7.12. Right door infilled frame behavior with different reinforcements.

The study reveals that the position of the door significantly effects the infill behavior. The closer the door is to the leeward column the more effect the door has on the behavior. Since racking loads can occur in any direction, openings should be positioned closer to the center to minimize their negative effects. Reinforcing the infill helps retain some of the lost strength due to having an opening.

7.6 Load Reversal

Lateral loads may vary in magnitude and direction. This section studies the effect of loading reversal on the infilled frame behavior. The study uses a typical infilled frame model. A complete load cycle is applied. The maximum load varies to examine its effect on the infilled frame behavior. The ultimate strength of a typical infilled frame under monotonic load is 156 kips. Figures 7.13, 7.14, and 7.15 show the load displacement curves for a typical infilled frame under a complete cycle up to a maximum load of 54%, 84%, and 100% of the ultimate strength respectively. Figure 7.13 reveals that the loading and unloading paths coincide in both directions of loading. Therefore, there is no significant plastic deformation if the load does not exceed about 50% of the ultimate. For higher load cycles, Figures 7.14 and 7.15, there are different paths for loading and unloading, and thus indicate that the model sustains plastic deformations. The load at maximum positive and negative displacements varies, e.g., 156 kips versus -142 kips, Figure 7.15. Two cycle loadings reveal that the first and second cycle maximum loads do not significantly vary, Figures 7.16 and 7.17. This conclusion applies on the positive direction since the model diverges before reaching the second cycle maximum negative displacement.

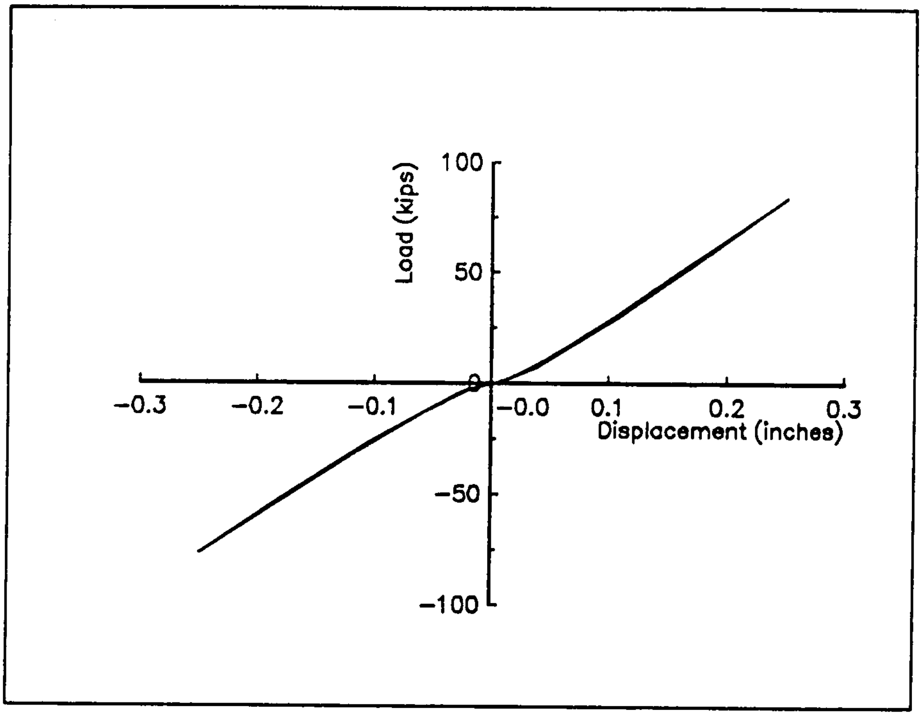

Figure 7.13. Infilled frame behavior under one load cycle up to 54% of the ultimate.

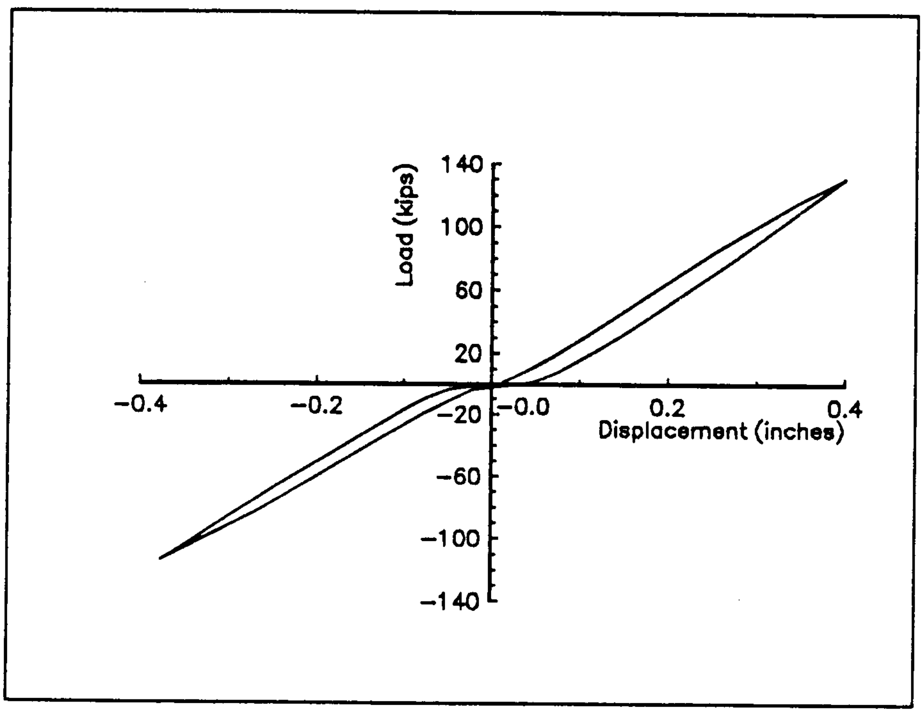

Figure 7.14. Infilled frame behavior under one load cycle up to 84% of the ultimate.

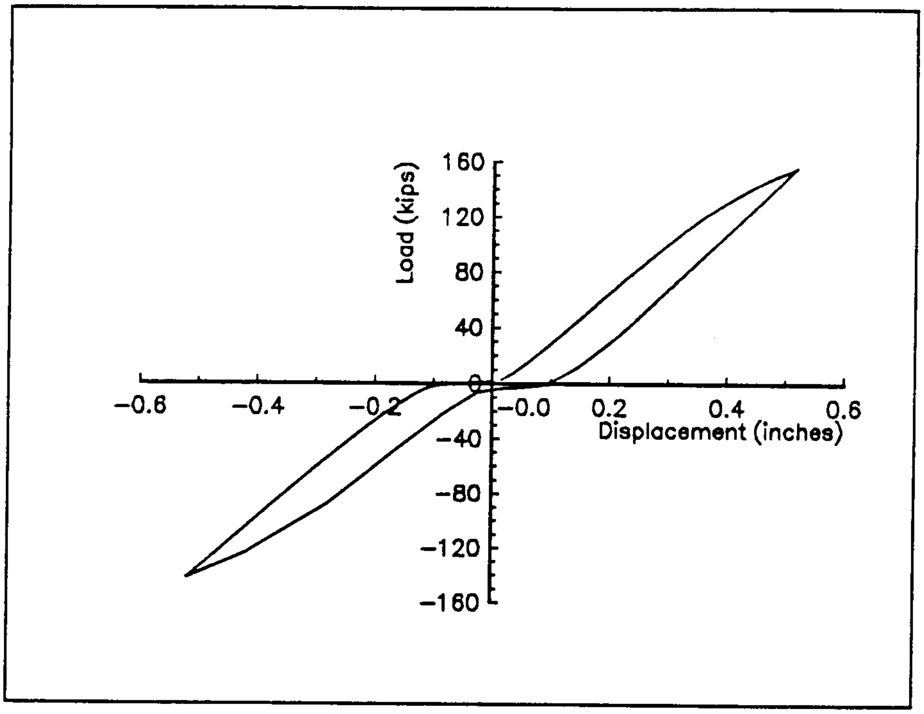

Figure 7.15. Infilled frame behavior under one load cycle up to 100% of the ultimate.

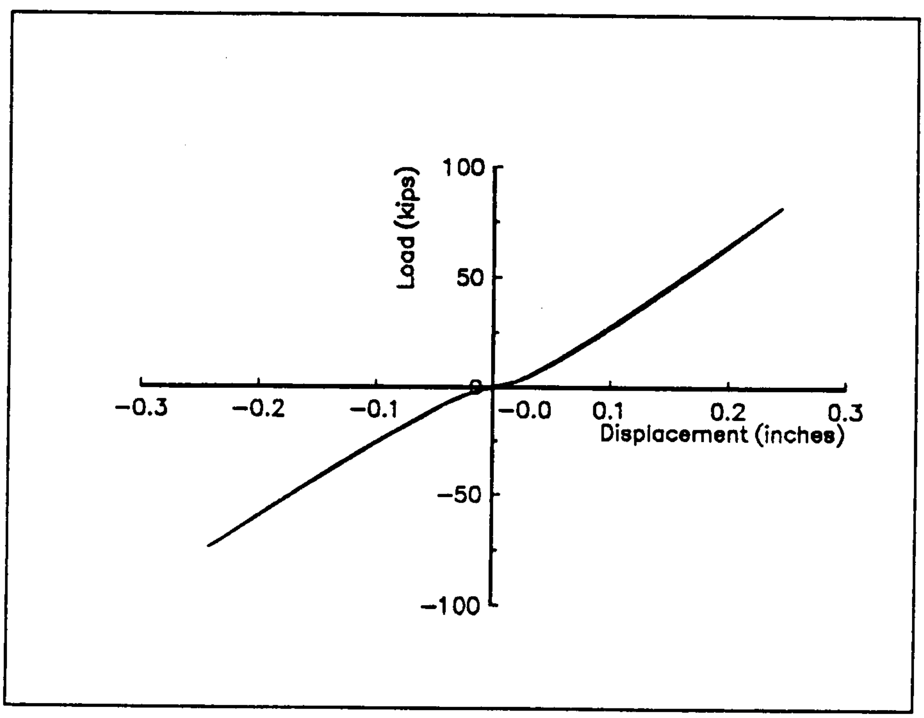

Figure 7.16. Infilled frame behavior under two load cycles up to 54% of the ultimate.

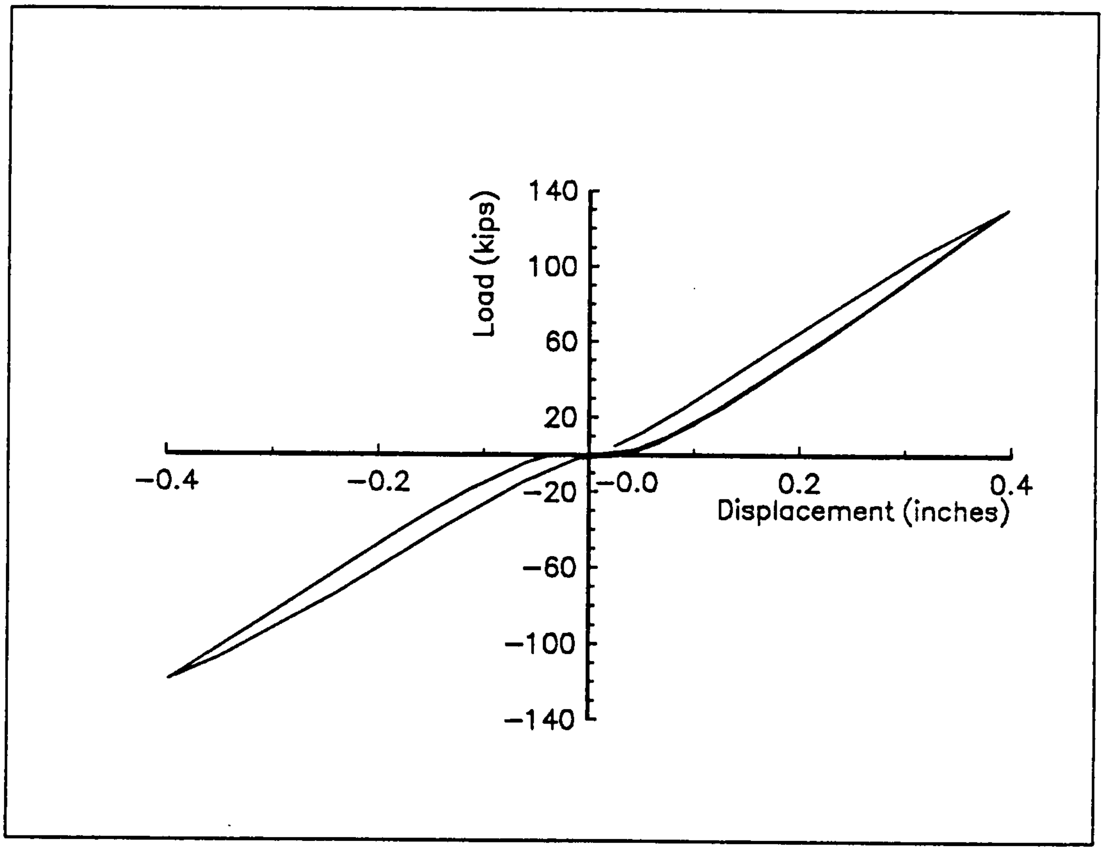

Figure 7.17. Infilled frame behavior under two load cycles up to 84% of the ultimate.

CHAPTER 8

CONCLUSIONS AND RECOMMENDATIONS

8.1 Introduction

A nonlinear finite element study was conducted to evaluate the in-plane behavior of concrete masonry infilled steel frames. ABAQUS was used to develop the finite element model and perform a parametric analysis. The model was verified by comparing the results with the experimental program series carried out at the University of Brunswick, Canada. These tests used hollow concrete block masonry. Hence, the results are primarily applicable to concrete block masonry, but the general concepts are applicable to all masonry.

The initial stiffness could be matched using elastic material properties with a frame-infill interface element. The ultimate load and secant stiffness could be matched using a nonlinear model. The ABAQUS nonlinear model used the concrete material model for the infill and an elastic-plastic material for the steel frame. A softened interface was used to account for the localized mortar crushing that tends to occur at the corners of infilled frames. This model was used to match the secant stiffness at approximately 50% of the ultimate load.

A parametric study was performed on the initial and secant stiffness, and the ultimate load. Results indicated that an appropriate equivalent strut model could closely match the infilled frame behavior. The model used the same frame beam and columns.

The masonry infill was replaced by an equivalent diagonal strut. The strut had the same net thickness and Young's modulus as the infill. An appropriate formula was used to estimate the strut effective width depending on whether the frame joints were hinged or rigid. The strut model connections were hinged regardless of the actual frame connections. When the frame columns differed, the average properties were used to obtain the relative stiffness which was used in the calculation for the strut effective width. However, the exact frame columns were still used in the strut model. Therefore, the infill behavior depended on the load direction. An average value could be used in estimating the structure ultimate load and stiffness, and thereafter, the natural frequency. The study included one and multiple bay infilled frames. Infilled frames under gravity loads were also considered. Other infilled frame parameters were examined such as initial gaps, openings, rebars, shear connectors, and cyclic loading.

8.2 Initial Stiffness Conclusions

For the initial stiffness strut model, it was found that Equation 2.1 (Stafford-Smith and Carter, 1969) was appropriate to estimate the diagonal strut effective width, α_c, for rigidly connected frames. A modified formula, Equation 4.1, was developed to reflect the reduction in stiffness due to frame hinged connections. The term λ was the frame-infill relative stiffness. The equivalent strut model successfully reflected the positive influence that vertical loads had on the infilled frame initial stiffness.

$$a_c = \frac{\pi}{2\ \lambda} \tag{2.1}$$

$$a_c = \frac{\pi}{2\sqrt{2}\ \lambda} \tag{4.1}$$

8.3 Secant Stiffness Conclusions

The same equations, 2.1 and 4.1, used for initial stiffness were adequate to calculate the effective strut width for the secant stiffness model. However, the strut used a secant modulus instead of the infill Young's elastic modulus. The secant modulus was calculated by multiplying the elastic modulus by a constant, 0.662. The study revealed the previous finding that the top beam moment of inertia had limited effects on the infilled frame stiffness. Vertical loads increased the infilled frame secant stiffness by improving the frame top beam and the infill contact and reducing the tensile stress in the windward column and sequentially decreasing the column elongation. The equivalent strut model successfully reflected the positive influence that vertical loads had on the infilled frame secant stiffness.

8.4 Ultimate Load Conclusions

For the ultimate load model, Equation 2.1 (Stafford-Smith and Carter, 1969) was used for rigidly connected infilled frames. Equation 4.1 was used to estimate the equivalent strut width for infilled frames with hinged connections. A constant, 0.387, was used as a penalty factor. The factor was used to reduce the infill failure strength due to the infill imperfect plasticity. The model failed when the windward column reached its yielding stress or the diagonal strut reached its ultimate compressive stress, Figure 5.12. Equations 5.6 and 5.7 calculated the infilled frame ultimate

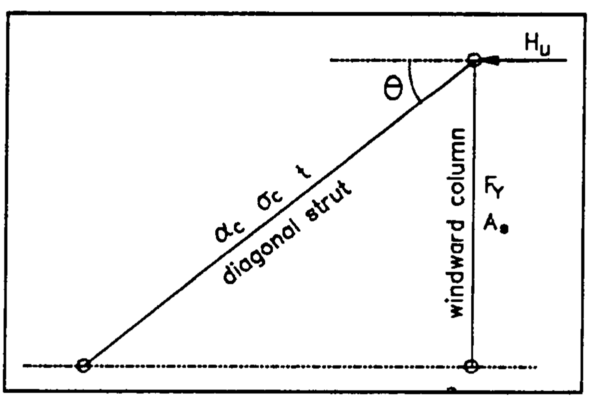

Figure 5.12. Ultimate strength strut model.

strength if it was controlled by the column or the strut strength, respectively. The equations gave the ultimate strength, H_u, in terms of the steel yielding stress, F_y, the frame column area, A_s the infill net thickness, t, the infill ultimate strength, σ_c, the strut effective width, α_c, the penalty factor, v_p, and the frame horizontal diagonal angle, θ. Vertical loads did not effect the ultimate load when the infill was weak. Under moderate vertical loads, the ultimate capacity of infilled frames with relatively strong infills was slightly increased. The reason for the increase was due to the improvement of the top beam-infill contact. Vertical loads did not increase the strut model ultimate load. This behavior was acceptable since it was on the safe side. Heavy gravity loads decreased the infilled frame ultimate strength. The reason for the decrease was due to the infill participation in supporting the heavy vertical load, and thus, its capacity to support lateral load was reduced. The strut model did not reflect the negative effects that heavy gravity loads had on the ultimate load since the model columns supported all the vertical loads. Therefore, under heavy vertical loads, the infill needs to be checked not only as a part of an infilled frame system but also as a bearing wall. The study found that the ultimate load of a multiple bay infilled frame was the sum of the ultimate strength of each individual one bay infilled frame. The middle column properties, area and moment of inertia, were equally divided between the two adjacent one bay infilled frames.

$$H_u = F_Y A_s \cot(\theta) \tag{5.6}$$

$$H_u = \sigma_c \, t \, \alpha_c \, v_p \cos(\theta) \tag{5.7}$$

8.5 Other Infilled Frame Parameter Conclusions

The study investigated different infilled frame parameters. These included infills connected to the frame by shear connectors, infills with openings, reinforced infills, or frame and infill initial gaps. The case of lateral load cycling was also considered.

The reinforcement of typical infills did not significantly affect the stiffness nor the ultimate load. Rebars did not influence the typical infill because it was primarily in compression.

Column and infill shear connectors drastically increased the infilled frame initial and secant stiffnesses. However, they caused premature failure of the infill due to tensile and shear stresses near the interface. Reinforcing the infill restored the infilled frame ultimate strength and kept the high stiffness. The reinforcements played a crucial role in this case by taking the tensile and shear forces.

Top beam frame and infill initial gap influence depended on the gap size. With a very small initial gap, the infill could survive and wedge into the strut position. With larger initial gaps, the infilled frame stiffness and ultimate load were drastically decreased.

Openings in general had negative effects on the infilled frame behavior. The closer the openings were to the compressive strut path the more the negative effects on the infilled behavior. Reinforcements were useful in the opening case; they offset the negative effects that an opening had.

8.6 Summaries

The study contributes to the understanding of the in-plane behavior of infilled frames. Table 8.1 summarizes the effects each infilled frame parameter has on the stiffness and ultimate load. A positive effect indicates that an increase in the parameter increases the stiffness or ultimate load.

The study provides a modest formula, Equation 8.1, to analyze infilled frames subjected to in-plane loading. The equation applies the necessary changes on the equivalent strut effective width, α_c, rather than on the infill Young's modulus of elasticity or the infill ultimate strength. The equation is applicable to hinged and rigidly connected infilled frames. The simplicity of the equation encourages considering infilled frames in the design of structures.

$$a_c = C_1\, C_2\, \frac{\pi}{2\,\lambda} \tag{8.1}$$

$$C_1 = \begin{array}{l} 1.0 \ \textit{for initial stiffness} \\ 0.66 \ \textit{for 50\% secant stiffness} \\ 0.39 \ \textit{for ultimate load} \end{array}$$

$$C_2 = \begin{array}{l} 1.0 \ \textit{for rigid frames} \\ 0.71 \ \textit{for hinged frames} \end{array}$$

8.7 Recommendations

Infills can drastically affect the structural behavior of frames subjected to lateral loads such as earthquakes and winds. Their influence is there whether or not they are considered in the original design. The difficulties in analyzing the infilled frame behavior and including them into the design are the reasons that designers were reluctant to include the infilled frames in the design. This study provides a modest model formulation to consider the infilled frame in the analysis of structures having infilled frames. This helps in taking advantage of having the infilled frame in the structure and achieving more realistic designs.

	initial stiffness	secant stiffness	failure load
infill net thickness	significant positive effect	significant positive effect	significant positive effect
frame height	negative effect	negative effect	maximum strength when aspect ratio is about 1.0
frame column moment of inertia	significant positive effect	significant positive effect	positive effect up to the beam moment of inertia, then slight effect
frame beam moment of inertia	negligible positive effect	marginal positive effect	positive effect up to the column moment of inertia, then no effect
gravity loads	positive effect	positive effect	depends on the vertical load and the infill frame characteristics (section 5.6)
frame-infill initial gap	significant negative effect	significant negative effect	significant negative effect if infill can not wedge to form strut
infill opening	significant negative effect	significant negative effect	significant negative effect;can be partially offset with reinforcing
infill reinforcements	no effect	no effect	no effect
frame-infill shear connectors	significant positive effect	significant positive effect	produces premature failure

Table 8.1. The effect of various infilled frame parameters on the behavior of infilled frames subjected to in-plane loadings.

REFERENCES

REFERENCES

ABAQUS Version 4-7-22, Hibbitt, Karlsson and Sorensen, Inc.

Achyutha, H., Rahman, S.S.U., and Karisiddappa (1988). "Effect of Position of Openings on the Behavior of Infilled Frames." Proceedings of the Eighth International Brick and Block Masonry Conference, Dublin, Ireland, 2, 1108-1121.

Amos, K.A. (1985). "The Shear Strength of Masonry Infilled Steel Frames." Thesis submitted in partial fulfillment of the requirements for the degree of Master of Science, University of New Brunswick, Canada.

Atkinson, R. H. and Yan, G.G. (1990). "Results of a Statistical Study of Masonry Deformability." The Masonry Society Journal 9, No 1.

Barua, H.K., and Mallick, S.K. (1977). "Behavior of Mortar Infilled Steel Frames Under Lateral Load." Building and Environment, 12, 263-272.

Chrysostomou, C.Z., Gergely, P., and Abel, J.F. (1988). "Preliminary Studies of The Effects of Degrading Infill Walls on The Nonlinear Seismic Response of Steel Frame." Technical Report NCEER-88-046, State University of New York at Buffalo.

Dawe, J.L., and Seah, C.K. (1989). "Behaviour of Masonry Infilled Steel Frames." Canadian Journal of Civil Engineering, 16, 865-876.

Dhanasekar, M., and Page, A.W. (1986). "Influence of Brick Masonry Infill Properties on the Behavior of Infilled Frames." Proceedings of the Institution of Civil Engineers, 81(2), 593-605.

Hendry, E. A. and Liauw, T. C. (1992). "Tests on Steel Frames With Reinforced Masonry Infill." The Third International Masonry Conference, London, England.

Holmes, M. (1961). "Steel Frames with Brickwork and Concrete Infilling." Proceedings of the Institution of Civil Engineers, 19, 473-478.

Klingner, R.E., and Bertero, V.V. (1976). "Infilled Frames in Earthquake-Resistant Construction." Earthquake Engineering Research Center, Report EERC 76-32.

Klingner, R.E., and Bertero, V.V. (1978). "Earthquake Resistance of Infilled Frames." Journal of the Structural Division, ASCE, 104(ST6), 973-989.

Klingner, R.E. (1980). "Mathematical Modeling of Infilled Frames." American Concrete Institute, SP-63, 1-25.

Klingner, R.E., Beiner, R., and Amrhein, J. (1987). "Performance of Masonry Structures in the Mexican Earthquake of September 19, 1985." Proceedings of the Fourth North American Masonry Conference, 70:1-70:14.

Liauw, T.C. (1970). "Elastic Behavior of Infilled Frames." Proceedings of the Institution of Civil Engineers, 46, 343-349.

Liauw, T.C., and Lee, S.W. (1977). "On the Behavior and the Analysis of Multi-Story Infilled Frames Subject to Lateral Loading." Proceedings of the Institution of Civil Engineers, Part 2, 63, 641-656.

Liauw, T.C., and Kwan, K.H. (1982). "Non-linear Analysis of Multistory Infilled Frames." Proceedings of the Institution of Civil Engineers, 73, Part 2, 441-454.

Liauw, T.C, and Kwan, K.H (1983). "Plastic Theory of Non-Integral Infilled Frames." Proceedings of the Institution of Civil Engineers, Part 2, 75, 379-396.

Liauw, T.C., and Kwan, K.H. (1984). "Nonlinear Behaviour of Non-Integral Infilled Frames." Computers and Structures, 18(3), 551-560.

Liauw, T.C., and Kwan, K.H. (1985). "Unified Plastic Analysis of Infilled Frames." Journal of Structural Engineering, ASCE, 111(7), 1427-1448.

Mallick, D.V., and Severn, R.T. (1967). "The Behavior of Infilled Frames Under Static Loading." Proceedings of the Institution of Civil Engineers, 38, 639-656.

Mallick, D.V., and Garg, R.P., (1971). "Effect of Openings on the Lateral Stiffness of Infilled Frames." Proceedings, Institution of Civil Engineers, 49(2), 193-209.

May, I.M., and Ma, S.Y.A. (1985). "A Rigid Plastic Method for the Determination of Collapse Loads of Infilled Panels with Openings." Journal of Strain Analysis, 21(1), 41-52.

McBride, R.T. (1984). "The Behavior of Masonry Infilled Steel Frames Subjected to Racking." Thesis submitted in partial fulfillment of the requirements for the degree of Master of Science, University of New Brunswick, Canada.

Moghaddam, H., and Dowling , P. (1988). "Earthquake Resistant Design of Brick Infilled Frames." Proceedings of the Eighth International Brick and Block Masonry Conference, 774-784.

Pook, L.L., and Dawe, J.L. (1986). "Effects of Interface Conditions Between a Masonry Shear Panel and Surrounding Steel Frame." Proceedings of the Fourth Canadian Masonry Symposium, Fredericton, NB, Canada, 910-921.

Richardson, J. (1986). "The Behaviour of Masonry Infilled Steel Frames." Thesis submitted in partial fulfillment of the requirements for the degree of Master of Science, University of New Brunswick, Canada.

Riddington, J.R., and Stafford-Smith, B. (1977). "Analysis of Infilled Frames Subject to Racking with Design Recommendations." The Structural Engineer, 55(8), 263-268.

Riddington, J.R. (1984). "The Influence of Initial Gaps on Infilled Frame Behavior." Proceedings of the Institution of Civil Engineers, Part 2, 77, 295-310.

Rivero, C.E. and Walker, W.H. (1982). "An Analytical Study of the Interaction of Frames and Infill Masonry Walls." A Report on a Research Sponsored by the National Science Foundation, University of Illinois at Urbana-Champaign.

Rivero, C.E., and Walker, W.H. (1985). "Model to Study the Interaction of Frames and Infill Masonry Walls." Proceedings of the Third North American Masonry Conference, 76:1-76:14.

Stafford-Smith, B. (1962). "Lateral Stiffness of Infilled Frames." Journal of the Structural Division, ASCE, 88, ST6, 183-199.

Stafford-Smith, B. (1966). "Behaviour of Square Infilled Frames." Journal of the Structural Division, ASCE, 92, ST1, 381-403.

Stafford-Smith, B., and Carter, C. (1969). "A Method of Analysis for Infilled Frames." Proceedings of the Institution of Civil Engineers, 44, 31-48.

STRUDL-II, The Structural Design Language, Civil Engineering Systems Laboratory, Massachusetts Institute of Technology Cambridge, Massachusetts.

Wolde-Tinsae, A., Lhadj, M., and Colville, J. (1987). "Finite Element Study of Semi-Confined Masonry Walls." Proceedings of the Fourth North American Masonry Conference, The Masonry Society, Denver, CO, 19-1 - 19-15.

Wood, R.H. (1978). "Plasticity, Composite Action and Collapse Design of Unreinforced Shear Wall Panels in Frames." Proceedings of the Institution of Civil Engineers, Part 2, 65, 381-411.

Yong, T.C. (1984). "Shear Strength of Masonry Infilled Panels in Steel Frames." Thesis submitted in partial fulfillment of the requirements for the degree of Master of Science, University of New Brunswick, Canada.

BIBLIOGRAPHY

BIBLIOGRAPHY

ABK (1984). "Methodology For Mitigation of Seismic Hazards in Existing Unreinforced Masonry Buildings: The Methodology." ABK-TR-08.

Achyutha, H., Jagadish, R., Rao, P.S., and Rahman, S.S. (1986). "Finite Element Simulation of the Elastic Behavior of Infilled Frames with Openings." Computers and Structures, 23(5), 685-696.

Achyutha, H., Rahman, S.S.U., and Karisiddappa (1988). "Effect of Position of Openings on the Behavior of Infilled Frames." Proceedings of the Eighth International Brick and Block Masonry Conference, Dublin, Ireland, 2, 1108-1121.

Ali, S., Page, A.W. (1987). "Non-linear Finite Element Analysis of Masonry Subject to Concentrated Loads." Proceedings of the Institution of Civil Engineers (London), 83(a), 815-832.

Ali, S., and Page, A.W. (1988). "Finite Element Model for Masonry Subjected to Concentrated Loads." Journal of Structural Engineering, ASCE, 114(8), 1761-1784.

Amos, K.A. (1985). "The Shear Strength of Masonry Infilled Steel Frames." Thesis submitted in partial fulfillment of the requirements for the degree of Master of Science, University of New Brunswick, Canada.

Amos, K.A., and Waugh, L.M. (1986). "Behavior of Perforated Masonry Shear Panels in a Steel Frame." Proceedings of the Eighth International Brick and Block Masonry Conference, Dublin, Ireland, 2, 569-580.

Anderson, C., and Held, L.C. (1986). "The Effect of Sand Grading on Mortar Properties and the Tensile Bond of Brickwork Specimens." Proceedings of the British Masonry Society, 1, 1-6.

Andreaus, U., Cerone, M., D'Asdia, P, and Iannozzi, F. (1985). "A Finite Element Model for the Analysis of Masonry Structures Under Cyclic Actions." Proceedings of Seventh International Brick and Block Masonry Conference, Australia, 479-489.

Andreaus, U., Ceradini, G., Cerone, M., and D'Asdia, P. (1985). "Masonry Columns Under Horizontal Loads: A Comparison Between Finite Element Modelling and Experimental Results." Proceeding of 7th International Brick and Block Masonry Conference, Australia, 469-526.

Andreaus, U., and Ceradini, G. (1992). "Failure Modes of Solid Brick Masonry under In-Plane Loading." Masonry International, 6(1), 4-8.

Andreaus, U. (1988). "A 3-D Finite Element Model for the Analysis of Masonry Structures." Proceedings of the Eighth International Brick and Block Masonry Conference, Dublin, Ireland, 3, 1405-1416.

Arya, S.K., and Hegemier, G.A. (1978). "On Nonlinear Response Predictions of Concrete Masonry Assemblies." Proceedings of the North American Masonry Conference, 19:1-19:24.

ASTM Committee C-10 (1924). "Report of Committee C-10 on Hollow Building Tile." ASTM Proceedings, 24, 411-422.

ASTM Committee C-10 (1926). "Report of Committee C-10 on Hollow Masonry Building Units." ASTM Proceedings, 26, 285-291.

Atkinson, R.H., Amadei, B., Sture, S., and Saeb, S. (1987). "Deformation and Failure Characteristics of Masonry Bed Joints Under Shear Loading." Proceedings of the Fourth North American Masonry Conference, 61:1-61:14.

Atkinson, R.H., Kingsley, G.R., Saeb, S., Amadei, B., and Sture, S. (1988). "A Laboratory and In-Situ Study of the Shear Strength of Masonry Bed Joints." Proceedings, Eighth International Brick and Block Masonry Conference, Dublin, Ireland.

Atkinson, R.H., Amadei, B.P., Saeb, S., and Sture, S. (1989). "Response of Masonry Bed Joints in Direct Shear." Journal of Structural Engineering, ASCE, 115(9), 2276-2296.

Backes, H., and Aroh, C. (1986). "The Strength and Deformation Characteristics of Masonry Subjected to Diagonal Tension." Proceedings of the Fourth Canadian Masonry Symposium, Fredericton, NB, Canada, 149-163.

Baker, L.R. (1979). "Some Factors Affecting the Bond Strength of Brickwork." Preprints of Papers to be Delivered at Fifth International Brick Masonry Conference, 43-46.

Barua, H.K., and Mallick, S.K. (1977). "Behavior of Mortar Infilled Steel Frames Under Lateral Load." Building and Environment, 12, 263-272.

Benedetti, D., and Benzoni, G.M. (1984). "A Numerical Model for Seismic Analysis of Masonry Buildings: Experimental Correlations." Earthquake Engineering and Structural Dynamics, 12(6), 817-831.

Bernardini, A., Modena, C., and Vescovi, U. (1982). "An Anisotropic Biaxial Failure Criterion for Hollow Clay Brick Masonry." International Journal of Masonry Construction, 2(4), 165-171.

Bernardini, A., Casellato, A., Modena, C., and Vitaliani, R. (1985). "Post-Elastic Behaviour of Plain Masonry Shear Walls." Proceedings of the Seventh International Brick Masonry Conference, Australia, 490-501.

Bertero, V., and Brokken, S. (1984). "Infills in Seismic Resistant Buildings." Journal of Structural Engineering, ASCE, 109(6), 1337-1361.

Borchelt, J.G., and Brown, R.H. (1978). "An Indirect Tensile Test for Masonry Units." Journal of Testing and Evaluation, ASTM, 6(2), 134-143.

Brown, R.H., and Palm, B.D. (1984). "Flexural Strength of Brick Masonry Using the Bond Wrench." Proceedings of the Second North American Masonry Conference, University of Maryland, College Park, Maryland, 1:1-1:15.

Carvalho, F., and Pires, F. (1992). "Shear Strength Tests of Brick Masonry." Proceedings, Sixth Canadian Masonry Symposium, Addendum.

Choubey, U.B., and Sinha, S.N. (1991). "Cyclic Compressive Loading Response of Brick Masonry." Masonry International, 4(3), 94-98.

Choubey, U.B., and Sinha, S.N. (1992). "Cyclic Compressive Loading Equations of Brick Masonry." Masonry International, 6(1), 36-39.

Chrysostomou, C.Z., Gergely, P., and Abel, J.F. (1988). "Preliminary Studies of the Effects of Degrading Infill Walls on the Nonlinear Seismic Response of Steel Frames." National Center for Earthquake Engineering Research, NCEER-88-0046.

Copeland, R.E., and Saxer, E.L. (1964). "Tests of Structural Bond of Masonry Mortars to Concrete Block." American Concrete Institute Proceedings, 61(11), 1411-1451

Dawe, J.L., Schriver, A.B., and Sofocleous, C. (1989). "Masonry Infilled Steel Frames Subjected to Dynamic Load." Canadian Journal of Civil Engineering, 16, 877-885.

Dawe, J.L., Yong, T.C. (1988). "An Investigation of Factors Influencing the Behavior of Masonry Infill in Steel Frames Subjected to In-Plane Shear." Proceedings of the Seventh International Brick Masonry Conference, Melbourne, Australia, 802-813.

Dawe, J.L., and Seah, C.K. (1989). "Behaviour of Masonry Infilled Steel Frames." Canadian Journal of Civil Engineering, 16, 865-876.

Dawe, J.L., Dukuze, A. Holder, J. (1992). "Dynamic Behaviour of Masonry Infilled Steel Frames: Experimental Analysis." Proceedings, Sixth Canadian Masonry Symposium, 341-350.

Dawe, J.L., and Dukuze, A. (1992). "Parametric Study of Masonry Infilled Frames Subjected to Dynamic Loads: Preliminary Results." Proceedings, Sixth Canadian Masonry Symposium, 351-363.

Dawe, J.L., Hatzinikolas, M.A. (1988). "Behavior of Masonry Infilled Panels In Steel Frames." Proceedings, Eighth International Brick and Block Masonry Conference, Ireland, 516-527.

Dawe, J.L., McBride, R.T. (1985). "Experimental Investigation of the Shear Resistance of Masonry Panels in Steel Frames." Proceedings of the Seventh International Brick Masonry Conference, Melbourne, Australia, 791-801.

Dhanasekar, M., Page, A.W., and Kleeman, P.W. (1985). "The Failure of Brick Masonry Under Biaxial Stresses." Proceedings, Institution of Civil Engineers, 79(2), 295-313.

Dhanasekar, M., Page, A.W., and Kleeman, P.W. (1982). "The Elastic Properties of Brick Masonry." International Journal of Masonry Construction, 2(4), 155-160.

Dhanasekar, M., Page, A.W., and Kleeman, P.W. (1985). "The Behavior of Brick Masonry Under Biaxial Stress With Particular Reference to Infilled Frames." Proceedings of Seventh International Brick Masonry Conference, Melbourne, Australia, 814-824.

Dhanasekar, M., and Page, A.W. (1986). "Influence of Brick Masonry Infill Properties on the Behavior of Infilled Frames." Proceedings of the Institution of Civil Engineers, 81(2), 593-605.

Dhanasekar, M., Kleeman, P.W., and Page, A.W. (1985). "Biaxial Stress-Strain Relations for Masonry." Journal of Structural Engineering, ASCE, 111(5), 1085-1100.

Drysdale, R.G., and Hamid, A.A. (1984). "Tension Failure Criteria for Plain Concrete Masonry." Journal of Structural Engineering, ASCE, 110(2), 228-244.

Drysdale, R.G., Hamid, A.A., and Heidebrecht, A.C. (1979). "Tensile Strength of Concrete Masonry." Journal of the Structural Division, ASCE, 105(ST7), 1261-1276.

Drysdale, R.G., and Hamid, A.A. (1982). "Tensile Strength of Brick Masonry." International Journal of Masonry Construction, 2(4), 172-178.

Elouali, T., Houde, J., and Tinawi, R. (1991). "Effect Des Murs De Remplissage En Maçonnerie Sur Las Période De Vibration Des Portiques." Canadian Journal of Civil Engineering, 18(2), 264-272.

Epperson, G.S., and Abrams, D.P. (1989). "Nondestructive Evaluation of Masonry Buildings." ACTC Document No. 89-26-03, University of Illinois, Champaign.

Erlin, B., and Hime, W.G. (1985). "Methods for Analyzing Mortar." Proceedings, Third North American Masonry Conference, 63:7-63:12.

Essawy, A.S., Drysdale, R.G., and Mirza, F.A. (1985). "Nonlinear Macroscopic Finite Element Model for Masonry Walls." New Analysis Techniques for Structural Masonry, ASCE, 19-45

Faella, G., Manfredi, G., and Realfonzo, R. (1992). "Cyclic Behaviour of Tuff Masonry Walls under Horizontal Loadings." Proceedings, Sixth Canadian Masonry Symposium, 317-328.

Fattal, S.G. (1977). "The Capacity of Unreinforced Masonry Shear Walls under Membrane Loads." NBS Building Science Series 106, 177-197.

Ganesan, T.P., and Ramamurthy, K. (1992). "Behavior of Concrete Hollow-Block Masonry Prisms under Axial Compression." Journal of Structural Engineering, ASCE, 118(7), 1751-1769

Ganz, H.R., and Thürlimann, B. (1985). "Plastic Strength of Masonry Shear Walls." Proceedings 7th International Brick and Block Masonry Conference, Australia, 837-847.

Ganz, H.R., and Thürlimann, B. (1985). "Shear Design of Masonry Walls." New Analysis Techniques for Structural Masonry, ASCE, 56-70.

Ganz, H.R., and Thürlimann, B. (1986). "Strength of Brick Walls under Normal Force and Shear." Proceedings of the British Masonry Society, 1, 27-29.

Gazzola, E., Drysdale, R., and Essawy, A. (1985). "Bending of Concrete Masonry Wallettes at Different Angles to the Bed Joints." Proceedings of the Third North American Masonry Conference, University of Texas, Arlington, Texas, 27-1 - 27-14.

Giovanni, M., and Roberto, G. (1987). "Reliability of Three Nonlinear Constitutive Laws in Predicting Masonry Deformations." Proceedings of the Fourth North American Masonry Conference, 22A:1-22A:14.

Govindan, P., Lakshmipathy, M., and Santhakumar, A.R. (1986). "Ductility of Infilled Frames." Journal of the American Concrete Institute, 83(4), 567-576.

Grimm, C.T. (1975). "Strength and Related Properties of Brick Masonry." Journal of the Structural Division, ASCE, 101(ST1), 217-232.

Hamid, A.A., and Drysdale, R.G. (1982). "Proposed Failure Criteria for Brick Masonry Under Combined Stresses." Proceedings of the Second North American Masonry Conference, 9:1-9:11.

Hamid, A.A., and Drysdale, R.G. (1981). "Proposed Failure Criteria for Concrete Block Masonry Under Biaxial Stresses." Journal of the Structural Division, ASCE, 107(ST8), 1675-1687.

Hamid, A.A., and Drysdale, R.G. (1980). "Behavior of Brick Masonry Under Combined Shear and Compression Loading." Second Canadian Masonry Symposium, 51-64.

Hamid, A.A., and Drysdale, R.G. (1982). "Effect of Strain Gradient on Tensile Strength of Concrete Blocks." Masonry: Materials, Properties, and Performance, ASTM STP 778, 57-65.

Hamid, A.A., and Drysdale, R.G. (1988). "Flexural Tensile Strength of Concrete Block Masonry." Journal of Structural Engineering, ASCE, 114(1), 50-66.

Hamid, A.A., Drysdale, R.G., and Heidebrecht, A.C. (1979). "Shear Strength of Concrete Masonry Joints." Journal of the Structural Division, ASCE, 105(ST7), 1227-1240.

Hamid, A.A., and Chukwunenye, A.O. (1986). "The Compression Behavior of Concrete Masonry Prisms." Journal of Structural Engineering, ASCE, 112(3), 605-614.

Hamid, A., and Drysdale, R.G. (1980). "Concrete Masonry Under Combined Shear and Compression Along the Mortar Joints." Journal of the American Concrete Institute, 77(5), 314-320.

Hathcock, B.D., and Skillman, E. (1918). "Test of Hollow Building Tiles." Technologic Papers of the Bureau of Standards No. 120.

Hegemier, G.A., Krishnamoorthy, G., and Nunn, R.O. (1977). "An Experimental Study of Concrete Masonry Under Seismic-Type Loading." Earthquake Resistant Masonry Construction, NBS Building Science Series 106, 114-153.

Hegemier, G.A., Krishnamoorthy, G., Nunn, R.O., and Moorthy, T.V. (1978). "Prism Tests for the Compressive Strength of Concrete Masonry." North American Masonry Conference, 18:1-18:17

Hegemier, G.A., Nunn, R.O., and Arya, S.K. (1978). "Behavior of Concrete Masonry Under Biaxial Stresses." North American Masonry Conference, 1:1-1:28.

Hegemier, G.A., Arya, S.K., Krishnamoorthy, G., Nachbar, W., and Fergerson, R. (1978). "On the Behavior of Joints in Concrete Masonry." Proceedings of the North American Masonry Conference, University of Colorado, Boulder, Colorado, 4:1-4:22.

Hendry, A.W. (1987). "Testing Methods in Masonry Engineering." Proceedings of the Fourth North American Masonry Conference, 49:1-49:13.

Holmes, M. (1961). "Steel Frames with Brickwork and Concrete Infilling." Proceedings of the Institution of Civil Engineers, 19, 473-478.

Holmes, M. (1963). "Combined Loading on Infilled Frames." Proceedings of the Institution of Civil Engineers, 25, 31-38.

Hughes, D.M., and Zsembery, S. (1980). "A Method of Determining the Flexural Bond Strength of Brickwork at Right Angles to the Bed Joint." Second Canadian Masonry Symposium, Ottawa, Canada, 73-86.

Isberner, A.W. (1985). "Composition of Hardened Masonry Mortar: A Critical Review of Test Methods and Calculations." Masonry: Research, Application, and Problems, ASTM STP 871, 3-14.

Johnson, F.B., and Matthys, J.H. (1973). "Structural Strength of Hollow Clay Tile Assemblages." Journal of the Structural Division, ASCE, 99(ST2), 259-275.

Kahn, L.F., and Hanson, R.D. (1979). "Infilled Walls for Earthquake Strengthening." Journal of the Structural Division, ASCE, 105(ST2), 283-296.

Karantoni, F.V., and Fardis, M.N. (1992). "Computed versus Observed Seismic Response and Damage of Masonry Buildings." Journal of Structural Engineering, 118(7), 1804-1821.

Karantoni, F.V., and Fardis, M.N. (1992). "Effectiveness of Seismic Strengthening Techniques for Masonry Buildings." Journal of Structural Engineering, 118(7), 1884-1902.

Kato, K., Matsumura, A., Endo, T., Kubota, T., and Nishiyama, M. (185). "Tests on Existing Buildings of Concrete Block Masonry Subjected to Horizontal Forces." Proceedings of the Third North American Masonry Conference, University of Texas, Arlington, Texas, 60:1-60:14.

Khattab, M.M., and Drysdale, R.G. (1992). "Tests of Concrete Block Masonry Under Biaxial Tension-Compression." Proceedings, Sixth Canadian Masonry Symposium, 645-656.

King, G.J.W., and Pandey, P.C. (1978). "The Analysis of Infilled Frames Using Finite Elements." Proceedings of the Institution of Civil Engineers, 65, 749-760.

Kingsley, G., and Noland, J. (1987). "A Note on Obtaining In-situ Load Deformation Properties of Unreinforced Brick Masonry in the United States Using Flatjacks." Evaluation and Retrofit of Masonry Structures, Joint USA-Italy Workshop, 215-224.

Kingsley, G.R., Noland, J.L., and Atkinson, R.H. (1987). "Nondestructive Evaluation of Masonry Structures Using Sonic and Ultrasonic Pulse Velocity Techniques." Proceedings of the Fourth North American Masonry Conference, 67:1-67-16.

Kingsley, G.R., and Noland, J.L. (1987). "An Overview of Nondestructive Techniques for Evaluating Structural Properties of Brick Masonry." Evaluation and Retrofit of Masonry Structures, Joint UAS-Italy Workshop, 225-238.

Klingner, R.E., and Bertero, V.V. (1978). "Earthquake Resistance of Infilled Frames." Journal of the Structural Division, ASCE, 104(ST6), 973-989.

Klingner, R.E., and Bertero, V.V. (1976). "Infilled Frames in Earthquake-Resistant Construction." Earthquake Engineering Research Center, Report EERC 76-32.

Klingner, R.E. (1980). "Mathematical Modeling of Infilled Frames." Reinforced Concrete Structures Subjected to Wind and Earthquake Forces. American Concrete Institute SP-63, 1-25.

Klingner, R.E., Beiner, R., and Amrhein, J. (1987). "Performance of Masonry Structures in the Mexican Earthquake of September 19, 1985." Proceedings of the Fourth North American Masonry Conference, 70:1-70:14.

Leuchars, J.M., and Scrivener, J.C. (1976). "Masonry Infill Panels Subjected to Cyclic In-Plane Loading." Bulletin of the New Zealand Society for Earthquake Engineering, 9(2), 122-131.

Lian, W., Qiyun, W., Jiahua, T., and Gnoying, D. (1980). "Inelastic Earthquake Response Analysis of Brick Infilled Frames." Seventh World Conference on Earthquake Engineering, 307-314.

Liauw, T.C., and Kwan, K.H. (1984). "Plastic Design of Infilled Frames." Proceedings of the Institution of Civil Engineers, Technical Note 412, 77, 367-377.

Liauw, T.C., and Kwan, K.H. (1985). "Unified Plastic Analysis of Infilled Frames." Journal of Structural Engineering, ASCE, 111(7), 1427-1448.

Liauw, T.C., and Kwan, K.H. (1984). "Nonlinear Behaviour of Non-Integral Infilled Frames." Computers and Structures, 18(3), 551-560.

Liauw, T.C., and Lo, C.Q. (1988). "Multibay Infilled Frames without Shear Connectors." ACI Structural Journal, 85(4), 423-428.

Liauw, T.C., and Lee, S.W. (1977). "On the Behavior and the Analysis of Multi-Story Infilled Frames Subject to Lateral Loading." Proceedings of the Institution of Civil Engineers, Part 2, 63, 641-656.

Liauw, T.C., and Kwan, K.H., (1985). "Static and Cyclic Behaviors of Multistory Infilled Frames with Different Interface Conditions." Journal of Sound and Vibration, 99, 275-283.

Liauw, T.C. (1972). "An Approximate Method of Analysis for Infilled Frames With or Without Openings." Building Science, 7, 233-238.

Liauw, T.C., and Kwan, K.H. (1983). "Plastic Theory of Infilled Frames with Finite Interface Shear Strength." Proceedings of the Institution of Civil Engineers, 75, 707-723.

Liauw, T.C. (1970). "Elastic Behavior of Infilled Frames." Proceedings of the Institution of Civil Engineers, 46,343-349.

Liauw, T.C., and Kwan, K.H. (1982). "Non-linear Analysis of Multistory Infilled Frames." Proceedings of the Institution of Civil Engineers, 73, Part 2, 441-454.

Liauw, T.C., and Kwan, K.H. (1983). "Plastic Theory of Non-Integral Infilled Frames." Proceedings of the Institution of Civil Engineers, 75, 379-396.

Mallick, D.V., and Garg, R.P., (1971). "Effect of Openings on the Lateral Stiffness of Infilled Frames." Proceedings, Institution of Civil Engineers, 49(2), 193-209.

Mallick, D.V., and Severn, R.T. (1967). "The Behavior of Infilled Frames Under Static Loading." Proceedings of the Institution of Civil Engineers, 38, 639-656.

Mallick, D.V., and Severn, R.T. (1968). "Dynamic Characteristics of Infilled Frames." Proceedings of the Institution of Civil Engineers, 39, 261-286.

Mann, W., Konig, G., and Otes, A. (1988). "Tests of Masonry Walls Subjected to Seismic Forces." Proceedings, 8th International Brick and Block Masonry Conference, 764-773.

Matthys, J.H. (1972). "Structural Performance of Hollow Clay Tile Wall Assemblages." Ph.D. Dissertation, The University of Texas at Austin.

May, I.M., and Ma, S.Y.A. (1985). "A Rigid Plastic Method for the Determination of Collapse Loads of Infilled Panels with Openings." Journal of Strain Analysis, 21(1), 41-52.

May, I.M., and Naji, J.H. (1991). "Nonlinear Analysis of Infilled Frames Under Monotonic and Cyclic Loading." Computers and Structures, 38(2), 149-160.

May, I.M. (1981). "Determination of Collapse Loads for Unreinforced Panels With and Without Openings." Proceedings of the Institution of Civil Engineers, 71, 215-233.

Mayes, R.L., and Clough, R.W. (1975). "A Literature Survey-Compressive, Tensile, Bond, and Shear Strength of Masonry." Earthquake Engineering Research Center Report 75-15, University of California, Berkeley, CA.

McBride, R.T. (1984). "The Behavior of Masonry Infilled Steel Frames Subjected to Racking." Thesis submitted in partial fulfillment of the requirements for the degree of Master of Science, University of New Brunswick, Canada.

McGinley, W.M. (1990). "IRA and the Flexural Bond Strength of Clay Brick Masonry." Masonry - Components to Assemblages, ASTM STP 1063, 217-234.

McNiven, H.D., and Mengi, Y. (1989). "A Mathematical Model for the In-Plane Non-Linear Earthquake Behaviour of Unreinforced Masonry Walls. Part 2: Completion of the Model." Earthquake Engineering and Structural Dynamics, 18, 249-261.

Mengi, Y., Sucuoglu, H., and McNiven, H.D. (1984). "A Linear Mathematical Model for the Seismic Inplane Behaviour of Brick Masonry Walls. Part 1: Theoretical Considerations." Earthquake Engineering and Structural Dynamics, 12, 313-326.

Mengi, Y., and McNiven, H.D. (1979). "A Mathematical Model of Masonry for Predicting Its Linear Seismic Response Characteristics." Earthquake Engineering Research Center, UCB/EERC-79/04.

Mengi, Y., and McNiven, H.D. (1986). "A Mathematical Model for Predicting the Nonlinear Response of Unreinforced Masonry Walls to In-Plane Earthquake Excitations." Earthquake Engineering Research Center, UCB/EERC-86/07.

Mengi, Y., and McNiven, H.D. (1989). "A Mathematical Model for the In-Plane Non-Linear Earthquake Behaviour of Unreinforced Masonry Walls. Part 1: Experiments and Proposed Model." Earthquake Engineering and Structural Dynamics, 18, 233-247.

Moghaddam, H., and Dowling, P. (1988). "Earthquake Resistant Design of Brick Infilled Frames." Proceedings of the Eighth International Brick and Block Masonry Conference, 774-784.

Motta, F., and D'Amore, E. (1985). "Numerical Modelling of the Structural Behavior of Masonry Buildings." Proceedings of the Seventh International Brick Masonry Conference, Australia, 510- 519.

Naraine, K., and Sinha, S. (1991). "Cyclic Behavior of Brick Masonry under Biaxial Compression." Journal of Structural Engineering, ASCE, 117(5), 1336-1355.

Naraine, K., and Sinha, S. (1989). "Behavior of Brick Masonry under Cyclic Compressive Loading." Journal of Structural Engineering, ASCE, 115(6), 1432-1445.

Naraine, K.S., and Sinha, S.N. (1990). "Energy Dissipation in Brick Masonry under Cyclic Compressive Loading." Proceedings of the British Masonry Society, 4, 18-20.

Naraine, K., and Sinha, S. (1991). "Cyclic Compression of Brick Masonry." ACI Structural Journal, 88(5), 603-609.

Naraine, K., and Sinha, S. (1992). "Stress-Strain Curves for Brick Masonry in Biaxial Compression." Journal of Structural Engineering, ASCE, 1451-1461.

Naraine, K., and Sinha, S. (1989). "Loading and Unloading Stress-Strain Curves for Brick Masonry." Journal of Structural Engineering, ASCE, 115(10), 2631-2644.

Naraine, K.S., and Sinha, S.N. (1990). "Geometrical Model for Brick Masonry Under Cyclic Compressive Loading." Proceedings of the British Masonry Society, 4, 13-17.

Noland, J.L., Kingsley, G.R., and Atkinson, R.H. (1990). "Nondestructive Evaluation of Masonry: An Update." Masonry - Components to Assemblages, ASTM STP 1063, 248-262.

Noland, J.L., Kingsley, G.R., and Atkinson, R.H. (1988). "Utilization of Nondestructive Techniques Into the Evaluation of Masonry." Proceedings of the Eighth International Brick and Block Masonry Conference, Dublin, Ireland.

Noland, J.L., Atkinson, R.H., and Baur, J.C. (1984). "An Investigation Into Methods of Non-Destructive Evaluation of Masonry Structures." Proceedings of the Second North American Masonry Conference, University of Maryland, Maryland 4:1-4:25.

Owada, Y., Kimura, H., Dumazawa, F., and Oakada, T. (1987). "Seismic Test of Existing Reinforced Concrete Block Masonry School Building." Proceedings of the Fourth North American Masonry Conference, 71:1-71:14.

Page, A.W. (1978). "Finite Element Model for Masonry." Journal of the Structural Division, ASCE, 104(ST8), 1267-1285.

Page, A.W., (1988). "Influence of Material Properties on the Behavior of Brick Masonry Shear Walls." Proceedings, 8th International Brick and Block Masonry Conference, Dublin, Ireland, 1, 528-537.

Page, A.W. (1983). "The Strength of Brick Masonry Under Biaxial Tension-Compression." International Journal of Masonry Construction, 3(1), 26-31.

Page, A.W. (1981). "The Biaxial Compressive Strength of Brick Masonry." Proceedings, Institution of Civil Engineers, 71(2), 893-905.

Page, A.W. (1980). "A Biaxial Failure Criteria for Brick Masonry in the Tension-Tension Range." International Journal of Masonry Construction, 1(1), 26-29.

Page, A.W., and Shrive, N.G. (1988). "A Critical Assessment of Compression Tests for Hollow Block Masonry." Masonry International, 2(2), 64-70.

Page, A.W., Kleeman, P.W., and Dhanasekar, M. (1985). "An In-Plane Finite Element Model for Brick Masonry." New Analysis Techniques for Structural Masonry, ASCE, 1-18.

Parsons, D.E., and Watstein, D. (1937). "Compressive Strength of Structural Tile Masonry." Journal of Research of the National Bureau of Standards, 18, Research Paper RP972, 215-226.

Parsons, D.E. (1931). "Factors Affecting the Strength of Masonry of Hollow Units." Bureau of Standards Journal of Research, 6, Research Paper RP310, 857-867.

Pei-Feng, Q., and Da, Q. (1985). "Analysis of Earthquake Damage to Brick Structures." Proceedings 7th International Brick and Block Masonry Conference, Melbourne, Australia, 1207-1212.

Plummer, H.C. (1962). "Brick and Tile Engineering." Brick Institute of America.

Polyakov, S.V. (1960). "On the Interaction Between Masonry Filler Walls and Enclosing Frame when Loaded in the Plane of the Wall." Translations in Earthquake Engineering, Earthquake Engineering Research Institute, San Francisco, 36-42.

Pook, L.L., Stylianov, M.A., and Dawe, J.L. (1986). "Experimental Investigation of the Influence of Compression on the Shear Strength of Masonry Joints." Proceedings of the Fourth Canadian Masonry Symposium, Fredericton, NB, Canada, 1053-1062.

Pook, L.L., and Dawe, J.L. (1986). "Effects of Interface Conditions Between a Masonry Shear Panel and Surrounding Steel Frame." Proceedings of the Fourth Canadian Masonry Symposium, Fredericton, NB, Canada, 910-921.

Prawel, S.P., and Reinhorn, A.M. (1985). "Seismic Retrofit of Structural Masonry Using a Ferrocement Overlay." Proceedings of the Third North American Masonry Conference, 59:1-59:59:19

Priestley, M.J.N., and Elder, D.M. (1983). "Stress-Strain Curves for Unconfined and Confined Concrete Masonry." American Institute of Concrete Journal, 80(2), 192-201.

Richardson, J., and Dawe, J.L. (1986). "Experimental Investigation of the Behavior of Masonry Infilled Steel Frames Subjected to Cyclic Racking Loads." Proceedings of the Fourth Canadian Masonry Symposium, Fredericton, New Brunswick, 922-934.

Richardson, J. (1986). "The Behaviour of Masonry Infilled Steel Frames." Thesis submitted in partial fulfillment of the requirements for the degree of Master of Science, University of New Brunswick, Canada.

Riddington, J.R. (1984). "The Influence of Initial Gaps on Infilled Frame Behavior." Proceedings of the Institution of Civil Engineers, Part 2, 77, 295-310.

Riddington, J.R., and Stafford-Smith, B. (1977). "Analysis of Infilled Frames Subject to Racking with Design Recommendations." The Structural Engineer, 55(8), 263-268.

Riddington, J.R., and Ghazali, M.Z. (1988). "Shear Strength of Masonry Walls." Proceedings, Eighth International Brick and Block Masonry Conference, Dublin, Ireland, 548-559.

Rivero, C.E., and Phan, D. (1985). "A First Approximation to the Development of a Failure Surface for Masonry Under a Biaxial State of Stress." Proceedings of the Third North American Masonry Conference, 67:1-67:14.

Rivero, C.E., and Walker, W.H. (1985). "A Model to Study the Interaction of Frames and Infill Masonry Walls." Proceedings of the Third North American Masonry Conference, 76:1-76:14.

Rossi, P.P. (1987). "Recent Developments of the Flat-Jack Test on Masonry Structures." Evaluation and Retrofit of Masonry Structures, Joint USA-Italy Workshop, 257-286.

Rossi, P.P. (1985). "Flat-jack Test for the Analysis of Mechanical Behavior of Brick Masonry Structures." Proceedings of the Seventh International Brick Masonry Conference, Melbourne, Australia, 1, 137-148.

Saeb, S., Amadei, B., and Atkinson, R.H. (1987). "Modeling Masonry Joint Response Under Constant or Variable Normal Stiffness Boundary Conditions." Evaluation and Retrofit of Masonry Structures, Joint USA-Italy Workshop, 287-306.

Samarasinghe, W., Page, A.W., and Hendry, A.W. (1982). "A Finite Element Model for the In-Plane Behavior of Brickwork." Proceedings, Institution of Civil Engineers, 71(2), 171-178.

Sarker, A., and Brown, R.H. (1987). "Flexural Strength of Brick Masonry Using the Bond Wrench." Research Report No. 20, Brick Institute of America.

Sawko, F., and Rouf, M.A. (1985). "A Numerical Model for Masonry." Proceedings of the Seventh International Brick Masonry Conference, Australia, 520-527.

Schmid, B.L. "Testing of URM Walls." Earthquake Hazard Mitigation of Unreinforced Masonry Buildings Built Prior to 1934.

Schmid, B., Kariotis, J., and Schwartz, E. (1979). "Tentative Los Angeles Ordinance and Testing Program for Unreinforced Masonry Buildings." Proceedings of the 1978 SEAOC Convention, Structural Engineers Association of California, San Francisco, California.

SCPI (1967). "Compressive, Transverse and Racking Strength Tests of Four-Inch Structural Clay Facing Tile Walls." Structural Clay Products Research Foundation Research Report Number 11.

Sheppard, P.F. (1985). "In-Situ Test of the Shear Strength and Deformability of an 18th Century Stone and Brick Masonry Wall." Proceedings of the Seventh International Brick Masonry Conference, Melbourne, Australia, 149-160.

Sheppard, P.F., and Tercelj, S. (1985). "Determination of the Seismic Resistance of an Historical Brick Masonry Building by Laboratory Tests of Cut-Out Wall Elements." Proceedings Seventh International Brick and Masonry Conference, Melbourne, Australia, 1383-1394.

Smolira, M. (1973). "Analysis of Infilled Shear Walls." Proceedings of the Institution of Civil Engineers, Part 2, 53, 895-912.

Snell, L.M. (1978). "Non-Destructive Testing Techniques to Evaluate Existing Masonry Construction." North American Masonry Conference, 73:1-73:6

Sofocleous, C. (1988). "Dynamic Response of Masonry Infilled Steel Frames." Thesis submitted in partial fulfillment of the requirements for the degree of Master of Science, University of New Brunswick, Canada.

Stafford-Smith, B., and Riddington, J.R. (1978). "The Design of Masonry Infilled Steel Frames for Bracing Structures." The Structural Engineer, 58B(1), 1-8.

Stafford-Smith, B. (1966). "Behavior of Square Infilled Frames." Journal of the Structural Division, ASCE, 92(ST1), 381-403.

Stafford-Smith, B. (1962). "Lateral Stiffness of Infilled Frames." Journal of the Structural Division, ASCE, 88(ST6), 183-199.

Stafford-Smith, B., and Carter, C. (1969). "A Method for the Analysis of Infilled Frames." Proceedings of the Institution of Civil Engineers, 44, 31-48.

Stafford-Smith, B. (1968). "Model Test Results of Vertical and Horizontal Loading of Infilled Frames." Journal of the American Concrete Institute, 65(8), 618-624.

Stang, A.H., Parsons, D.E., and Foster, H.D. (1926). "Compressive and Transverse Strength of Hollow-Tile Walls." National Bureau of Standards Technologic Paper 311, Volume 20, 317-353.

Stockbridge, J.G. (1979). "Evaluating the Condition of Masonry Buildings in Service." Preprints of Papers to be Delivered at Fifth International Brick Masonry Conference, 165-167.

Sucuoglu, H., Mengi, Y., and McNiven, H.D. (1984). "A Linear Mathematical Model for the Seismic Inplane Behavior of Brick Masonry Walls. Part 2: Determination of Model Parameters Through Optimization Using Experimental Data." Earthquake Engineering and Structural Dynamics, 12, 327-346.

Sucuoglu, H., Mengi, Y., and McNiven, H.D. (1982). "A Mathematical Model for the Response of Masonry Walls to Dynamic Excitations." Earthquake Engineering Research Center, UCB/EERC-82/24.

Thiruvengadam, V. (1985). "On the Natural Frequencies of Infilled Frames." Earthquake Engineering and Structural Dynamics, 13(3), 401-419.

Thomas, F.G. (1953). "The Strength of Brickwork." The Structural Engineer, 31(2), 35-46.

Thomas, R.D. (1989). "Concrete Masonry Infilled Frames: The Efficient Alternative." Master of Science Thesis, The University of Texas at Arlington.

van der Pluijm, R. (1992). "Material Properties of Masonry and Its Components under Tension and Shear." Proceedings, Sixth Canadian Masonry Symposium, 675-686.

West, H.W.H (1976). "The Flexural Strength of Clay Masonry Determined From Wallette Specimens." Proceedings, Fourth International Brick Masonry Conference, Paper 4.a.6.

Whittemore, H.L., and Hathcock, B.D. (1923). "Some Compressive Test of Hollow-Tile Walls." U.S. Bureau of Standards Technologic Paper No. 238, Vol. 17, 513-527.

Whittemore, H.L., Stang, A.H., and Parsons, D.E. (1938). "Structural Properties of Six Masonry Wall Constructions." U.S. National Bureau of Standards Building Materials and Structures Report BMS5.

Wolde-Tinsae, A., Lhadj, M., and Colville, J. (1987). "Finite Element Study of Semi-Confined Masonry Walls." Proceedings of the Fourth North American Masonry Conference, The Masonry Society, Denver, CO, 19-1 - 19-15.

Wolde-Tinsae, A., Raj, B. (1986). "Behavior of Semi-confined and Fully Confined Externally Reinforced Masonry Walls." Proceedings of the Fourth Canadian Masonry Symposium, Fredericton, NB, Canada, 1038-1053.

Wood, R.H. (1958). "The Stability of Tall Buildings." Proceedings of the Institution of Civil Engineers, 11, 69-102.

Wood, R.H. (1978). "Plasticity, Composite Action and Collapse Design of Unreinforced Shear Wall Panels in Frames." Proceedings of the Institution of Civil Engineers, Part 2, 65, 381-411.

Woodward, K., and Rankin, F. (1985). "Shear Resistance of Unreinforced Hollow Concrete Block Walls." Proceedings of the Third North American Masonry Conference, The Masonry Society, 38:1-38:15.

Yettram, A.L., and Hirst, M.J.S. (1972). "The Collapse Load for Square Concrete Infill Panels." Building Science, 7, 95-100.

Yokel, F.Y., Fattal, G.S. (1976). "Failure Hypothesis for Masonry Shear Walls." Journal of the Structural Division, ASCE, 102(ST3), 515-532.

Yong, T.C. (1984). "Shear Strength of Masonry Infilled Panels in Steel Frames." Thesis submitted in partial fulfillment of the requirements for the degree of Master of Science, University of New Brunswick, Canada.

Zarnic, R., and Tomazevic, M. (1985). "Study of the Behavior of Masonry Infilled Reinforced Concrete Frames Subjected to Seismic Loading." Proceedings, Seventh International Brick and Block Masonry Conference, Melbourne, Australia, 1315-1326.

Zarnic, R., and Tomazevic, M. (1989). "Behaviour of Repaired Masonry Infilled R/C Frames: First Year Report." Report to US-Yugoslav Joint Board on Scientific and Technological Cooperation, Grant No. JF786/NSF.

Zarnic, R., and Tomazevic, M. (1990). "Behaviour of Repaired Masonry Infilled R/C Frames: Second Year Report." Report to US-Yugoslav Joint Board on Scientific and Technological Cooperation, Grant No. JF786/NSF.

VITA

Bassam Jamal was born in Damascus, Syria on May 10, 1956. He attended elementary schools in the Maza area (Damascus). In May, 1974 he graduated from Assaad Abdula High. In September, 1974 he entered the University of Damascus and received a degree of Bachelor of Science in Civil Engineering in 1980. In September, 1985 he started his graduate studies at the University of Tennessee in Knoxville. In June, 1987 he received a Master of Science degree in Civil Engineering. In May, 1993 he received a Doctor of Philosophy degree in Civil Engineering.